Electrical Load Disaggregation and Demand Response in Commercial Buildings

Imran Rahman

Dissertation submitted to the faculty of the Virginia Polytechnic Institute and State University in partial fulfillment of the requirements for the degree of

Doctor of Philosophy
in
Electrical Engineering

Saifur Rahman
Manisa Pipattanasomporn
Jaime De La Reelopez
Harpreet S. Dhillon
Lei Zuo

December 17th, 2019

Arlington, Virginia

Key Words: Load Disaggregation, Demand Response, Double-Auction, Bid Price, Load Scheduler, Load Priorities, User Preferences

Electrical Load Disaggregation and Demand Response in Commercial Buildings

Imran Rahman

Abstract

Electrical power systems consist of a large number of power generators connected to consumers through a complex system of transmission and distribution lines. Within the electric grid, a continuous balance between generation and consumption of electricity must be maintained., ensuring stable operation of the grid. In recent decades due to increasing electricity demand, there is an increased likelihood of electrical power systems experiencing stress conditions. These conditions lead to a limited supply and cascading failures throughout the grid that could lead to wide area outages. Demand Response (DR) is a method involving the curtailment of loads during critical peak load hours, that restores that balance between demand and supply of electricity. In order to implement DR and ensure efficient energy operation of buildings, detailed energy monitoring is essential. This information can then be used for energy management, by monitoring the power consumption of devices and giving users detailed feedback at an individual device level.

Based on the data from the Energy Information Administration (EIA), approximately half of all commercial buildings in the U.S. are 5,000 square feet or smaller in size, whereas the majority of the rest is made up of medium-sized commercial buildings ranging in size between 5,001 and 50,000 square feet. Given that these medium-size buildings account for a large portion of the total energy demand, these buildings are an ideal target for participating in DR. In this dissertation, two broad solutions for commercial building DR have been presented.

The first is a load disaggregation technique to disaggregate the power of individual HVACs using machine learning classification techniques, where a single power meter is used to collect aggregated HVAC power data of a building. This method is then tested over a number of case studies, from which it is found that the aggregated power data can be disaggregated to accurately predict the power consumption and state of activity of individual HVAC loads.

The second work focuses on a DR algorithm involving the determination of an optimal bid price for double auctioning between the user and the electric utility, in addition to a load scheduling algorithm that controls single floor HVAC and lighting loads in a commercial building, considering user preferences and load priorities. A number of case studies are carried out, from which it is observed that the algorithm can effectively control loads within a given demand limit, while efficiently maintaining user preferences for a number of different load configurations and scenarios.

Therefore, the major contributions of this work include- A novel HVAC power disaggregation technique using machine learning methods, and also a DR algorithm for HVAC and lighting load control, incorporating user preferences and load priorities based on a double-auction approach.

Electrical Load Disaggregation and Demand Response in Commercial Buildings

Imran Rahman

General Audience Abstract

Electrical power systems consist of a large number of power generators connected to consumers through a complex system of transmission and distribution lines. Within the electric grid, a continuous balance between generation and consumption of electricity must be maintained., ensuring stable operation of the grid. When electricity demand is high, Demand Response (DR) is a method that can be used to reduce user loads, restoring the balance between demand and supply of electricity.

Based on data from the Energy Information Administration (EIA), half of all commercial buildings in the US measure 5,000 square feet or smaller in size, whereas the majority of the other half is made up of medium-sized commercial buildings measuring in at between 5,001 to 50,000 square feet. This makes these commercial buildings an ideal target for participating in DR. In this dissertation, two broad solutions for commercial building DR have been presented.

The first is a load disaggregation technique, where power consumption and activity of individual HVACs can be obtained, using a single power meter. The second work focuses on a DR algorithm, that controls single floor HVAC and lighting loads in a commercial building, based on a user generated bid price for electricity, user preferences and load priorities, when electricity demand is at its peak.

Acknowledgements

I would like to begin by thanking my advisor Dr. Saifur Rahman, for giving me the opportunity to pursue my PhD degree. This dissertation would not have been possible without his guidance and motivation throughout my time as a graduate student, for which I am grateful.

I would like to express my gratitude to Dr. Manisa Pipattanasomporn, Dr. Jaime De La Ree, Dr. Harpreet S. Dhillon and Dr. Lei Zuo, for serving on my PhD committee, and providing me with valuable comments and suggestions. I would also like to thank Dr. Murat Kuzlu, for his guidance in research and encouragement throughout my PhD program.

Lastly, I would like to thank my family and friends, for their endless support and belief in my ability, ultimately getting me through to the end. Thank You.

Table of Contents

List of Figures

List of Tables

1. Introduction

The introduction to this dissertation begins with a brief background of the underlying concepts that have been explored in this work. These are power disaggregation of electrical loads and demand response. This is then followed by the motivation behind the work that has been carried out – the objectives and scope of this dissertation. Finally, the specific tasks that were completed are listed along with their accompanying contributions.

1.1 Background

Buildings have been identified as a major energy consumer worldwide, accounting for 20%-40% of the total global energy consumption. In addition to being a major energy consumer, it has been proven that buildings account for a significant portion of energy wastage as well. Significant energy wastage poses a threat to sustainability, therefore making energy efficiency of buildings extremely critical.

Energy monitoring is crucial in ensuring the energy efficient operation of complex systems, such as residential and commercial buildings. This information can also be used to analyze the power consumption of individual devices/appliances within a building. This provides information for energy management by providing feedback to the user at an individual device level. Power disaggregation or Non-Intrusive Load Monitoring (NILM) involves decomposing an aggregated power signal to give the details of operation of individual electrical loads. Individual device data have great benefits to consumers since energy saving opportunities can be identified for a DR event, and faulty components can also be recognized.

An electrical grid comprises of generating plants, transmission lines, substations, transformers, and distribution lines. Within an electrical grid there must be a continuous balance between the amount of electricity that is generated and the amount being consumed at all times. A recent trend is allowing commercial customers or private entities acting on behalf of customers, to submit bid prices to the active energy market in order to determine the price of electricity and load usage patterns, during peak load hours. DR is a process by which the electrical load consumption is modified instead of changing the electrical power generation, enabling the power balance between electrical generation and consumption to be maintained. Consumers can bid into the market to purchase electricity during peak load conditions, and in turn change their electrical load consumption to facilitate in peak load reduction.

This dissertation focuses on two broad solutions- disaggregation of aggregated HVAC loads, and a novel DR algorithm for HVAC and lighting load control in commercial buildings.

1.2 Motivation

In order to ensure sustainability, efficient energy management with minimized energy wastage is required. The use of smart meters in buildings has made the collection of energy consumption data at a building and individual site level feasible. Therefore, data driven and statistical prediction models have been made possible, to ensure energy efficient operation of buildings.

Building level electrical load data are often recorded in an aggregated form. This aggregated data must then be disaggregated in order to identify which devices are in operation at any given moment in time, allowing the fine-grained monitoring and control of the individual devices within a particular area of a building. Knowledge of individual device usage is essential in implementing demand response, for peak load reduction and also to evaluate the demand response potential of a particular site.

Heating, ventilation and air-conditioning (HVAC) systems account for about 40% of the energy usage of commercial buildings. Therefore, implementing demand response in commercial HVAC systems is essential for maintaining the electrical power supply and demand equilibrium. Another type of controllable loads that are considered and can take part in demand response are lighting loads, which can be dimmed based on user comfort and ambient brightness to facilitate in peak load reduction.

Therefore, to enable efficient energy usage in commercial buildings, there is a need for the development of an efficient DR algorithm that can make use of disaggregated real-time energy consumption data, of individual controllable devices such as HVAC and lighting loads.

1.3 Scope and Objectives

To address the needs that have been outlined in the motivation section, this dissertation focuses on three main objectives:

1. Disaggregate aggregated identical HVAC power consumption data to get individual HVAC device usage data, to be used for DR.

2. Improve peak load reduction and energy efficiency in smart buildings by implementing a novel DR algorithm, controlling HVAC and lighting loads.

3. Quantify the peak load reduction and energy savings by measuring the DR potential.

1.4 Tasks and Contributions

To achieve the mentioned objectives, the tasks to be achieved along with their accompanying contributions are:

1. Use machine learning classification algorithms to disaggregate the power consumption of identical aggregated loads (HVAC). This would reduce costs and enhance security as fewer power meters would be required.

2. Develop a DR algorithm that controls HVAC and lighting loads to implement DR response. This algorithm would also consider the user's preferences and opinions, and result in the maximum possible peak reduction and energy savings for the user.

3. Quantify and analyze the DR potential. This will also give utilities insight into DR potentials among their users, and usage patterns.

2. Literature Review

2.1 Disaggregation of Electrical Loads

Disaggregation is crucial to understanding the power consumption of individual loads in residential and commercial buildings. Individual load information is of great benefit to consumers, since it identifies energy savings and demand response opportunities as well as mal-functioning loads. It also increases awareness of how energy is being used in a building by providing detailed load-level feedback.

Non-Intrusive Load Monitoring (NILM) involving discerning loads from aggregated data, acquired from a single point of measurement was initiated by Hart [1], as an alternative to sub-metering all appliances. Since then, a number of techniques have been developed for the purpose of power disaggregation. Load classification categorizes appliances to several classes based on how the appliances are used. In [2] power mapping functions (PMFs) are established between the power consumption and states of data center servers. These PMFs are then used to disaggregate the aggregated power data of an entire data center. Load disaggregation of residential appliances has been achieved using sparse approximations [3], using sparse data models that were learnt from individual appliances. Using this technique sparse coefficients were found for each appliance, after which a sparse optimization problem is solved, giving the load profile for individual appliances. Multi-state finite state machines [4] have also been used to model

appliances. Appliance states are modelled as unique vectors of power consumptions, recorded at successive time instants.

Load disaggregation has also been carried out using electrical signatures based on electrical transients and current-voltage phase shift during steady-state conditions [5]. Using these features decision tree classification has also been used [6], where discrete events such as appliance operational time and appliance switching, are considered. Karhunen Loéve expansion has been used to disaggregate the power consumption of residential appliances. The uncorrelated spectral components of a power signal are used to generate a unique appliance signature, which is then used for disaggregation. Load control techniques have also been used such as- shedding, shifting and dimming of loads [7] [8], in addition to using different power levels [9] [10] [11] to classify different load types. There has also been significant work carried out using latent variable models that take advantage of appliance features [12], [13].

The concept of power edges has also been used for event detection [14] using subtractive clustering. Appliance signatures have also been built using a dynamic fuzzy C-Means clustering [15] algorithm, based on the active and reactive power of appliances. A comparison has been carried out between K-Means and Gaussian Mixture Models (GMM) for load disaggregation in [16]. While there are differences between the two algorithms, both rely on Expectation Maximization algorithm to determine cluster centers.

Artificial Neural Networks (ANNs) [17] have been used for load disaggregation, where low sampling data was used to detect changes in the active power consumption of devices. Back Propagation Neural Networks [18] have been used to disaggregate residential loads. Disjunctive Factored Four-Way Conditional Restricted Boltzmann Machines (DFFW-CRBM) and Factored Four-Way Conditional Restricted Boltzmann Machines (FFW-CRBM) are examples of deep learning mechanisms [19] used for disaggregation. Both of these algorithms are cable of multiple load classification and prediction.

K-Means clustering has been used to develop a genetic algorithm [20], where power states of electrical appliances are used for power disaggregation. Factorial Hidden Markov Modelling (FHMM) is used for modelling appliances, that uses a set of appliances states, where similar states have been merged together. Residential loads have also been modelled as Hidden Markov models (HMMs) where Segmented Integer Quadratic Constraint Programming (SIQCP) [21] is used to find individual load profiles. Power states of individual devices have been incorporated into an algorithm using FHMM and Viterbi algorithm [22] for disaggregation. Active devices are detected based on probability calculations made by the Viterbi algorithm. In [23] the features of the devices in [24] are adaptively estimated, leading to improved accuracy in the disaggregation technique. Load classification has been carried out using graph signal processing [25], where features such as active power and device status have been used. Distributed Wavelet Transform (DWT) has also been used [26], where features from a current wave have been used.

An auxiliary feedback method that incorporates the use of semi-supervised shift-invariant weighted non-negative matrix factorization [27] and device status, has been tested for load disaggregation. The methods of pulse extraction, pulse classification and clustering [28] have

also been used as a multi-stage process for disaggregation. The operation of each appliance is mapped to a discrete set of pulses, that has been decomposed from smart meter data. Another matrix factorization method that has been used for disaggregation is the Sum-to-K constrained Non-Negative Matrix Factorization (S2K-NMF) [29]. This method is able to extract meaningful results from aggregated data, by enforcing certain constraints such as the non-negative and sum-to-k constraint. Activation coefficients are calculated by the process of matrix factorization, from which the power consumption of individual devices is calculated. Occupancy data consisting of a mix of with Ultra-Wideband (UWB) radar and power signals [30] have also been tested for disaggregation. The UWB data records the movement of individuals within the considered environment, improving the accuracy of disaggregation. A number of features such as- impulsion, return temperature, and compressor state has been used in an unsupervised approach [31], for disaggregation of individual HVAC equipment.

Many early attempts at power disaggregation had also been attempted, such as representing the power signature of appliances by current waveforms [32]. A technique using voltage monitoring [33] has also been tested, where power jumps of different devices is mapped to voltage variations. These transients are then used to determine which connected devices are active at any given moment in time. Multiple clustering techniques have also been used for load disaggregation, such as an unsupervised approach [34] where rising and falling power edges are used to create models, from which features are extracted. K-means clustering in conjunction with edge detection [35], has also been used for the disaggregation of air conditioning units. In this process certain key elements of the units are detected, which are then used to determine device activity. In [36] a comparison is made between a two-step change filter and Sobel edge detector. Features are then extracted from these edges in the form of real and reactive powers, which surround the edges. Gaussian distribution in addition to Expectation-Maximization (EM) clustering algorithm [37], has been used to model different appliances and calculate clusters based on power edges. These clusters are then used to obtain the number and activity status of different appliances.

In earlier work, a number of electrical features had been used to enhance the performance of load disaggregation [38-41]. Examples of such features include- real/reactive power, Electromagnetic Interference (EMI), transient waveforms, current waveforms, instantaneous admittance waveforms, and voltage readings.

Power of lighting loads, and submeters from aggregated commercial building submetering data, has also been disaggregated using Fourier series models [42]. Statistics based on motif mining techniques [43], where motifs comprise of frequent shapes and patterns, within load curves have also been used. Load curves are then reconstructed based on this data to disaggregate active devices.

Load probabilities have been used to develop approaches for disaggregation [44], where the probability of active loads at any given time are known. These probabilities are then matched with the aggregated power data to determine the activity of loads, using the concept of probability maximization. In place of clustering, the method of Discrete Time Warping (DTW)

[45] has been used for disaggregation, which produced more accurate results when compared to K-Means clustering. Instead of looking at the output of devices, inputs were investigated [46] where devices were modelled as SISO (Single Input Single Output) devices, for the purpose of load disaggregation.

2.2 Electrical Load Prediction

Buildings are a major consumer of energy but are also responsible for a significant portion of energy wastage. Therefore, the need to make buildings as energy efficient as possible is crucial in ensuring sustainability. In this context, it is important to be able to make predictions regarding a buildings' power consumption.

Artificial Neural Networks (ANNs) have been used extensively in performing the task of electrical load forecasting. One of the simplest forms that has been investigated for load forecasting, is a multi-layer perceptron neural network [47] using historical data. ANN's trained using a small amount of training data, and average temperature of the day before [48] as an input to consider the inertia of the system, have also been used to predict the total power consumption of a university building in Spain. Deep neural networks using Long Short-Term Memory (LSTM) have been used in building load forecasting [49] to predict the active power consumption of the total building load in the next time step. Two types of LSTM models- LSTM- based Sequence to Sequence (S2S) and standard LSTM architecture were tested, using different time interval electricity consumption data. Between the two variants, the S2S architecture performed most accurately over different time interval data. A Radial Basis Function Neural Network (RBFNN) has been used for hourly electric load forecasting [50]. Features such as historical load data and weather data have been used as inputs, which have seen to yield accurate predictions, during different ambient conditions. In [51] an IoT (Internet of Things) based deep learning system automatically extracts features from captured data to give a two-step forecasting scheme, which forecasts the daily total consumption of an area of loads first, based on which the intra-day load variation is predicted. Short term electrical load forecasting (STLF) using Back Propagation ANN's (BP-ANN) have been used in [52]. A number of different system models are formulated, considering various combinations of parameters such as base load component, day of the week, load inertia, short term trends, autocorrelation, length of the past data, etc. These parameters are then used to predict the hourly loads for the following day. Recurrent Neural Networks (RNNs) [53] have been used to develop a load forecasting management model for the city of London. Using historical load data, Recurrent Cartesian Genetic Programming evolved Artificial Neural Networks (RCGPANN), have been used for day-ahead electrical load prediction. A hybrid RNN neuro-fuzzy inference model [54] has also been used to predict HVAC load in commercial buildings. The performance of three different neural network models- Feed Forward Neural Network model (FFNN), RNN and Neural Network-based nonlinear autoregressive exogenous model (NARX) [55] have been compared, in short term load forecasting for a building in Korea. Of the three models, it is found that the

NARX model yields the most accurate results. The Levenberg–Marquardt neural network model [56] has been used to model occupant behavior, for building cooling load prediction.

Various Regression techniques have also been used for the purpose of electrical load forecasting. Using historical thermal and demand data, an optimal fit line generated from quadratic regression [57], is used to predict a building's electrical load for demand resource planning. In another study, three different regression techniques- Random Forest (RF), Regression Trees (RT) and Support Vector Regression (SVR) were tested and compared [58], when predicting the hourly electricity usage if two educational buildings in Florida. 11 input features consisting of meteorological data, occupancy data and time related data were used when predicting the hourly electricity usage. Of the three models, the RF model was found to be most accurate. Linear regression models [59] using input features such as -weather, occupancy and office hours, are used to make day-ahead predictions of electricity consumption for a particular floor of an office building in Sweden. The results show that occupancy is correlated with appliance load, and outdoor temperature and a temporal variable defining work hours are connected with ventilation and cooling load. A clustering-based hybrid model [60] consisting of fuzzy c-means clustering (FCM) to cluster together similar days and hours based on electricity consumption, in addition to using support vector regression (SVR) has been used to predict the day-ahead hourly electric demand in a number of hotel buildings.

In a number of studies, the performance between various ANN's and regression techniques has been compared. A 7-step ahead [61] load prediction model for simulated loads was tested using both SVR and ANN, and the results were compared, from which it was found that SVR made more accurate predictions than ANN, and that the training time of SVR is approximately 72 times faster than ANN's. An ultra-short-term heating load prediction model has also been developed [62] using Principal Component Analysis (PCA), Correlation Analysis (CA), and Wavelet Decomposition (WD) to determine input features. These inputs are used in support vector regression (SVR) and the multilayer layer perceptron neural network (MLP), from which it is found that the MLP provides greater accuracy in prediction. Short-term electrical load prediction of HVAC has been carried out using different models [63], including Artificial Neural Network (ANN), Multiple Linear Regression (MLR), and Bagged Decision Tree (BDT). BTU of air-conditioning units have been used in conjunction with weather features to make predictions. In addition to temperature and humidity as predictors, additional factors such as room size are used as input features as well. The results show that among the three models the ANN model using all possible input predictors is most accurate. A Non-linear Auto Regressive model with exogenous input (NARX) neural network has been used [64] to forecast the day ahead, week ahead and month ahead power consumptions for a commercial building. This model incorporates input features such as temperature, auto regressive features from historical data, and also contextual information such as day of the week, time of day and also type of day. The accuracy of this model is compared with a SVR model given the same inputs. Forecasting accuracy for both types of models are comparable, with the NARX neural network performing slightly better than SVR. Medium-term load forecasting for hourly electric load prediction of peak loads of different days or hourly loads throughout the day [65], has been carried out using SVR and

ANN's. Though ANN's provide slightly more accurate results than SVR, they require a large amount of training data resulting in high memory requirements and processing time. Therefore, with similar accuracy and significantly less processing time, the SVR model is preferred for medium-term load forecasting. An improved entropy method [66], that groups together similar days is used for short-term electrical load forecasting of HVAC in commercial buildings using both General Regression Neural Networks (GRNN) and Support Vector Machine (SVM). The load data were obtained using an energy simulation software called DEST to simulate an office building in a business park in Beijing. The proposed method yielded high forecast accuracy and fast computation speed. In [67] the performance in forecasting short term demand of three different models- neural networks, decision trees and Conditional Restricted Boltzmann Machines (CRBM) algorithms are compared. In general, it is found that of the three models, neural networks perform most accurately at day-ahead forecasting. Short and medium-term forecasting of a water source heat pump [68], has been carried out using six different models- Multiple linear regression, Gaussian process regression, tree bagger, boosted tree, bagged tree and neural network. The six models tested have comparable results, with neural networks performing the most accurately.

Besides ANN's and regression, there have been a number of other approaches applied to electrical load forecasting. Box- Jenkins Methodology from which the Seasonal Autoregressive Integrated Moving Average (SARIMA) [69] models are obtained, has been developed for short-term electricity load forecasting for university buildings in Thailand. An Extreme Learning Machine (ELM) algorithm based on the Moore-Penrose generalized inverse matrix theory [70], is used for energy consumption forecasting of an air conditioning system. Another HVAC load forecasting method involves selecting similar days based on combined weights [71]. Errors of similar conditions are calculated using weather and day data. A Case Based Reasoning (CBR) approach [72] has also been used to predict the energy demand of a commercial building in Quebec. This method is used to provide a three-hour ahead energy demand prediction, using only weather forecasts. Another method used for HVAC energy forecasting involves frequency domain spectral density analysis [73]. This process captures the dynamics of building energy system such as weather, schedule, and ventilation rate, and is able to forecast the energy consumption of the HVAC system with an accuracy of greater than 90%, in under two minutes.

2.3 Demand Response Techniques

Demand response plays an important role in peak load reduction, that benefits the utility in terms of load curtailment and can also benefit the consumer, in terms of financial reward.

A number of different machine learning algorithms have been used in implementing demand response algorithms. A price-based Demand Response (DR) strategy using ANN's and mixed-integer linear programming [74] has been developed, which controls HVAC and considers user preferences. The thermal preference levels of occupants are modeled using ANN's which are directly integrated into the DR scheduling. The optimization problem for DR, incorporating the

occupant's thermal discomfort and the buildings thermal response is then solved using mixed-integer linear programming. A Model Predictive Control (MPC) framework using a Nonlinear Autoregressive Neural Network (NARNET) has been used [75] to determine the optimal control of a HVAC system during demand response. Thermal behavior of the building is modelled using the NARNET and the optimal control problem is formulated as a Mixed-Integer Non-Linear Programming (MINLP). Autonomous control of multiple lighting systems during a DR event using Reinforcement Learning (RL) has been proposed [76], taking into account the occupants illuminance comfort. A novel state action space Q-learning technique has been presented to control lighting loads. The problem is modelled as a Markov Decision Process, and an optimization approach based on RL is proposed. Another Q-learning approach that controls the illuminance level by adjusting lights and blinds [77] in a smart building has been developed. The system uses the occupants' perceptions of the surroundings as a feedback signal through a human-machine interface, while the illuminance level is recorded periodically by a light sensor. A comfort model is then built based on the feedback signal and illuminance, which helps determine the occupants comfort state. Accordingly, a control policy is determined by a Q-learning controller, which is used to operate actuators that adjust the surroundings, until users are satisfied.

There are a number of DR techniques that are based on the concepts of load priorities, scheduling, and user comfort. A new DR approach for HVAC has been developed based on Predicted Mean Vote (PMV) [78]. This enables DR to take place with minimal thermal discomfort to the user. Load shedding by means of dimming control of lighting systems in a building [79], without affecting user comfort have been investigated. Based on the load shedding flexibilities of the respective groups of loads, the methods of proportional load shedding and load shedding equalizing relative illumination changes are implemented for DR. When compared to uniform load shedding, this approach meets the minimum illumination requirement for all load groups and sheds a larger amount of load than uniform load shedding. In order to reduce the power consumption of home appliances during peak-demand hours, task scheduling [80] is used to control the operation of time-shiftable loads. Symbiotic Organisms Search (SOS) and Cuckoo Search (CS) algorithms, are two heuristic optimization methods that have been tested. Results show that the SOS algorithm outperforms the CS algorithm. An automated DR algorithm has been proposed and tested where in an interruptible load scheme, buildings participate as an aggregated load [81]. During a DR event, the electricity demand is reduced by controlling the centrifugal fan of the air conditioning system. If this is not enough, further load curtailment is achieved by shedding loads based on their assigned load priorities until the electricity demand has reached an acceptable level. In [82] an Automated Demand Response with an Assessable impact on Loads and Occupant Comfort (ADRALOC) program has been presented. During a DR event, this program can both directly and indirectly control HVAC loads. Predicted features such as load consumption, occupant behavior and indoor environmental properties allow DR events to be scheduled. An optimal scheduling DR program for [83] residential homes has also been discussed. During a DR event, thermostat set points are adjusted to minimize the energy consumption, while the operation of other loads is shifted to maximize the load reduction further. This problem is formulated as a Mixed-Integer Linear Program (MILP), to minimize peak load

under certain constraints that represent the operation of time-shiftable loads. In another study, a random forest regression approach for predictive control of HVAC systems in a commercial building [84] has been carried out. An optimal HVAC schedule operation is generated, that minimizes the HVAC energy consumption, while also ensuring that the indoor temperature is within a predefined temperature range.

There have also been some DR approaches based on occupancy detection only. Lighting set point tuning has been controlled for office zones based on occupancy sensing [85]. During the day time, in the case of sufficient daylight entering through the windows, the lights were turned off after a delay of six minutes, whereas the lights were turned on with no delay if there was insufficient daylight. Optimal daylight harvesting and occupancy detection have been used in [86] to control lighting load energy consumption in an office space. This is achieved using a co-located notion and light sensor within each of the luminaires spread throughout an office building. Significant savings are found when a combination of occupancy detection and daylight harvesting were used. A similar approach is taken in [87] using a ZigBee wireless network. A central controller receives the net average illuminance and occupancy from respective sensors. Brightness of lighting loads are then adjusted for peak load reduction.

DR approaches based on load priorities, scheduling, user comfort, and various other methods have also been investigated. Two transactive control strategies- with and without precooling [88] to control residential HVAC systems during a DR event has been investigated, with the heating or cooling set point of the thermostat adjusted based on the market price signal. The effectiveness of this method is tested on a group of 100 homes using the GridLAB-D simulation platform. The cost savings used by each of the methods is quantified and the results show that the strategy without precooling yielded the most savings. A transactive control approach is taken in [89] that uses market mechanisms to control HVAC loads in a commercial building, during a DR event. The process involves bidding and clearing of electricity prices. A number of case studies were conducted, from which it was found that this transactive approach was effective at peak load reduction. In [90] a transactive control method for lighting loads has been presented, in which lighting loads are treated as price-sensitive loads. Using pricing signals, an energy management system calculates the lighting illumination level of the desired areas, making sure the illumination level falls within a predetermined range. The illumination level is then adjusted using a lighting controller. HVAC load curtailment, where each consumer is described by a forecast of their thermal response profile computed using a statistical model [91] has been carried out. From this, a load scheduling algorithm based on solving a convex problem is used to control the HVAC energy consumption of a group of consumers. The energy signatures of individual rooms are considered as individual agents, and then a multi-agent Minority Game (MG)-based demand response management system, reduces the peak demand. Residential HVAC control within a microgrid based on game theory [93] has also been presented. A Stackelberg Game-based Demand Response (SGDR) algorithm is proposed. In this approach the HVAC unit is the demand-side responsive resource, whereas the load serving entity is considered the leader and the microgrid a follower. Optimization of lighting power consumption using a nature inspired Fish School Search (FSS) and weighted FSS algorithm [94] has also been

investigated. Between FSS and weighted FSS, the latter was found to show more accurate results with a small execution time. HVAC DR control through thermostats (as wireless sensors) using a rule-based technique [95] has also been investigated. In this approach, the thermostat acts as a central unit, making decisions based on a number of defined rules. Prior and real-time information from the thermostats are compared, which is then used to determine the optimal HVAC control technique.

2.4 Double-Auctioning

Double-Auction algorithms have been used for the transaction of electricity and resources in a number of different scenarios.

A number of different double-auction techniques have been used in the implementation of a transactive energy market in microgrids. In [96] a double-sided auction is broken down into two separate single auction games. The single auctions are coupled as a joint potential quantity, with updates being made to the potential related to the top responses of players in each single auction. A peer-to-peer transactive energy market platform in [97] uses a double-auction with average mechanism. In this mechanism the market cleared price is calculated from the mean of the bids and reservation prices of all the participants in the current market. Energy is then allocated following a greedy manner from the sellers with lowest price to the buyers with higher bids. An iterative approach is taken in [98] where an aggregator receives bids from the buyers, and also available energy for trade from the sellers. It then allocates energy to the buyers proportionally, and iteratively converges to the market clearing price. Another iterative approach has been developed in [99] where a microgrid controller implements a distributed algorithm to maximize social welfare of the participants.

Block chain technology has been used to develop a peer to peer platform for transaction of energy in the absence of a trusted third party [100]. Block chain technology is used to maintain the lawful behavior of the peers when trading. This mechanism enables local energy trade while also minimizing energy loss due to transmission. The distances among the pair of buyer-seller peers is reduced, and then cleared market price is calculated from their bid prices. A Continuous Double Auction (CDA) mechanism using block chain has been developed in [101]. Given fluctuations in the CDA market, an adaptive aggressiveness strategy is used, by which bids and ask prices can be adjusted based on current market prices. An adaptive attitude bidding strategy in CDA is described in [102], where heuristic rules and reasoning mechanisms are incorporated. A risk-based auction using an artificial immune system-based algorithm [103], has been used for profit maximization. The algorithm is applied on a typical study case network to optimize the generation, where assumptions are made on realistic market prices for power and distributed generators bids, that reflect realistic operational costs. This work has been extended in [104], where a hybrid-immune-system-based particle swarm optimization minimizes the generation fuel costs, based on the priorities of the consumer. A risk-based auctioning technique is implemented,

where risk associated with a bid is assessed after which the agents and proceed accordingly in order to maximize profit.

An iterative double auction approach where sellers are equipped with photovoltaic panels in [105] and the optimal allocation and sizing of wind power generators [106] for profit maximization, are examples of renewable integrated double auction mechanisms. Autonomous coordination of buildings in a smart microgrid [107] has also been carried out using double auction. Demand devices and in-house energy supply participate to maximize economic benefit and autonomy of the microgrid. This system enables every generation/consumption device within the microgrid to participate in the auctioning process. A novel strategy-proof online double auction (SODA) scheme in [108] has been developed for transaction of resources between microgrids. Here the excess and insufficient microgrids in the system are treated as sellers and buyers, respectively. The microgrid center controller matches the buyers and sellers in order to maximize social welfare. A multi-round double-auction among microgrids has also been developed in [109]. In this algorithm, each participant is modeled as an agent, in a multi-round double-auction, where offers are taken into consideration even after a fixed bidding period, which leads to improved fairness.

A number of double-auction schemes focused on controlling a particular type of load have also been developed. A HVAC control double-auction system that responds to a combination of user specified internal setpoints and external market signals through a controller has been described in [110]. The internal setpoint temperature of a HVAC unit is adjusted based on the current market cleared price. Generated bid prices are based on whether the internal air temperature is higher or lower than the desired setpoint. A reinforcement learning HVAC control bidding strategy has been developed in [111]. Once again, the bid prices are a function of the indoor temperature in comparison to user defined set points.

A double-auction technique for Electric Vehicles (EVs) is discussed in [112] and [113], where Vehicle-to-Grid (V2G) technology is used to implement DR during smart grid outages. The sellers comprise of EVs that have surplus electrical energy, whereas the EVs with insufficient energy serve as buyers. Through use of a public key, the bids are encrypted when sent to the auctioneer whose role is being fulfilled by the microgrid controller. A location privacy preserving auction scheme has been developed in [114] where individual EVs in addition to multiple parking lots, comprise the trading platform for energy sharing. This ensures free energy trading between EVs while also increasing the energy supply available for a microgrid, in the event of an outage.

Double-auction mechanisms used for resource allocation in cellular networks has been discussed in [115] where bids and asks, of active cell-edge users and idle users respectively have been marked up. This gives different idle users (sellers) the incentive to match up with different cell-edge users (buyers), to share cellular resources. Double-auction for harvested renewable energy resources among cellular base stations has been explored in [116]. Base stations with surplus harvested energy share this energy with base stations that have an energy deficit. Energy

deficient base stations are also stimulated to purchase energy from surplus energy base stations in order to reduce the consumption of non-renewable energy.

Cloud computing resources have also been shared using double-auction schemes, such as in [117] where an iterative scheme has been implemented, to maximize social welfare. A combinatorial double-auction technique has been applied to cloud resource allocation in [118]. Several factors are considered, such as provider and user credit, in addition to energy costs, which in turn resists dishonesty within the auctions. This meets user demand for diversity of service resources, in addition to avoiding monopoly among resource transactions.

2.5 Evaluation of Demand Response Potential

Evaluating the demand response potential can also give the utility insight into load curtailment strategies and the usage characteristics of its consumers.

In many cases machine learning algorithms have been used to evaluate demand response potential. A smart meter driven Real-Time Demand Response Potential Evaluation (RTDRPE) method in [119] uses a Gaussian Mixture Model (GMM), to learn probabilistic behaviors of electricity consumers from historical data. The RTDRPE then facilitates in the real-time decision-making process for DR implementation. Cluster Analysis in conjunction with Bayes method [120] has also been used to evaluate a consumers' DR potential. Based on load data, consumers are divided into patterns after which Bayes method is used to predict the users' behavior patterns using features such as temperature and day type. Using this information, a consumers' DR potential can be calculated. A Markov chain-based approach for evaluating DR of residential loads is presented in [121], simulated in Matlab. Markov chain-based occupant behavior models are created, used in conjunction with common residential load models, to predict minute by minute variation in residential load patterns.

Besides the machine learning methods mentioned above, there are a number of other methods that have been used in evaluating DR potential. User preferences have been incorporated [122] into evaluating the DR potential of residential HVAC loads. As residential HVAC loads are flexible, this method assesses the DR potential of these loads, taking into account the temperature preferences of the user. Electricity consumption is then adjusted, while ensuring the temperature range satisfying user comfort is maintained. The model is tested for a number of different seasons, and it is found that temperature dead-bands have a significant effect on DR potential, which correspond to how willing users are to accept changes in their comfort. The DR potential of ventilation fan systems [123] has also been evaluated. A building HVAC system is simulated in a Python model, where the objective is to minimize electricity consumption in addition to the CO2 level in the air. Experimental results show there is a need to aggregate several HVAC systems in order to enable prolonged load sheds during a DR event while still maintaining acceptable air quality. Using a Genetic Algorithm (GA) to evaluate the DR potential of HVAC systems [124] has also been investigated. Inputs to the model include building cooling

load profiles and historical electricity pricing. Dynamic pricing in addition to time of use are the two different electricity pricings that are considered. The use of alternate energy sources in office buildings [125] to reduce the peak demand from the electric grid has been investigated. The integration of energy systems such as solar PV, thermal or electrochemical storage systems, could be used to generate power in place of load shedding during a DR event.

There are a number of building energy simulation tools that have been used to evaluate DR potential. A Direct Load Control (DLC) [126] program that considers consumer comfort, is used to implement demand reduction at the consumer end, to control the operation of HVAC systems. Building energy models are simulated in GridLAB-D, both with and without implementing DR, from which the DR potential is found. Another study has been carried out using GridLAB-D to evaluate the effect of various factors on the DR potential of residential homes [127]. Case studies were carried out to investigate the effects of different factors such as – thermal storage capacity for different buildings, impact of dynamic price signal, temperature variation, rebound effect and also, day time and seasonal factors. The effects of zonal cooling set point strategies on peak load reduction have been evaluated in [128]. The concept of building centered productiveness, is used to analyze demand response potential for a commercial cooling system. Virtual tests are carried out using HAMBase/Simulink simulations, which are then validated with recorded onsite measurements. Another significant contribution of this study is that it provides a cost-effective strategy for evaluation of peak load reduction potential, during cooling operations in an office building. A DR potential model for a Model Predictive Controller (MPC) of space heating has been developed in EnergyPlus [129]. The study focuses on controlling space heating optimally, as to minimize the electricity costs in addition to minimizing the CO2 level in the air.

3. HVAC Power Disaggregation Using Supervised Machine Learning Algorithms

3.1 Introduction

The energy efficient operation of residential and commercial buildings can be ensured from the use of detailed energy monitoring. This detailed energy data can then be used to analyze the power usage of loads at an individual device level, thus providing a foundation for applications in energy management and feedback given to the user in the form of usage patterns. Although the use of smart appliances will become widespread in the future, legacy devices will still be present, which are incapable of reporting their device status and energy consumption in real-time. Load monitoring of appliances broadly falls under two categories: 1) distributed direct sensing, also known as sub metering and 2) single-point power disaggregation. In the case of distributed direct sensing, individual appliances are monitored using submetering sensors to record quantities such as: current, voltage, power, etc. This technique has been proven to be effective, however this hampers economic feasibility as well as complexity, given a large number of dedicated meters are required to monitor individual devices. An alternative to this involves increasing smart meter deployment, and promoting the importance of energy savings in what is known as Non-Intrusive Load Monitoring System (NILMS). This process requires simple installation techniques, while monitoring current and voltage signals, thereby determining the activity of different loads based on the changes observed in monitored signals. It has been proven that smart meters are capable of transmitting detailed energy data back and forth with the utility, with a higher frequency in comparison to classical meters. There is however, a need for yet more detailed information on power consumption at an individual device level, to unravel actions that could be taken to enable higher energy savings.

A number of power disaggregation techniques have been developed, which are used to disaggregate signals for a number of aggregated loads. However, power disaggregation of aggregated data for a number of identical devices, in order to determine the state of activity at any given moment in time, is problem that has not yet been fully addressed. Considering smart buildings, power disaggregation is a technique that involves separating the power consumption of a number of devices, that has been recorded by a single power meter. An application of this would be during a Demand Response (DR) event, where the power consumption of individual HVAC units would be required, in order to effectively control them. Installing individual power meters to monitor each HVAC unit is not economically feasible, therefore meaning that their data must be aggregated and collected by a single power meter. This power data must then be disaggregated, to retrieve the power consumption data for each individual HVAC unit.

3.2 Methodology

The following sections describe the performance and accuracy of a number of supervised classifiers that have been simulated, for the purpose of power disaggregation of several aggregated identical HVAC units. The classifiers that have been tested include: Decision Trees (DT), Discriminant Analysis (DA), Support Vector Machine (SVM) and k-Nearest Neighbors (k-NN). The main contributions presented in this work are as follows:

1. A novel power disaggregation technique for multiple identical HVAC units, whose power data has been collected and aggregated by the use of a single power meter. This will enable the fine-grained monitoring of the individual devices, thus identifying the activity status and power consumption of individual HVAC units. This would therefore, reduce costs and enhance security, due to the use of fewer power meters.

2. Using simple machine learning classification algorithms and features such as real power, reactive power and phase currents, obtained from smart meter data, the problem of power disaggregation of aggregated loads can be solved.

Power disaggregation is carried out for five HVAC compressors installed throughout a single floor of a commercial building. This is achieved using machine learning classifier models, trained using features such as real and reactive power, and phase currents of each HVAC compressor and corresponding air handler unit. Index values representing the combination of active compressors based on power consumption are also included as a training input features. The classifiers then determine which compressors are active at any given moment in time by matching input power consumption data to a particular index value, based on the training data. This technique achieves a high degree of accuracy in determining the device status throughout a defined test period.

3.3 Supervised Classifiers

Supervised classification is the process by which input features are used to predict a corresponding class output, based on data used to train the model. These class outputs are referred to as target values, categories or labels. In the following sub sections, the supervised classifiers that have been tested for load disaggregation are briefly described.

3.3.1 Decision Trees

The concept of Decisions Trees (DT) is based on a tree-like structure, where different input features within the data set are represented by branches, whereas the outputs are represented as leaves on the branches. Given a set of input features, the model traverses the branches of the tree

by first calculating entropy and then information gain, which is then used to separate different classes. Decision trees can be classified into two major types- models that output continues values are referred to as regression trees, whereas models that predict discrete values are referred to as classification trees, and it is classification trees that have been used in this work.

Entropy is defined as:

$$\sum_{i=1}^{J} p_i log_2 p_i \qquad (1)$$

where p_i are fractions that add up to 1 and represent the percentage of each class present in the child node, once splitting takes place from a parent node within the tree.

Information Gain = Parent Entropy– Weighted Sum of Children Entropy

$$IG(T, a) = H(T) - H(T|a) \qquad (2)$$

At each step when building the tree, information gain is used to decide on which feature, splitting occurs. The creation of a small tree with low model complexity is ensured by a splitting technique that results in the purest possible child nodes at each step.

3.3.2 Discriminant Analysis

Discriminant analysis (DA) is a classification technique where the model is given prior knowledge of output classes, which are then used to classify new data points to known output classes based on the input features. This technique uses a score-based system where, each output class has an associated score which is calculated based on its corresponding input features, during the training phase of the model. Hence the model can effectively determine the output class given a particular set of input features.

3.3.3 Support Vector Machine

Support Vector Machines (SVM) also has two variants- one that used for classification, which is used in this work and another that can be used for regression referred to as Support Vector Regression (SVR). SVM is a non-probabilistic binary linear classifier, mapping a set of input features to a particular output class. The model uses hyperplanes which are used to divide a space

into a number of different categories. Therefore, data points belonging to different categories are divided by the maximum possible separation. Once data points are inserted into this space, they are categorized depending on which side of the hyperplane they are located in. A hyperplane can be defined as,

$$f(x) = \beta_o + \beta^T x \qquad (3)$$

where β_o is the *bias* and β is known as the weight vector.

There are an infinite number of ways of defining the optimal hyperplane by scaling of β and β_o. The representation chosen in this work is,

$$|\beta_o + \beta^T x| = 1 \qquad (4)$$

where the training examples nearest to the hyperplane are represented as x. Support vectors are defined as the training examples nearest to the hyperplane.

The distance between a point *x* and a hyperplane (β, β_o) is calculated using the following,

$$\text{distance} = \frac{|\beta_o + \beta^T x|}{||\beta||} \qquad (5)$$

For canonical hyperplanes, the numerator is equal to one and the distance to the support vectors is calculated as follows,

$$\text{distance}_{\text{ support vectors}} = \frac{|\beta_o + \beta^T x|}{||\beta||} = \frac{1}{||\beta||} \qquad (6)$$

M is defined as a margin that is twice the distance to the closest examples,

$$M = \frac{2}{||\beta||} \qquad (7)$$

The problem of maximizing M can be modelled as the problem of minimizing a function $L(\beta)$ subject to certain constraints. This constraints-based model that classifies the training examples x_i based on input features, to a particular output class is given below.

$$\min_{\beta,\beta_o.} L(\beta) = \frac{1}{2}||\beta||^2 \text{ subject to } y_i(\beta_o + \beta^T x_i) \geq 1 \quad \text{for} \quad \text{all } i \qquad (8)$$

Here y_i represents each of the labels of the training examples. This is a problem of Lagrangian optimization that can be solved using Lagrange multipliers to obtain the weight vector β and the bias β_o of the optimal hyperplane.

In equation (8), y_i represents each unique output label given in the training examples. The problem is defined as a Lagrangian optimization, which when solved using Lagrange multipliers, gives the weight vector β and the bias β_o of the optimal hyperplane.

3.3.4 k-Nearest Neighbors

The k-Nearest Neighbors (k-NN) algorithm is an example of a non-parametric supervised classifier, given the model complexity increases with the size of the training data. When classifying an input data point, the model considers its input features in addition to considering the most common output classes assigned to its neighboring data points. For a particular data point, the average of the outputs of its 'k' nearest neighbors are calculated and then used to assign a particular output class.

$$D = \{(x_1, y_1), \ldots, (x_n, y_n)\} \quad (9)$$

D is the set of training data consisting of a set of input features (x_n) and their corresponding output classes (y_n).

$$f(x) = y_k, \text{ where } k = \text{argmin}_i\, d(x, x_i) \quad (10)$$

f(x) is the output of the classifier, calculated by computing the minimum difference between an input data point and objects given in the training data. Based on this computation, the input data point is assigned to a particular output class.

3.4 Data Collection

3.4.1 Thermostats and Compressors

In Fig. 1 Below, the floor plan of the second floor of the commercial building in Alexandria, VA is shown, from where data was collected for the purpose of load disaggregation. Each of the labelled thermostats in the figure, control a single HVAC compressor. Thermostat 1 is located inside an office room, whereas thermostat 4 is located inside a computer lab. The remaining thermostats- 2,3 and 5 are located in different hallways throughout the floor. Using separate power meters to monitor and record the power consumption of individual compressors is not economically feasible, therefore a single power meter is used to collect the aggregated power data for five HVAC compressors.

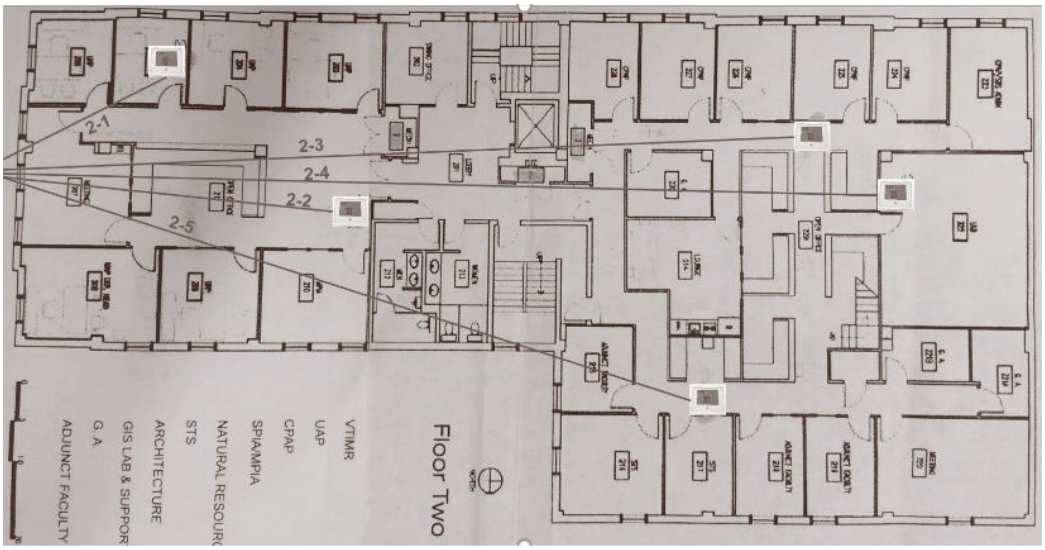

Figure 1. Location of the five thermostats on the second floor controlling HVAC compressors.

3.4.2 Training Data

Training Data Training data for the classification models had been collected over several months- April through September of 2017, from a single floor of a commercial building in Alexandria, VA. The Data was collected at a resolution of one-minute intervals, consisting of both compressor and air handler unit data. The training data consists of:

- Real Power
- Reactive Power
- Phase Currents
- Index Values

The real power values for the HVAC compressors vary between 0kW for when all compressors are turned off, to a value just under 14kW, when all five compressors are turned on, during which time the maximum reactive power is around 5kVar. The value for the combined phase currents vary between 0A and 50A. When a particular number of compressors are active, the real and reactive power readings are quite similar, therefore distinguishing between different combinations of active compressors is challenging. Due to this, additional features such as the effect on phase currents was also investigated. It was found that there was significant change in phase currents, for different compressor combinations, and phase currents were therefore also included as input features for the load disaggregation models.

Training data was collected using BEMOSS™ (Building Energy Management Open Source Software) developed by Virginia Tech - Advanced Research Institute for small and medium-sized commercial buildings. Data was collected for each of the 32 combinations of five different HVAC

compressors. For each combination, an index value was assigned corresponding to the power and current data for that particular compressor combination. For each index, 30 minutes of training data was used, when training the classifier models for load disaggregation. In Table 1 below, the list of indexes corresponding to the combination of active compressors is given.

Table 1. List of compressor indexes.

Index	**Active Compressor(s)**
0	**All Are Off**
1	1
2	2
3	3
4	4
5	5
6	1,2
7	1,3
8	1,4
9	1,5
10	2,3
11	2,4
12	2,5
13	3,4
14	3,5
15	4,5
16	1,2,3
17	1,3,4
18	1,4,5
19	1,2,4
20	1,3,5
21	1,2,5
22	2,3,4
23	2,4,5
24	2,3,5
25	3,4,5
26	1,2,3,4
27	1,3,4,5
28	1,2,4,5
29	1,2,3,5
30	2,3,4,5
31	1,2,3,4,5

3.4.3 Test Data

Test data for the case studies in section 3.5 was collected for a period of 24 hours during June 2017, when the outdoor temperature was among the highest for the month. The test data for the case studies in section 3.6 was collected over five separate 24-hour periods in August 2017, again during days having some of the highest outdoor temperatures.

3.5 Case Studies

3.5.1 Compressor Models

Classifiers for the compressor models are trained using input features such as: real and reactive powers in addition to phase currents using only compressor data. The output portion of the training data are the corresponding index values. In this section, predicted index values for each of possible 32 combinations (starting from 0 to 31) is plotted, in comparison to the true recorded values of the indexes at those particular time instances. In the figures given below, the power consumption is shown to reflect the change in power consumed, with a change in index values.

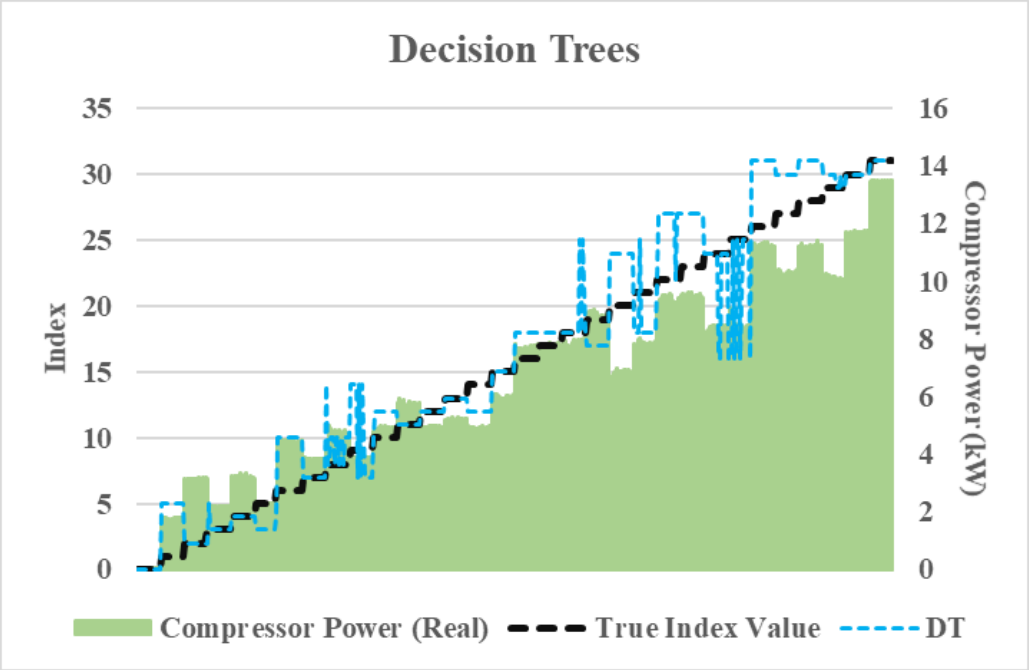

Figure 2. Indexes generated by DT model plotted against the true index value of the compressors.

In Fig. 2 we observe that compressor DT model does not perform accurately at predicting the index values, with an accuracy of only 60%.

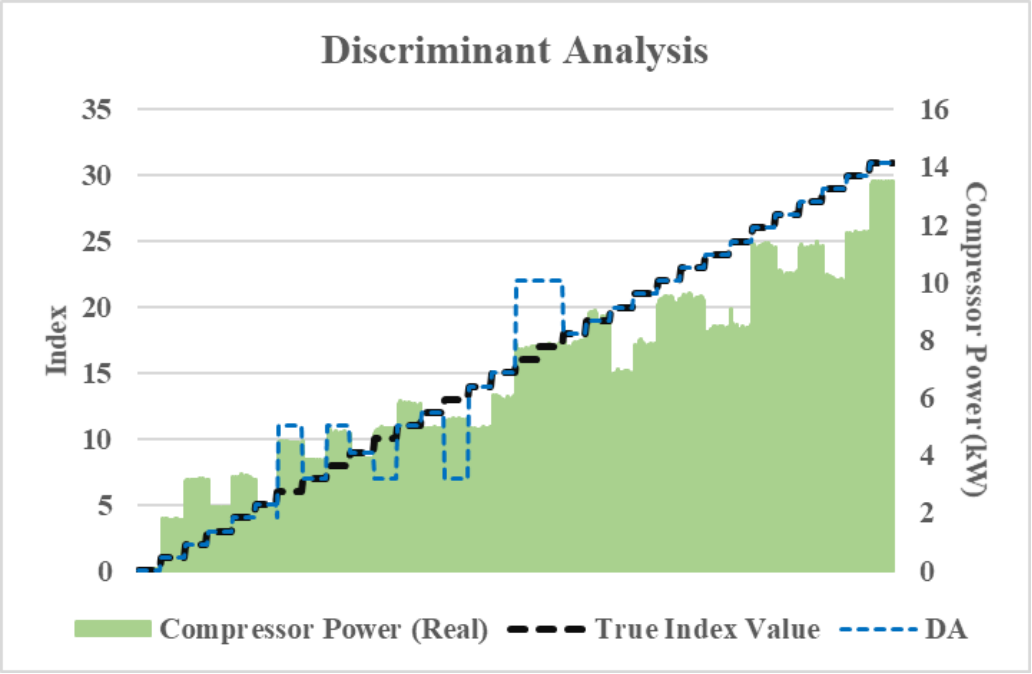

Figure 3.Indexes generated by DA model plotted against the true index value of the compressors.

From Fig. 3 we see that the accuracy of the compressor DA model is greater, where predicted indexes are accurate to within 89% of the true index values.

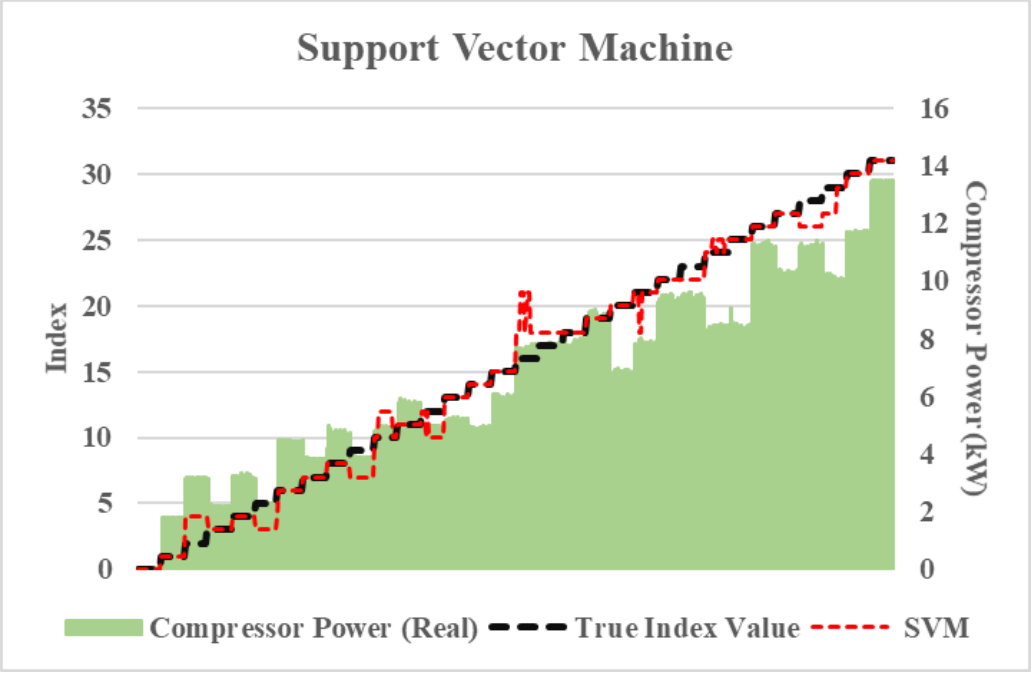

Figure 4. Indexes generated by SVM model plotted against the true index value of the compressors.

Fig. 4 has a few more rises and drops, therefore SVM higher error compared to DA, with an accuracy of 81%.

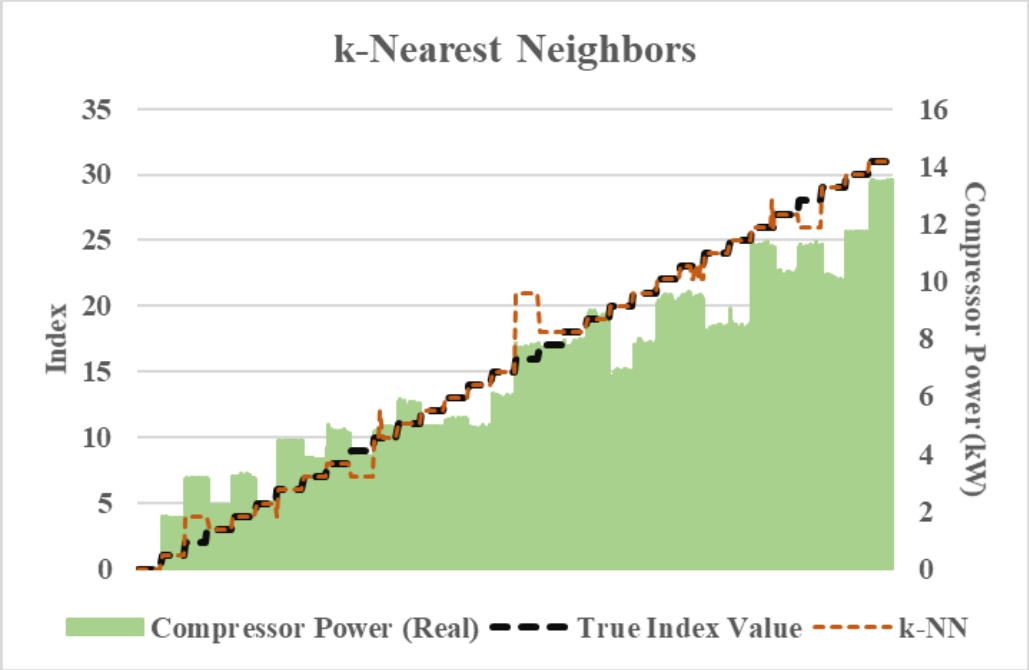

Figure 5. Indexes generated by k-NN model plotted against the true index value of the compressors.

Fig. 5 illustrates the accuracy of the compressor k-NN model to be significantly higher where predicted indexes are accurate to within 96% of the true index values.

In Fig. 2-5, the accuracy of indexes predicted by four different classifiers is compared against the true index values recorded at those times, for each of the possible 32 HVAC compressor combinations sequentially. From the results seen here, k-NN is seen to perform most accurately.

3.5.2 Combined Compressor and Air Handler Models

Classifiers for the combined compressor and air handler models are trained using input features such as: real and reactive powers in addition to phase currents using both compressor and air handler data. Once again, output portion of the training data are the corresponding index values. As in the previous section, the predicted index values for each of possible 32 combinations (starting from 0 to 31) is plotted, in comparison to the true recorded values of the indexes at those particular time instances.

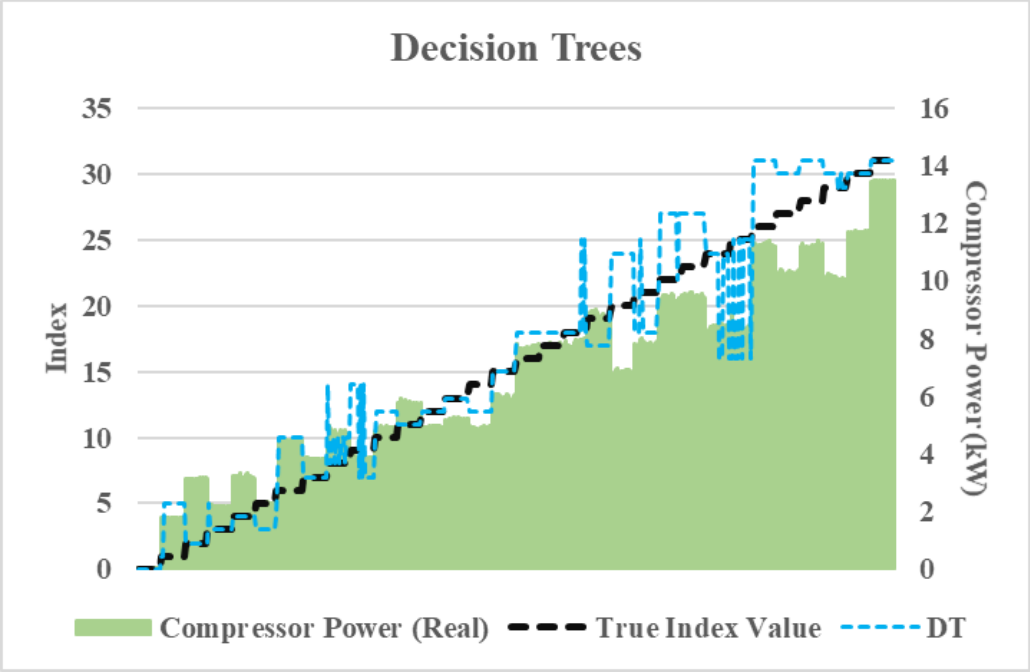

Figure 6. Indexes generated by Decision Trees model plotted against the true index value of the compressors.

From Fig. 6 we can observe there are still large deviations between the predicted and true index value line, with the combined DT model accurate to within 60% of the true index values.

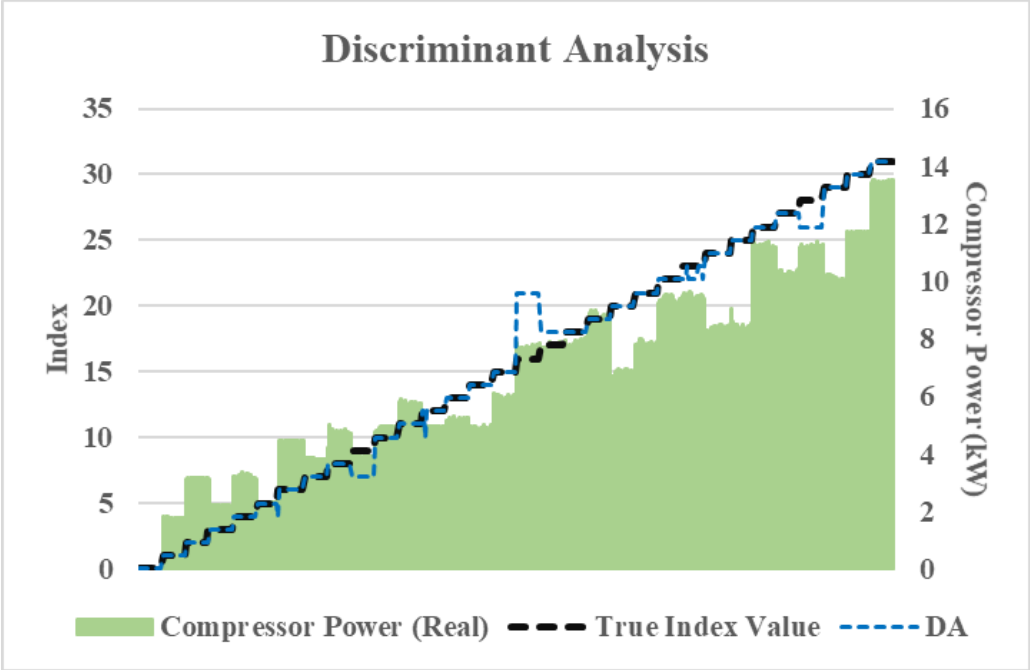

Figure 7. Indexes generated by DA model plotted against the true index value of the compressors.

In Fig. 7 we see that combined DA performs significantly better at predicting indexes and is accurate to within 96% of the true index values.

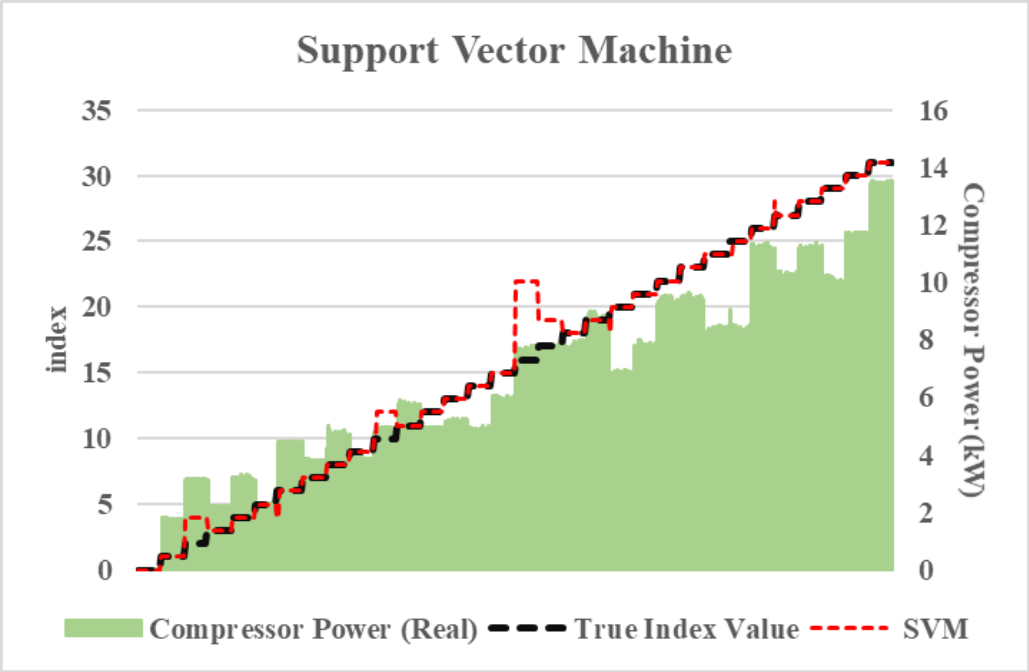

Figure 8. Indexes generated by SVM model plotted against the true index value of the compressors.

Fig. 8 illustrates how the combined SVM classifier has a few more variations from the true index value line, with a prediction accuracy of 90%.

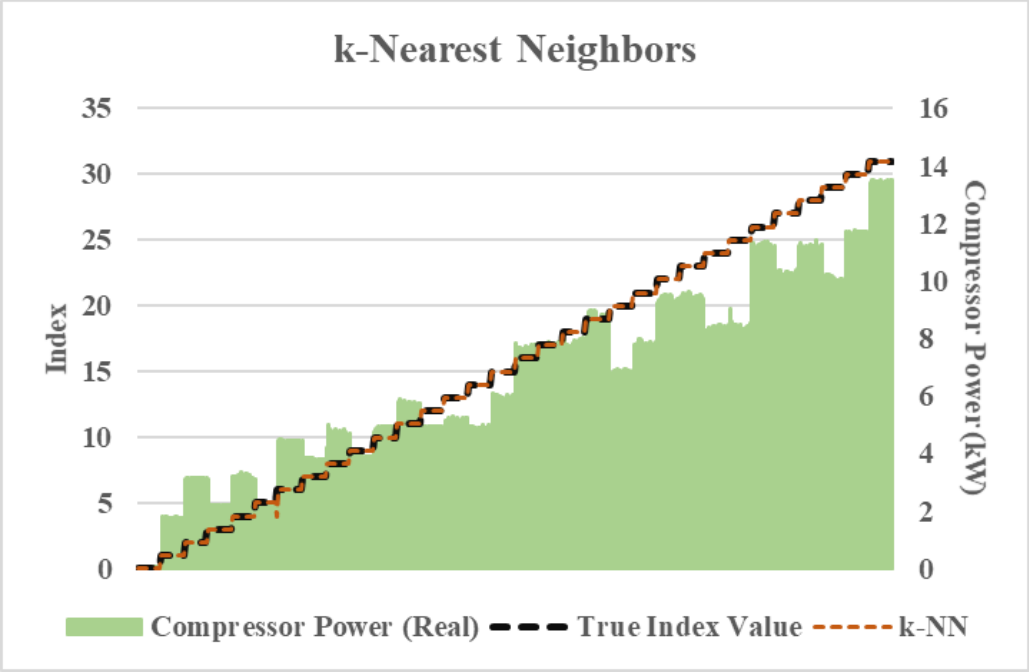

Figure 9. Indexes generated by k-NN model plotted against the true index value of the compressors.

Fig. 9 shows the combined k-NN model is the most accurate, where predicted indexes are accurate to within 99% of the true index values.

With the exception of the DT model, Fig. 6-9 illustrate improved accuracy for the classifier models at predicting the index values, in comparison to the compressor only models of section 3.5.1.

3.6 Case Studies

The most accurate k-NN model that uses both compressor and air handler data, was used to predict indexes and the corresponding power consumption of the five aggregated HVAC compressors for five different days during August 2017, when the average temperature was among the highest for the entire month. This test was carried out to see if the predicted indexes were consistent with the pattern of aggregated real power consumption for the compressors. The true value of the compressor indexes is not known in this case, however the goal is to see how accurately the model can predict power consumption using the indexes it predicts, given power and phase current data. The figures below show the predicted power consumption (red line) for five different days in comparison to the real recorded power data (blue line).

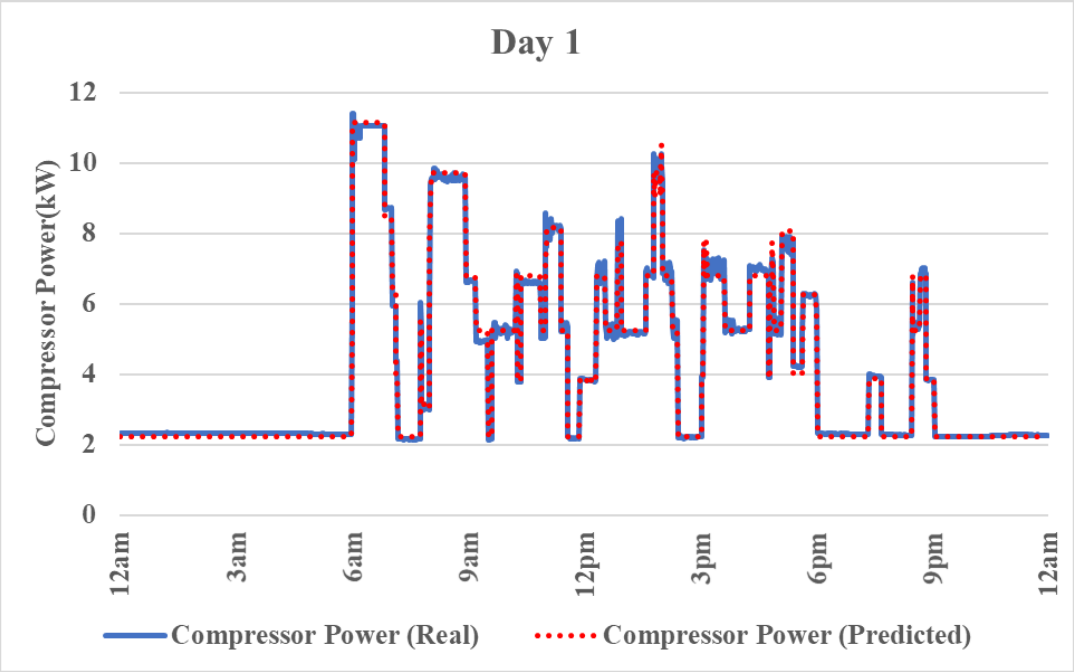

Figure 10. Comparison between real and predicted aggregated compressor power consumption for Day 1.

Fig. 10 illustrates the pattern of the predicted power consumption in comparison to real power consumption for Day 1, where the average RMSE over the 24-hour test period is 1.13kW out of a total maximum load of 11.40 kW.

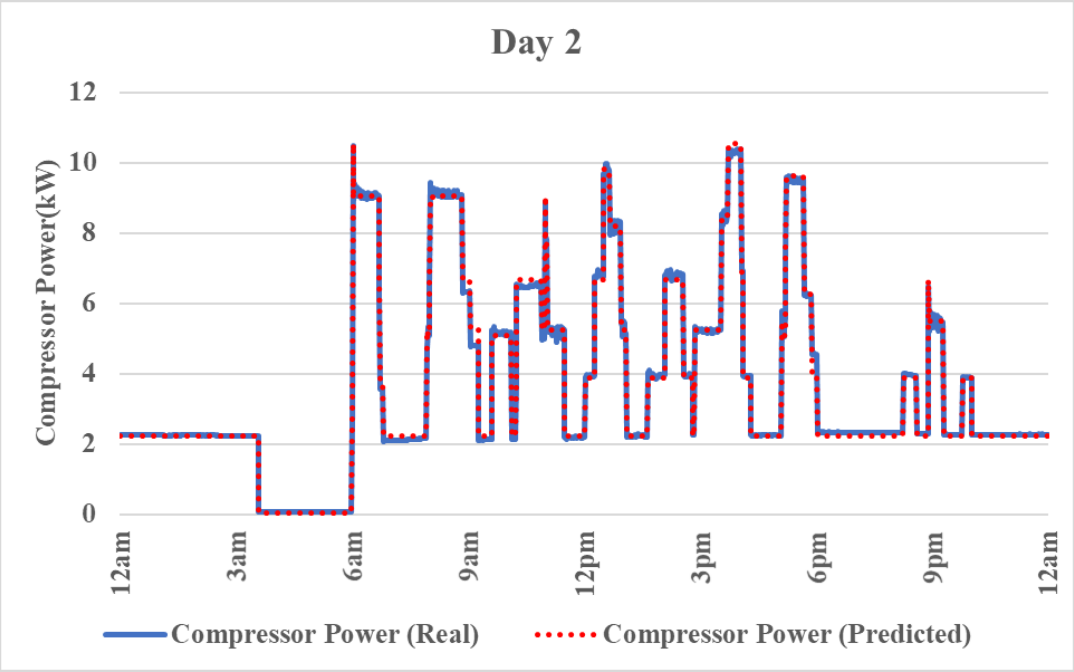

Figure 11. Comparison between real and predicted aggregated compressor power consumption for Day 2.

Fig. 11 compares the pattern of the predicted and real power consumption for Day 2, where the average RMSE over the 24-hour test period is 0.91kW out of a total maximum load of 10.48 kW.

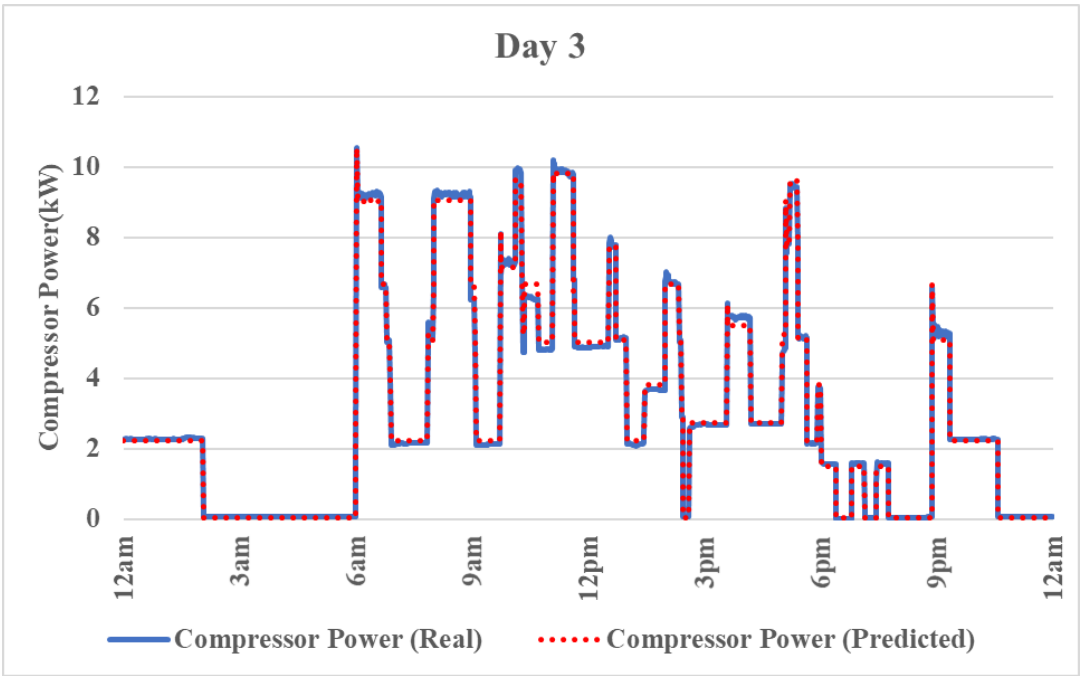

Figure 12. Comparison between real and predicted aggregated compressor power consumption for Day 3.

Fig.12 shows results for Day 3 of testing, where the average RMSE over 24 hours is 0.99 kW out of a total maximum load of 10.53kW

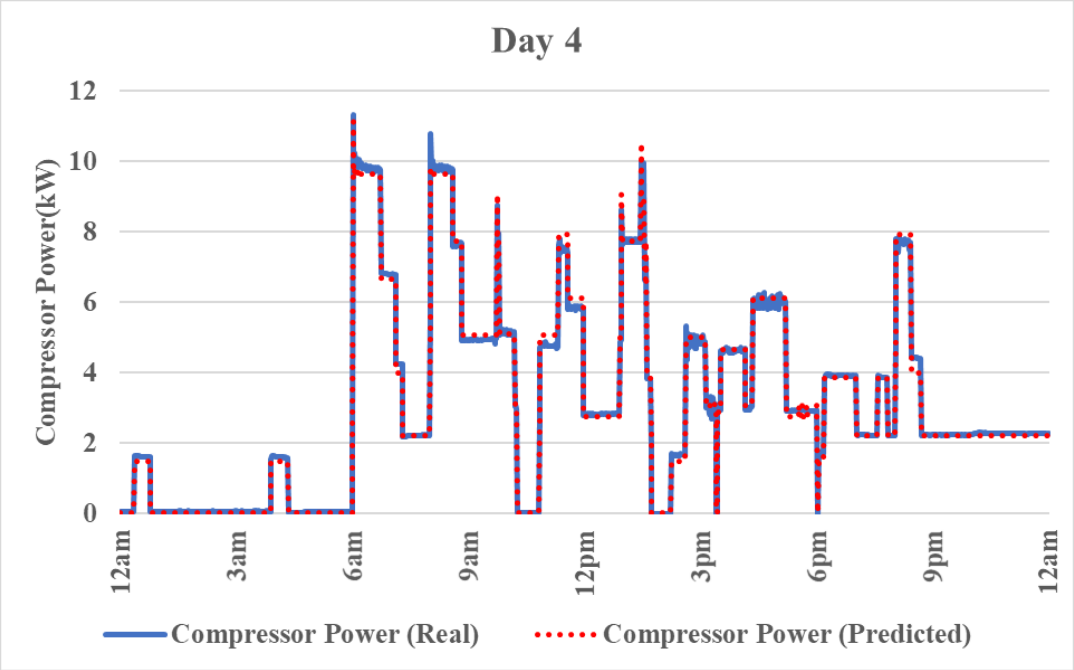

Figure 13. Comparison between real and predicted aggregated compressor power consumption for Day 4.

In Fig. 13 the average RMSE over the 24-hour period in Day 4 is 1.14kW out of a total maximum load of 11.44kW.

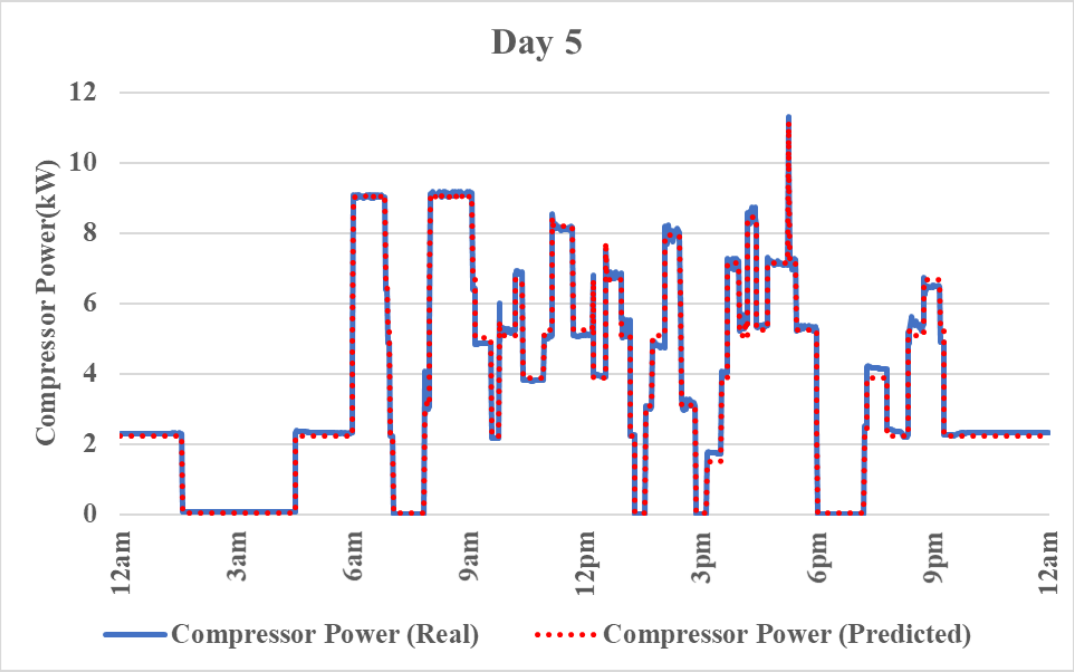

Figure 14. Comparison between real and predicted aggregated compressor power consumption for Day 5.

Fig. 14 illustrates the pattern of the predicted power consumption in comparison to real power consumption for Day 5, where the average RMSE over the 24-hour period is 1.06kW out of a total maximum load of 11.32kW.

Fig. 10-14 show the comparison of the real aggregated compressor power with the predicted power corresponding to the predicted indexes, over 5 different test days.

3.7 Results and Discussion

Using training data that had been collected over a period of several months, the performance of four different supervised classifiers was evaluated in a number of different case studies. First, the models were trained and then used to predict each of the possible 32 indexes representing each combination of five active HVAC compressors, consecutively during a 24-hour period in the month of June 2017. Figures were used to visualize the accuracy of predicted indexes in comparison to the recorded true index values at corresponding time instances. Among the tested classifiers in the case of both the compressor only, and combined compressor and air handler models, the Decision Trees classifier was least accurate, whereas the k-NN model was most accurate at correctly predicting index values. Table 2 summarizes the accuracy of each of the tested models when predicting each of the 32 possible index values consecutively.

Table 2. The accuracy of tested classifiers.

Model	DT	SVM	DA	k-NN
Compressor Model	60%	81%	89%	96%
Combined Model	60%	90%	96%	99%

In general, we observe that the combined compressor and air handler models have increased accuracy over the compressor only models, when predicting index values. A possible reason for inaccuracies in the combined models could be attributed to the fact that air handler units sometimes remain in operation for a few minutes even after the compressor has been switched off. With the exception of the k-NN classifiers, it was found that the models experience an accuracy of less than 50% when predicting the following index values- 9,16,17,23 and 28. This could be due to the limitations in performance of each of the classifiers as phase current values for index 9 and 7 are very close to each other, making it difficult for the classifiers to distinguish between them. Indexes 16 and 17, have phase current values almost identical to that of index 21, which are also comparable with corresponding values for indexes 18 and 22, resulting in prediction errors. Both the compressor and air handler data for index 23 and 22 are almost identical and comparable with that of index 27, again leading to errors in predicted index values. In the case of index 28, there are similarities in the compressor data with that of index 26, whereas similarities in the air handler data are found with index 31. These similarities with data associated with other index values, account for a significant portion of error.

Among all the classifier models that were tested, Decision Trees performed least accurately in both the compressor only and also combined models. Entropy and information gain are used to split different output classes based on the input features, however in the case of power disaggregation of combined HVAC compressors, many features are shared among individual devices. Therefore, Decision Trees are unable to efficiently split the input features, which results in a large number of prediction errors. The score-based method that is employed by Discriminant Analysis, results in greater accuracy than Decision Trees and has the second highest accuracy at predicting indexes in the case of the combined models. Considering both sets of models, the hyperplane-based SVM classifier performs more consistently, but still has some errors as using hyperplanes to distinguish between closely associated data points is challenging. The k-NN classifiers have been found to perform most accurately, with accuracies of 96% and 99% when predicting indexes for the compressor and combined models respectively. The fact that this algorithm considers the output values of closely associated data points, means that this method can distinguish between data points having to some degree similar input features.

As the k-NN classifier model trained using compressor and air handler data has the greatest accuracy when predicting each of the 32 compressor indexes, this k-NN model is then used to predict the indexes and corresponding power consumption of the aggregated compressor load in

five separate 24-hour long test cases. The results in the form of average RMSE, for each of the five test cases is summarized in Table 3.

Table 3. RMSE of predecited power consumption.

Test Case	Average RMSE (kW)	Total Maximum Load (kW)
Day 1	1.13	11.40
Day 2	0.91	10.48
Day 3	0.99	10.53
Day 4	1.14	11.44
Day 5	1.06	11.32

For each of the test cases Day 1- Day 5, the average RMSE over the 24-hour test period is 9.6%, 8.6%, 9.4%, 9.9% and 9.3% of the total maximum load respectively. Thus, a claim can be made that the combined k-NN classifier model is not only predicting the correct index at any given time, but also predicting the corresponding power consumption of the aggregated compressors, further validating the results.

4. Double-Auction Demand Response of HVAC and Lighting Loads Using Machine Learning and User Preferences

4.1 Introduction

In recent decades due to increasing electricity demand, there is an increased likelihood of electrical power systems experiencing stress conditions, due to increased load during critical peak hours. These conditions can result in. a limited supply and cascading failures throughout the grid that could lead to wide area outages. Demand Response (DR) is a method involving the curtailment of loads during critical peak load hours, that restores the balance between demand and supply of electricity as well as increasing the efficiency of operation for the electric utility, in addition to reducing the peak load and demand charge for customers during these times.

Significant changes in the electric power industry will be brought about by the implementation of DR programs such as dynamic pricing schemes as well as building energy management (BEM) systems. A fully automated DR program is achievable when implemented using a BEM system, as the system is capable of monitoring different types of loads and controlling their operations based on user preferences. Many DR programs have been developed that control different types of loads, however the work presented here focuses on developing a double-auction based DR program that controls single floor HVAC and lighting loads, based on user preferences, in commercial buildings. This is a problem that has not yet been fully addressed.

4.2 Methodology

In the following sections, different components of the DR algorithm are described in detail, in addition to the results from various case studies. The main contributions in this work are as follows.

1. A double-auction DR algorithm that controls HVAC and lighting loads in commercial buildings, that takes into consideration the user's preferences and load priorities which results in the maximum possible peak reduction and energy savings for the user.
2. A novel customer bid price equation, that considers the impact of HVAC and lighting loads.
3. A load scheduling technique based on machine learning that considers user preferences and load priorities.

The auctioning process is referred to as a double-auction as both the customer and utility submit their bid prices and asking prices, after which the cleared price is calculated in the DR server. The devices being controlled are distributed throughout a single floor of a commercial building, and are controlled using the DR algorithm that would be implemented in a BEM system.

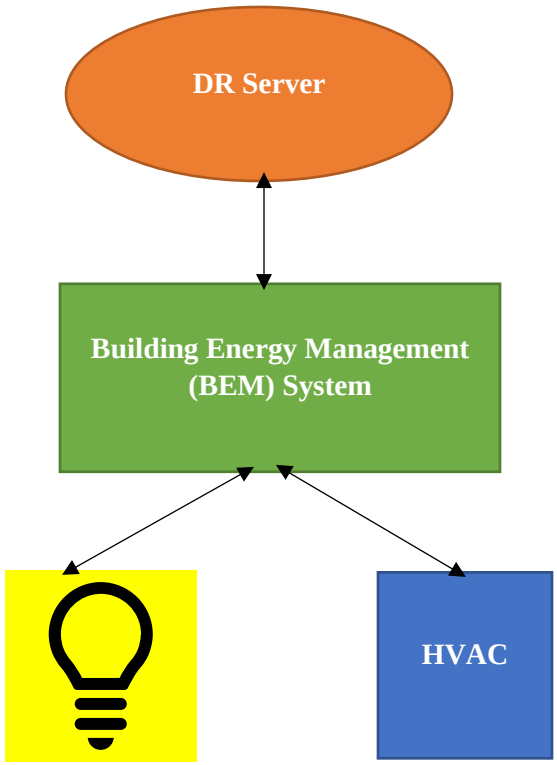

Figure 15. Flow chart of entities involved in DR.

As summarized in Fig. 15 based on the cleared price of the double-auction between the user and the DR server, using the allocated demand limit from the DR server, user preferences and load priorities set in the BEM system, the DR algorithm determines an optimal load configuration and monitors device status at each time step, updating the load configuration when possible. Using this technique, it is possible to reduce peak load while maintaining user comfort levels to a high degree, during a DR event.

4.3 The Demand Response (DR) Algorithm

A DR event can be defined as a period of time during which the total load of a customer must be kept under a certain specified demand limit. In this study, customers taking part in the DR event are informed beforehand of the demand limit (kW) and duration (hours) through a BEM. In this work, the objective is to operate as many HVACs as needed, keep lighting within certain brightness levels, both to maintain the desired user comfort level, while staying below the allocated demand limit. It is assumed that plug loads are kept constant and their power consumption cannot be changed.

For ‘n’ number of HVAC units, this can be formulated as the following maximization problem:

$$\text{Maximize P} = \sum_{k=1}^{n} P_{\text{Hk}} + P_{\text{L}} + P_{\text{p}} \tag{11}$$

Subject to,

$$P \leq D$$

$$P_{\text{H}}, P_{\text{L}}, P_{\text{p}} \geq 0$$

$$P_{\text{p}}\ is\ a\ constant$$

Here given in kW,

P = Total power consumption

P_{H} = Power consumption of n HVAC units

P_{L} = Total power consumption of lighting load

P_{p} = Total power consumption of plug loads

D = Demand Limit

The schematic below gives a brief overview of the DR algorithm that has been developed.

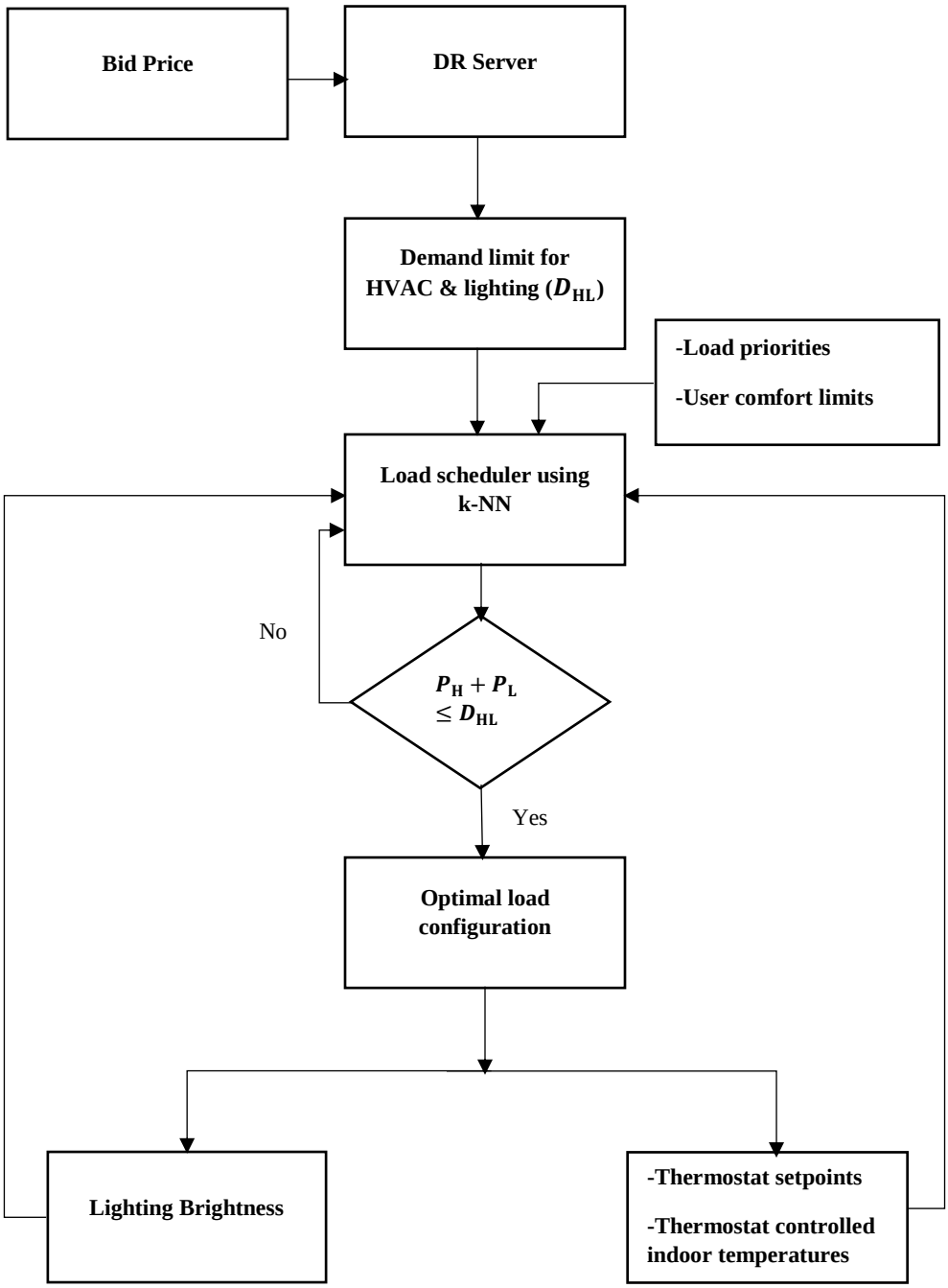

Figure 16. Flow chart of overall DR algorithm.

At each time step, based on the allocated demand limit from the cleared bid price, the load scheduler calculates all possible load configurations. Then based on load priorities and user comfort limits, the optimal load configuration is found. The power consumption of this optimal load configuration is compared with the demand limit for HVAC and lighting load $\boldsymbol{D_{HL}}$, which if satisfied, is the configuration taken by the HVACs and the lighting load. Or else the process is repeated to find the next best configuration, until a suitable load configuration is found. Once the loads are set to a particular configuration, they feed back their current status and surrounding indoor temperature information at each time step back to the load scheduler, so that when a change occurs, the load configuration is once again updated.

In the following sub-sections, a number of the important components of the DR algorithm are explained.

4.3.1 Double-Auction and Bid Price Calculation

A double-auction market is based on the concept of a two-way market, where both the buyer and the seller submit bids consisting of price and quantity, simultaneously into a single energy market. In this work, the seller is the electric utility whereas the buyer is the customer (user) occupying a single floor of a commercial building with their dedicated energy meter. In order for a user to participate in a transactive market, it must be able to do the following:

1. Determine a bid price based on the current state of controllable loads and historical electricity prices.

2. Adjust its load configuration according to the cleared price and allocated demand limit.

The DR server, clears the price and quantity of electricity that is traded by matching the customer bid with the closest asking bid from the seller. Once the auction is resolved, the cleared price and demand limit (kW) in addition to the duration of the DR event are conveyed back to the customer from the DR server to the customer's BEM system. This highly scalable approach enables both the buyer and seller to participate in determining the price and quantity of traded electricity between them. In addition to price signals, the prices at which electricity was traded at hourly intervals for the previous 24-hours is sent to the customers, as this data is taken into consideration when the customer bid price is generated.

At a set time before the DR event, the BEM of the customer will generate a bid price using a number of parameters given in the following formula:

$$P_{bid} = P_{avg} + \sum_{k=1}^{n} \frac{(Tk_{cur} - Tk_{des)} * (Sk_H - Sk_{L)} * P_{dev}}{(Tk_{max} - Tk_{min)}} + (L_B * P_{dev}) + G \qquad (12)$$

Where,

Tk_{cur} = The current indoor air temperature (°F) of area controlled by k^{th} thermostat

Tk_{des} = The desired temperature setpoint (°F) of k^{th} thermostat

Tk_{min} = Minimum acceptable indoor temperature (°F) of area controlled by k^{th} thermostat

Tk_{max} = Maximum acceptable indoor temperature (°F) of area controlled by k^{th} thermostat

Sk_H = Standard deviations between Tk_{des} and Tk_{max} of k^{th} thermostat

Sk_L = Standard deviations between Tk_{des} and Tk_{min} of k^{th} thermostat

L_B = Desired lighting brightness

G = Pricing gain

P_{dev}= Standard deviation of price in 24-hour window

P_{avg} = Average price in 24-hour window ($/kWh)

P_{bid} = Bid price of the customer sent to the DR server ($/kWh)

Among the quantities stated in equation (12), the gain value G will be a value that is user-defined, and L_B is fraction of lighting brightness with a value that varies between 0 to 1. This formula generates the bid price such that if $Tk_{cur} > Tk_{des}$ a bid price that is higher than P_{avg} is generated, and vice versa. This is achieved by calculating bid prices based on the standard deviations of electricity prices from the mean taken over a previous 24-hour window. The use of standard deviations makes this formula adaptable for different regions, and price schemes. In this work, equation (12) is used to generate bid prices when the thermostats are in cooling mode, as the assumption is that the heating system is gas based and not electric.

4.3.2 Load Scheduler

The load scheduler receives the demand limit for HVAC and lighting loads from the BEM, and based on this calculates all possible load configurations using this demand limit. This is achieved using a k-NN classification algorithm, that matches the demand limit for HVAC to indexes that represent different combinations of active HVAC units, while reserving a quantity of power corresponding to the minimum level of acceptable lighting brightness. Once all the configurations are known, the load scheduler uses the pre-defined load priorities and user comfort limits to determine the optimal load configuration. Once the configuration of HVACs is determined, if there is unused power left over from the demand limit, the level of brightness for lighting is increased to a point that ensures the maximum possible user comfort is being maintained. An example of the k-NN training data used to find load configurations for 5 HVAC units is given in Table 4.

Table 4. Power consumption of HVACs and their corresponding indexes.

Power (kW)	Index	Active Compressor(s)
0.04	0	All Are Off
1.8	1	1
3.12	2	2
2.55	3	3
3.58	4	4
3.66	5	5
5.44	6	1,2
4.66	7	1,3
5.82	8	1,4
4.35	9	1,5
4.52	10	2,3
6.93	11	2,4
5.96	12	2,5
5.91	13	3,4
4.66	14	3,5
6.31	15	4,5
10.48	16	1,2,3
9.11	17	1,3,4
7.75	18	1,4,5
9.04	19	1,2,4
7.19	20	1,3,5
8.13	21	1,2,5
10.18	22	2,3,4
10.14	23	2,4,5
8.9	24	2,3,5
9.26	25	3,4,5
12.47	26	1,2,3,4
11.51	27	1,3,4,5
11.97	28	1,2,4,5
10.94	29	1,2,3,5
12.26	30	2,3,4,5
16.19	31	1,2,3,4,5

4.3.3 Load Priorities

In this work, the user defines different load priorities to individual HVAC units. This ensures that the desired indoor temperatures are best maintained for areas given the highest priorities. However, the algorithm is designed in such a way that, if the indoor temperature in a particular area increases beyond the user comfort limit, the thermostat controlling this area will take the highest priority. If multiple thermostats violate the user comfort limits, the HVACs will activate

based on the priorities previously set among the individual thermostats. An example of how load priorities change when the user comfort limit is violated if indoor temperature rises above 72°F, for three different thermostats: T1, T2 and T3 in three different time steps: t_1, t_2 and t_3, is shown in Table 5.

Table 5. Example of load priority allocation.

t_1			
Thermostat	**Setpoint (°F)**	**Indoor Temperature (°F)**	**Priority**
T1	70	72	1
T2	70	72	2
T3	70	72	3
t_2			
Thermostat	**Setpoint (°F)**	**Indoor Temperature (°F)**	**Priority**
T1	70	72	2
T2	70	72	3
T3	70	73	1
t_3			
Thermostat	**Setpoint (°F)**	**Indoor Temperature (°F)**	**Priority**
T1	70	72	3
T2	70	73	1
T3	70	73	2

In the first time-step **t_1**, the three thermostats - T1, T2 and T3 are assigned priorities of 1, 2 and 3 respectively based on user preferences, with 1 being the highest priority. In the second time-step **t_2**, the indoor temperature of the area controlled by T3 rises above the user comfort limit and hence takes the highest priority, whereas T1 takes the next highest priority of 2 and T2 takes the lowest priority of 3. In the third time-step **t_3**, the comfort limit for the area controlled by T2 is violated, and therefore T2 takes the highest priority of 1, as it initially had a higher user set priority than T3. This results in T3 now having the second highest priority, and T1 the least priority as the indoor temperature of the area it controls is still within the comfort limits.

4.4 Case Studies

The developed DR algorithm was tested using real data collected from BEMOSS™ platform, that has been deployed in a commercial building in Alexandria, Virginia. This is in addition to testing using simulated data, to represent a number of different scenarios. For each case study that has been carried out, the DR event takes place between 1pm-4pm, with bid prices being generated by the customer 30 minutes before the DR event takes place. Following which the double auction between the customer and the DR server takes place, and a clearing price as well

as the demand limit for the customer is determined. In each case, equation (12) using setpoint and indoor temperature data, user preferences, and price data for the previous 24 hours leading up to the DR event, were used to generate bid prices for electricity. An example of the price data for a 24-hour period prior to a DR event, retrieved from an online database is given in Table 6.

Table 6. Example of electricity prices over a 24-hour period.

Time	**Price($/kWh)**
13:00	0.036
14:00	0.052
15:00	0.049
16:00	0.026
17:00	0.024
18:00	0.023
19:00	0.020
20:00	0.020
21:00	0.019
22:00	0.019
23:00	0.017
0:00	0.017
1:00	0.018
2:00	0.018
3:00	0.019
4:00	0.020
5:00	0.024
6:00	0.025
7:00	0.026
8:00	0.037
9:00	0.030
10:00	0.042
11:00	0.020
12:00	0.038

During the double-auction, the users bid price for electricity is submitted to the DR server, where it is matched with the closest asking price and corresponding demand limit that has been submitted by the electric utility. For each of the case studies, to represent the participation of the electric utility in the double-auction, the following price and corresponding demand limit structure has been used.

Table 7. Pricing and corresponding demand limit.

Price ($/kWh)	Demand Limit (kW)
0.000	0
0.020	5
0.040	10
0.060	15
0.080	20
0.100	25
0.120	30
0.140	35
0.160	40
0.180	45
0.200	50

The lighting load considered in the case studies is assumed to be dimmable, and during the DR event, the brightness of lighting within user comfort limits is adjusted based on the power consumption of HVAC loads and available demand limit. The power consumption of, lighting load for different brightness levels was obtained from a previously conducted lab experiment, where the brightness of a lighting load is varied and its corresponding power consumption is recorded. The results of this experiment are given in the Table 8.

Table 8. Effect of brightness on lighting load power consumption.

Brightness of Lighting Load	% Power Consumption
100	100
95	100
90	100
85	100
80	100
75	94.64
70	90.14
65	82.58
60	77.99
55	70.43
50	65.83
45	58.28
40	53.01
35	48.42
30	43.92
25	38.66
20	34.07
15	24.21

10	12.15
5	9.09
0	0.00

In the case studies, during DR the lighting brightness level is maintained between a minimum of 50% and maximum of 75%. The power consumption (kW) of lighting load for different brightness levels is given in the Table 9.

Table 9. Brightness and corresponding lighting load power consumption

Brightness %	**Power (kW)**
75	2.37
70	2.23
65	2.06
60	1.95
55	1.76
50	1.63

For each of the test cases, the values of the following parameters from equation (12) are set as follows:

$Tk_{max} = Tk_{des} + 2$

$Tk_{min} = Tk_{des} - 1$

$L_B = 75/100$

$$G = \frac{\text{Total number of HVAC loads}}{1000}$$

During the DR event, thermal behavior of the areas controlled by thermostats are simulated using a statistical building model, based on historical data collected over a period of two years- during 2016 and 2017. The BEM system records HVAC and lighting data at one-minute intervals.

4.4.1 Case Studies Using Real Data

Four different test cases during days with some of the highest average outdoor temperatures in July 2018 were carried out, in which the actual data recorded by BEMOSS™, in addition to user

inputs, was used to generate bid prices for electricity prior to the DR event on that day. In each case, the controllable loads were five HVACs and the brightness levels of the total lighting load on a single floor of the building. Load priorities for HVACs, controlled by their thermostats, (T1-T5) are given in the following order- T1>T2>T3>T4>T5. An amount of 2kW- the maximum power consumption of the total plug load, is subtracted from the allocated demand limit in each case, as the operation of these loads do not change during a DR event. The DR algorithm based on the received demand limit, begins to control loads 15 minutes before the DR event, to ensure the total load is below the demand limit when the DR event starts.

Case 1

In this test case, prior to the DR event when the user bid price is generated, all five HVAC units are in operation, as each of the thermostats (T1-T5) recorded an indoor temperature greater than the set point, which was set to 70°F.

Table 10. Indoor temperatures, electricity prices and demand limit for case1.

T1 (°F)	T2 (°F)	T3 (°F)	T4 (°F)	T5 (°F)	Bid Price ($/kWh)	Cleared Price ($/kWh)	Demand Limit (kW)
74	72	71	71	73	0.066	0.060	15

Based on the results of the double-auction, the total demand limit is 15kW, of which 2kW is for plug loads, a minimum of 1.63kW is for lighting at 50% brightness, which can go up to a maximum of 2.37kW for 75% brightness therefore leaving 11.37kW for HVAC loads.

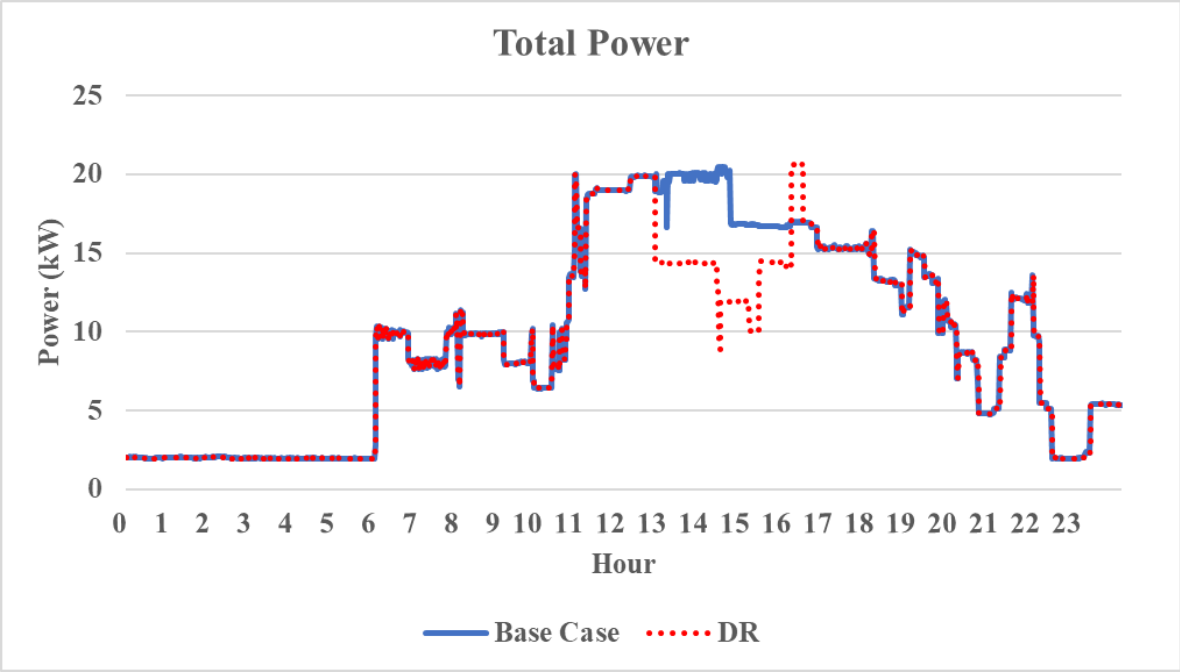

Figure 17. Comparison of 24-hour total power consumption for case 1.

From Fig. 17 we see that during the DR event between 1pm-4pm, the red line representing power consumption using the DR algorithm stays within the 15kW demand limit. In comparison, the blue line representing the base case, rises to a maximum power consumption of 20.49kW during this time. During the DR event, the total energy consumption using DR is 40.12kWh compared to 55.23kWh for the base case. Therefore, the total energy saving using the DR algorithm is 15.15 kWh (27.44%).

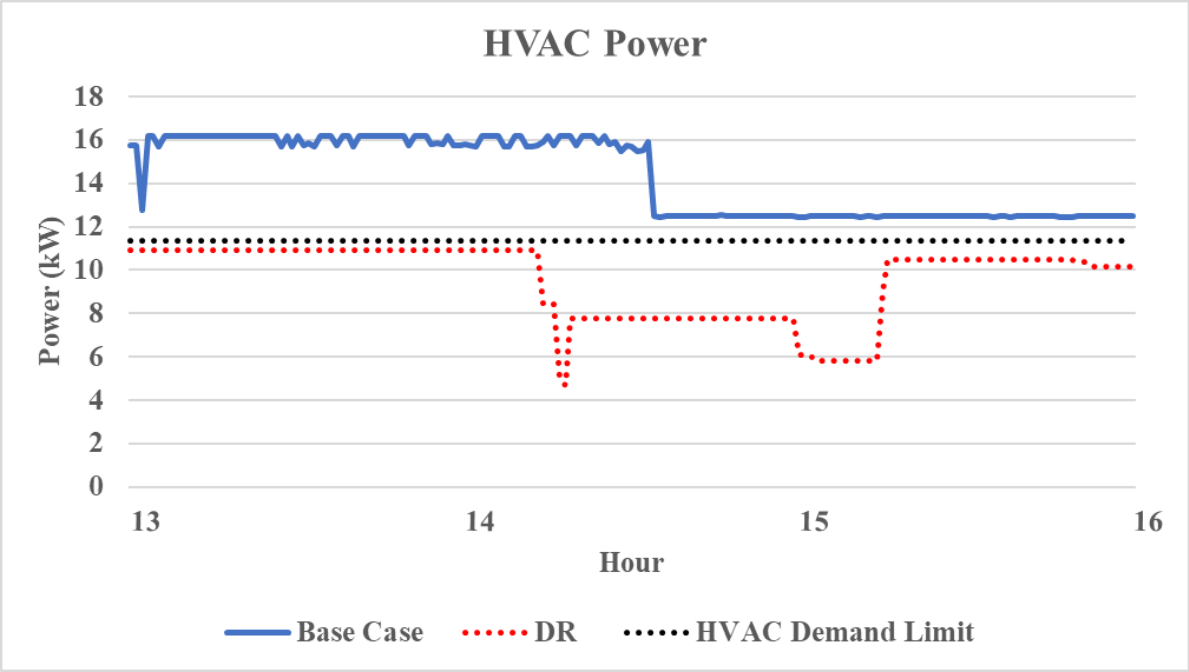

Figure 18. Comparison of HVAC power consumption for case 1.

Fig. 18 shows the red DR line stays within the DR limit of 11.37kW for HVAC loads. whereas without DR, the power consumption never falls below 12.46 kW. During the DR event, the HVAC energy consumption using DR is 28.81kWh compared to 43.12kWh for the base case. The total HVAC energy saving from using the DR algorithm is 14.31kWh (33.20%).

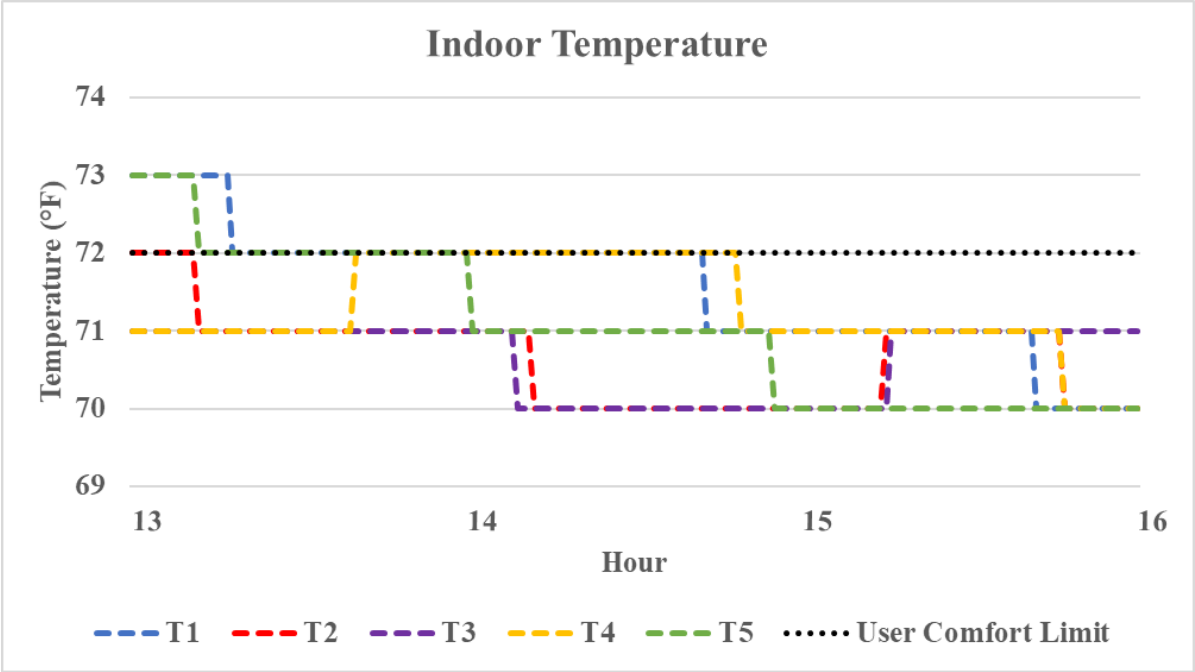

Figure 19. Variation of indoor temperatures during case 1.

The indoor temperature readings from Fig. 19 show that only 2 thermostats- T1 and T5 initially have a higher temperature than the user comfort limit due to higher initial indoor temperatures at the start of the DR event, however once brought within the comfort level, they both manage to reach the set point temperature of 70°F, and later stay within the comfort limit. The indoor temperatures of T1and T5 violate the user comfort limit no more than 10% and 6.77% of the DR event duration respectively.

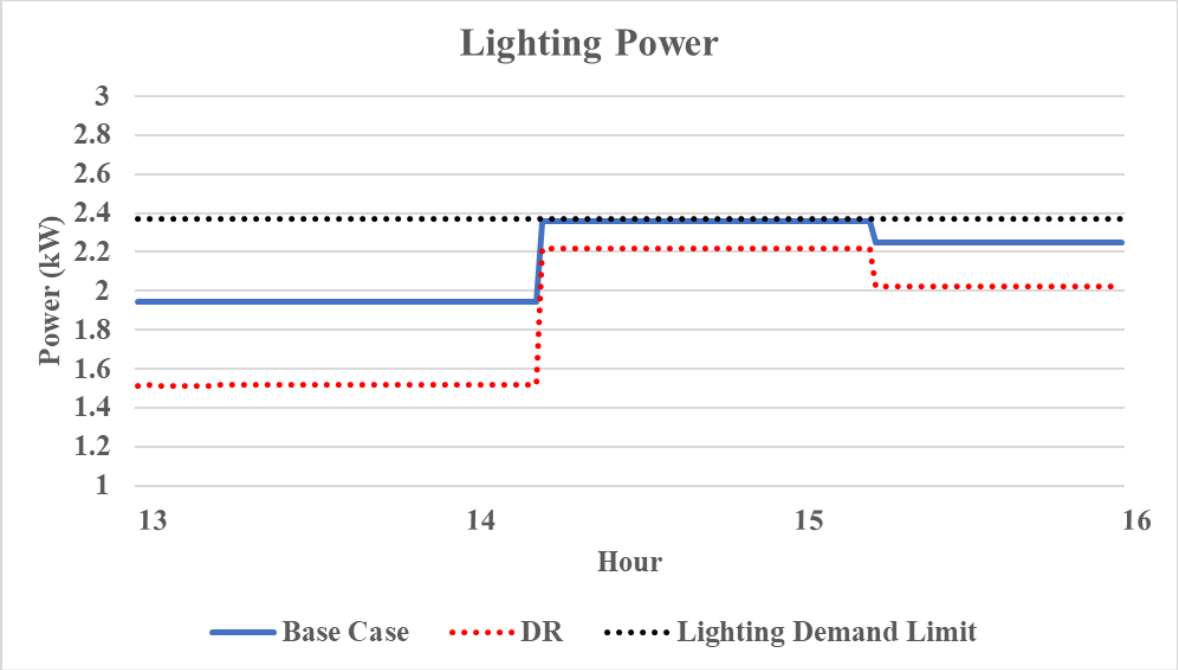

Figure 20. Comparison of lighting power consumption for case 1.

From Fig. 20 we observe the maximum Demand limit for lighting loads of 2.37kW is never reached, as not all the lighting loads are turned on. During the DR event, the lighting energy consumption using DR is 5.64kWh compared to 6.48kWh for the base case. The total lighting energy saving from using the DR algorithm is 0.84kWh (12.96%).

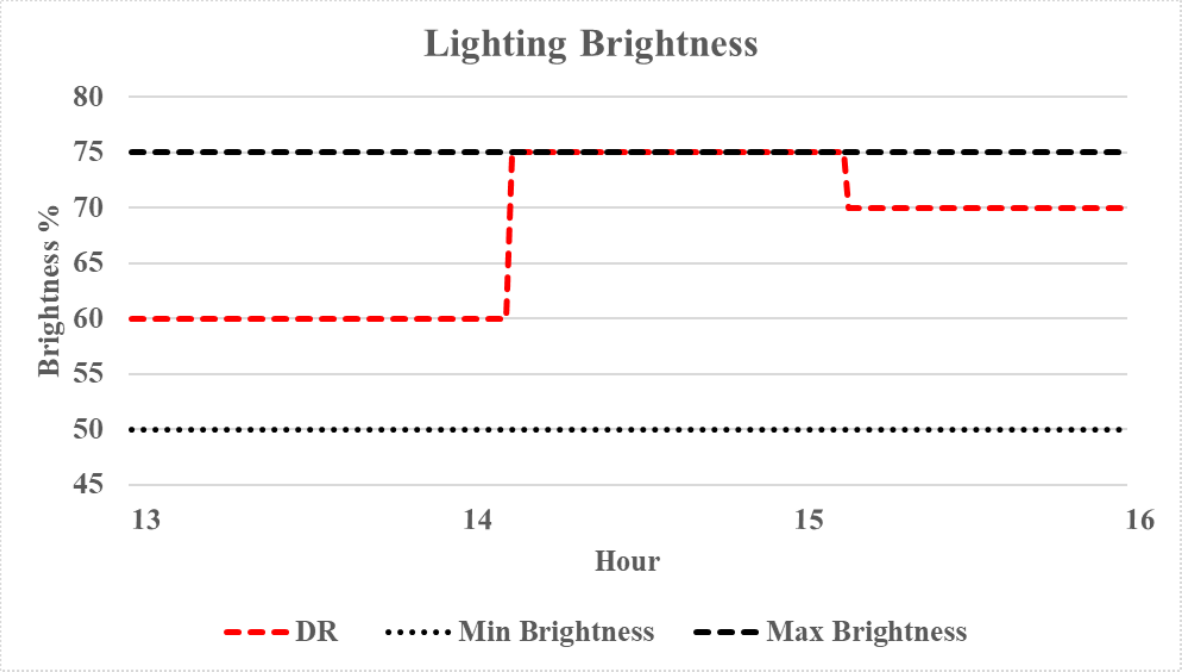

Figure 21. Variation of lighting brightness during case 1.

Fig. 21 shows us that the lighting brightness using the DR algorithm is always kept within the user comfort limits and always above the minimum comfort level, at times reaching the maximum permitted brightness of 75% during the DR event. Initially the brightness is set at 60%, since at the beginning of the DR event, four HVACs are active and there is not enough power left over within the demand limit for a higher brightness level. Once the HVAC controlled by T3 becomes inactive, the brightness is increased to 75%. At this time, HVACs controlled by T1, T2 and T5 are active, and there is a sufficient amount of power left in the demand limit to do so. Later in the DR event, brightness decreases to 70%, when HVACs controlled by T1, T2 and T4 are active, and there is not enough power left over to maintain 75% brightness.

Case 2

In this case, four of the five HVACs (T1-T3 and T5) are active, with indoor temperatures above the 70°F setpoint, when the user bid price is generated.

Table 11. Indoor temperatures, electricity prices and demand limit for case 2.

T1 (°F)	T2 (°F)	T3 (°F)	T4 (°F)	T5 (°F)	Bid Price ($/kWh)	Cleared Price ($/kWh)	Demand Limit (kW)
72	73	71	70	72	0.059	0.060	15

Table 11 shows that after the bid price is cleared at the DR server, the total demand limit is 15kW, of which 2kW is for plug loads, and once again a minimum of 1.63kW is for lighting loads, therefore leaving 11.37kW for HVAC loads.

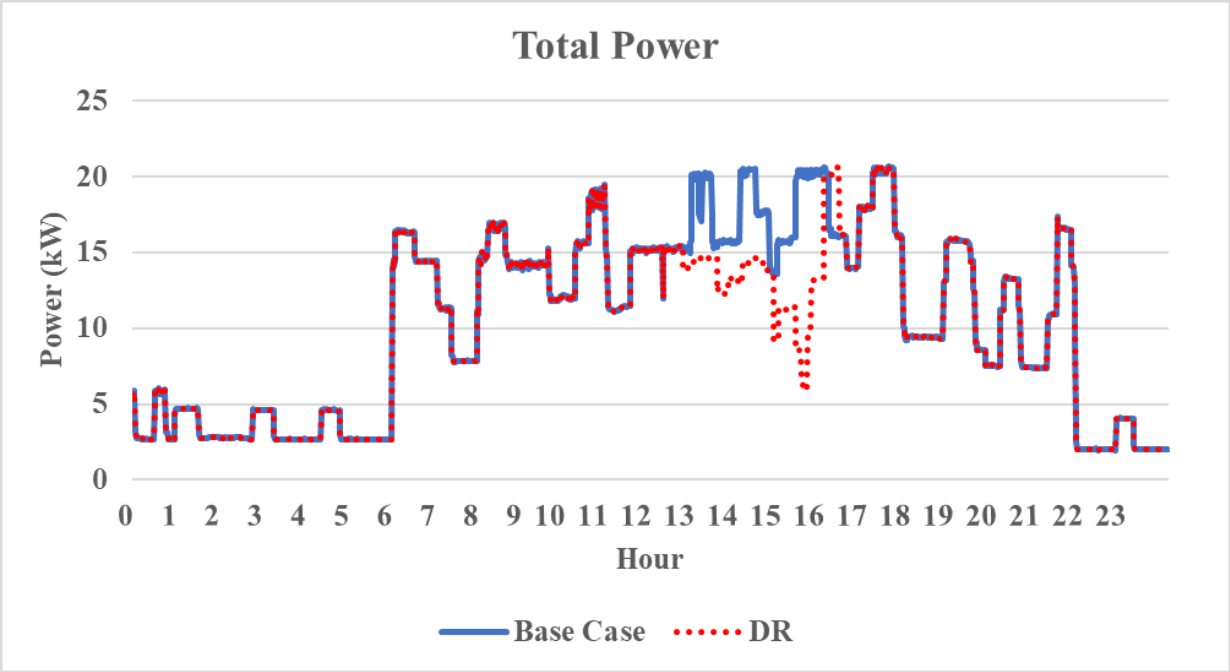

Figure 22. Comparison of 24-hour total power consumption for case 2.

Fig. 22 shows the red DR line stays within the 15kW demand limit, during the entire DR event between 1pm-4pm. However, during this time the blue base case line reaches a maximum power consumption of 20.53kW. During the DR event, the total energy consumption using DR is 37.67kWh compared to 53.60kWh for the base case. The total energy saving throughout the DR event is 15.93kWh (29.71%).

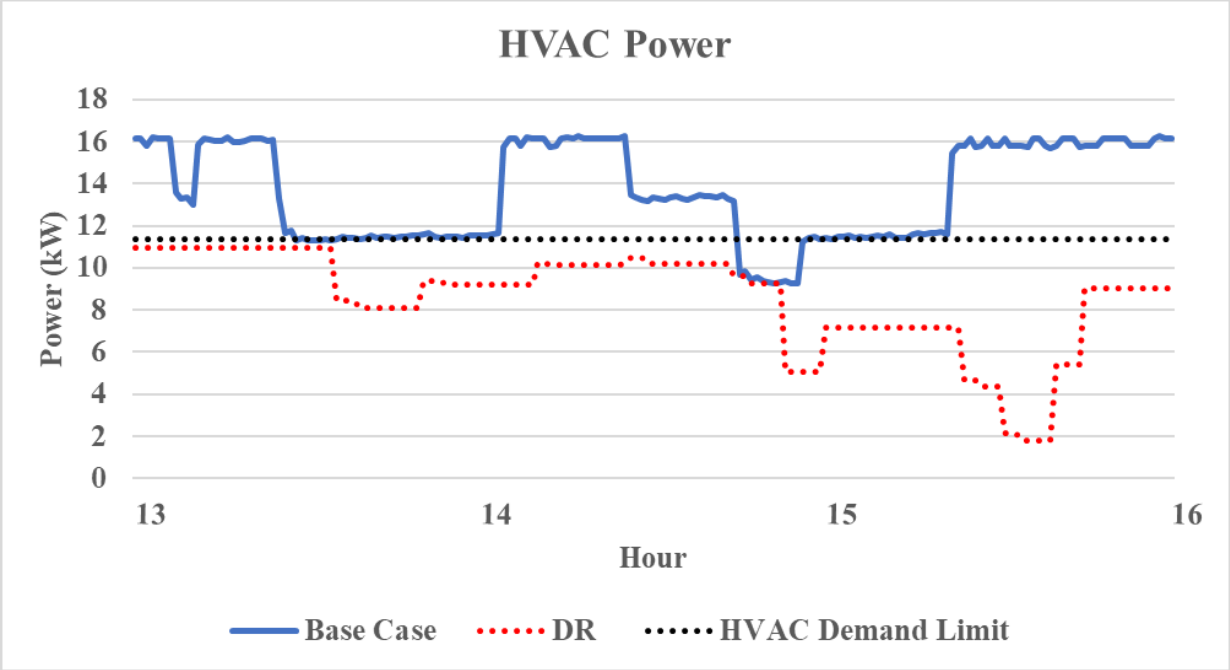

Figure 23. Comparison of HVAC power consumption for case 2.

In Fig. 23 we see the red DR line stays within the DR limit of 11.37kW for HVAC loads, whereas the base case line reaches a maximum load of 16.28kW. During the DR event, the HVAC energy consumption using DR is 25.84kWh compared to 41.21kWh for the base case. Using the DR algorithm, 15.38kWh (37.31%) of HVAC energy is saved.

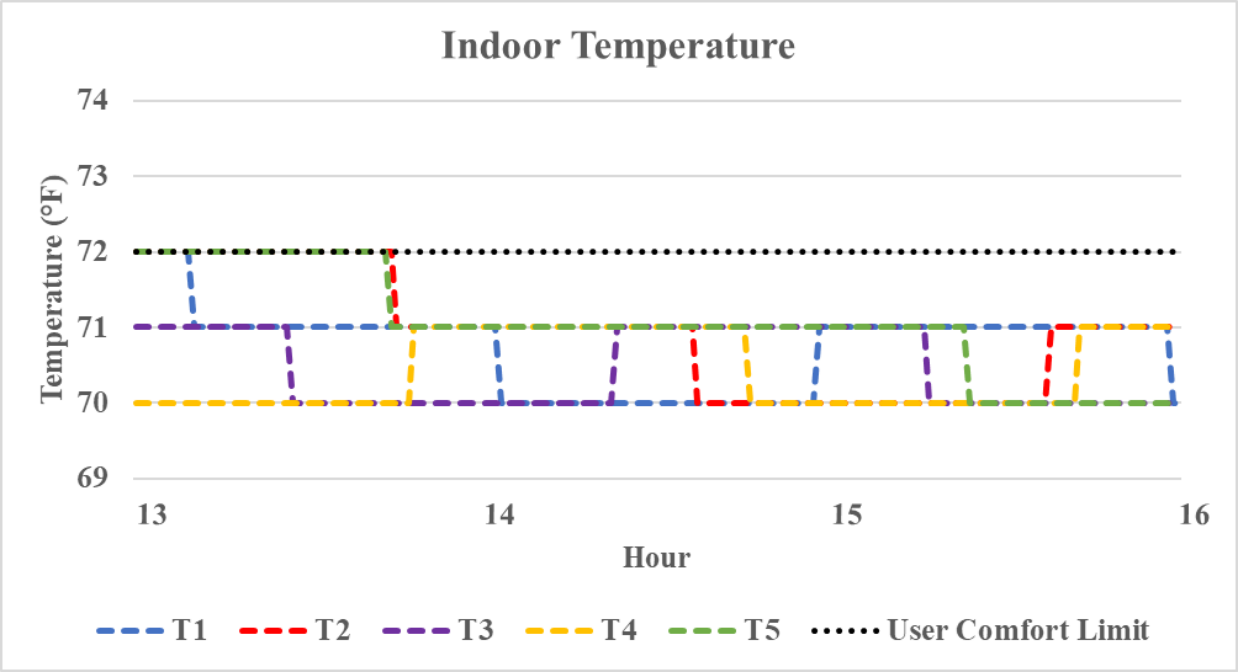

Figure 24. Variation of indoor temperatures during case 2.

Fig. 24 illustrates the fact that using the DR algorithm, all thermostats reach the cool setpoint of 70°F, and the indoor temperature for each remains within the user comfort limit throughout the DR event.

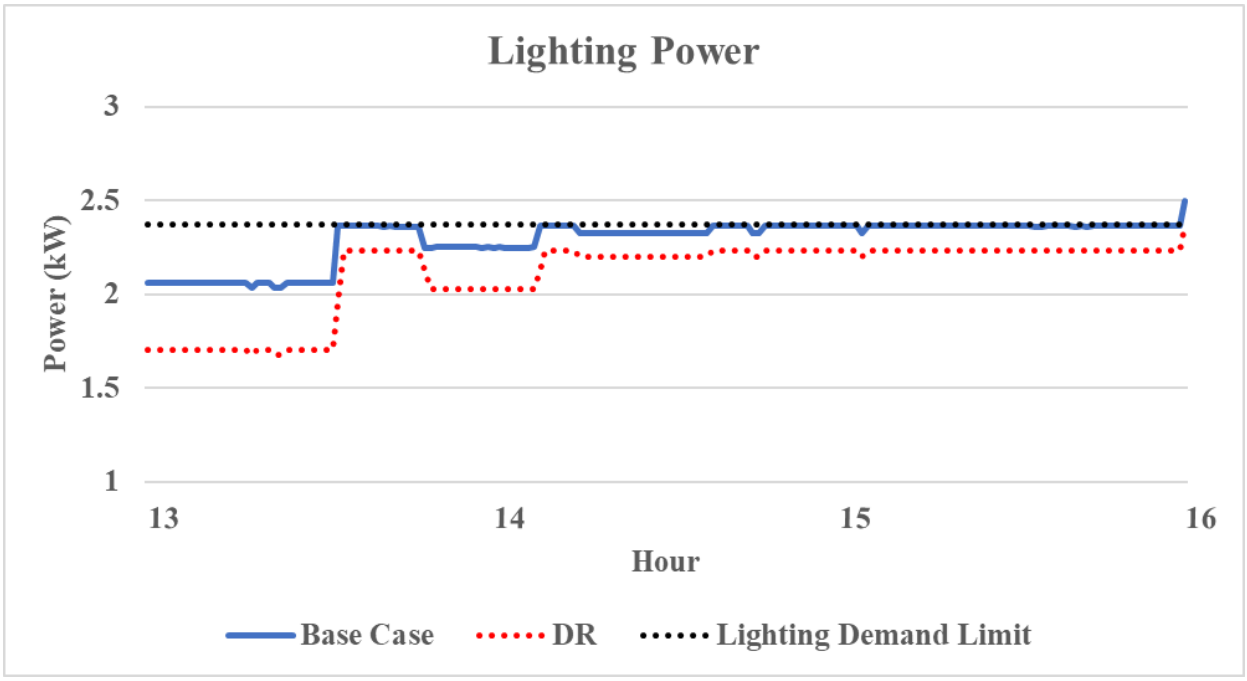

Figure 25. Comparison of lighting power consumption for case 2.

In Fig. 25 we see that the lighting power consumption always remains below the maximum demand limit. During the DR event, the lighting energy consumption using DR is 6.32kWh compared to 6.87kWh for the base case. Using the DR algorithm, we find an energy saving of 0.55kWh (7.94%) for lighting loads.

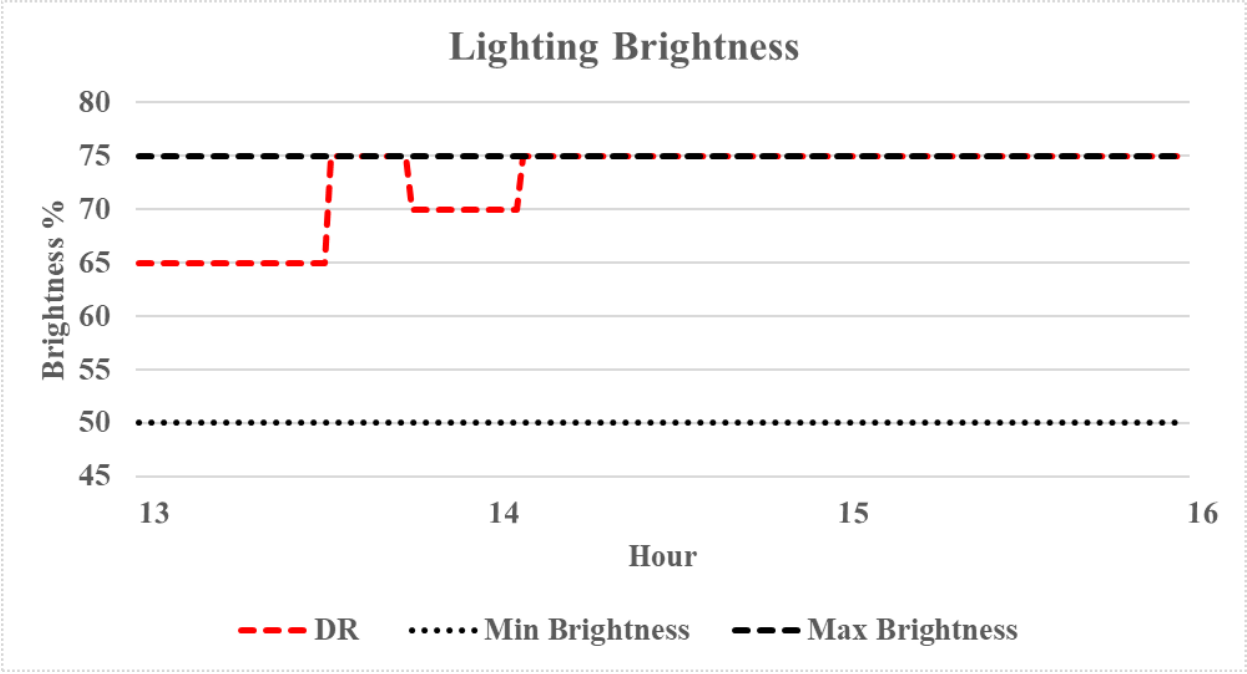

Figure 26. Variation of lighting brightness during case 2.

Fig. 26 shows us that the lighting brightness using the DR algorithm is always kept above within the user comfort limits and always above the minimum comfort level, and is kept at the maximum 75% brightness for the majority of the DR event. Initially four HVACs controlled by thermostats T1, T2, T3 and T5 are active, and based on the power left over within the demand limit, the maximum brightness is set to 65%. The brightness increases to 75% when the HVAC controlled by T3 becomes inactive, and later on drops for a short period of time to 70% when the HVAC controlled by T4 becomes active. After some time, the brightness returns to 75% when the HVAC controlled by T1 turns off, and stays at this level for the remainder of the DR event.

Case 3

Three of the five HVACs (T1, T4 and T5) have higher indoor temperatures than the 70°F setpoint and are therefore active when the bid price for DR is generated.

Table 12. Indoor temperatures, electricity prices and demand limit for case 3.

T1 (°F)	T2 (°F)	T3 (°F)	T4 (°F)	T5 (°F)	Bid Price ($/kWh)	Cleared Price ($/kWh)	Demand Limit (kW)
71	70	70	71	71	0.047	0.040	10

From Table 12 we see the double-auction yields a demand limit of 10kW. This will therefore leave 6.37kW for HVAC operation, after the minimum power consumption for lighting and plug loads are truncated from the demand limit.

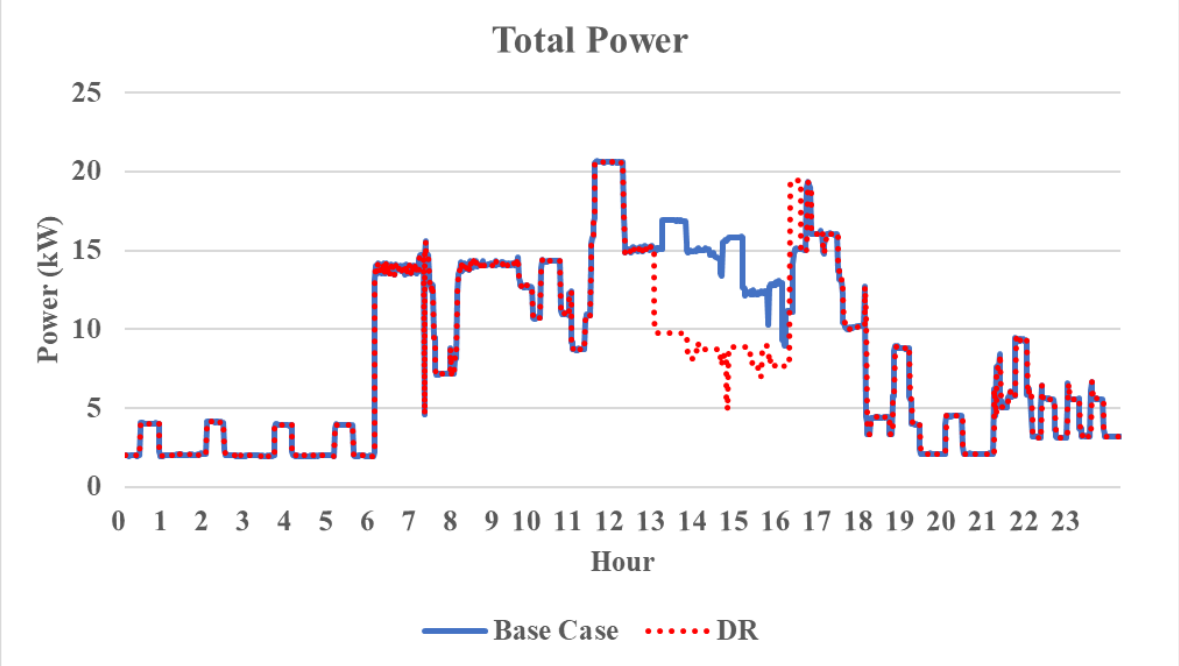

Figure 27. Comparison of 24-hour total power consumption for case 3.

Fig. 27 once again shows us that using the DR algorithm, the total demand limit of 10kW is maintained during the DR event, whereas the base case reaches a maximum total load of 20.67kW. During the DR event, the total energy consumption using DR is 25.62kWh compared to 42.97kWh for the base case. Throughout the DR event, 17.35kWh (40.37%) of energy is saved.

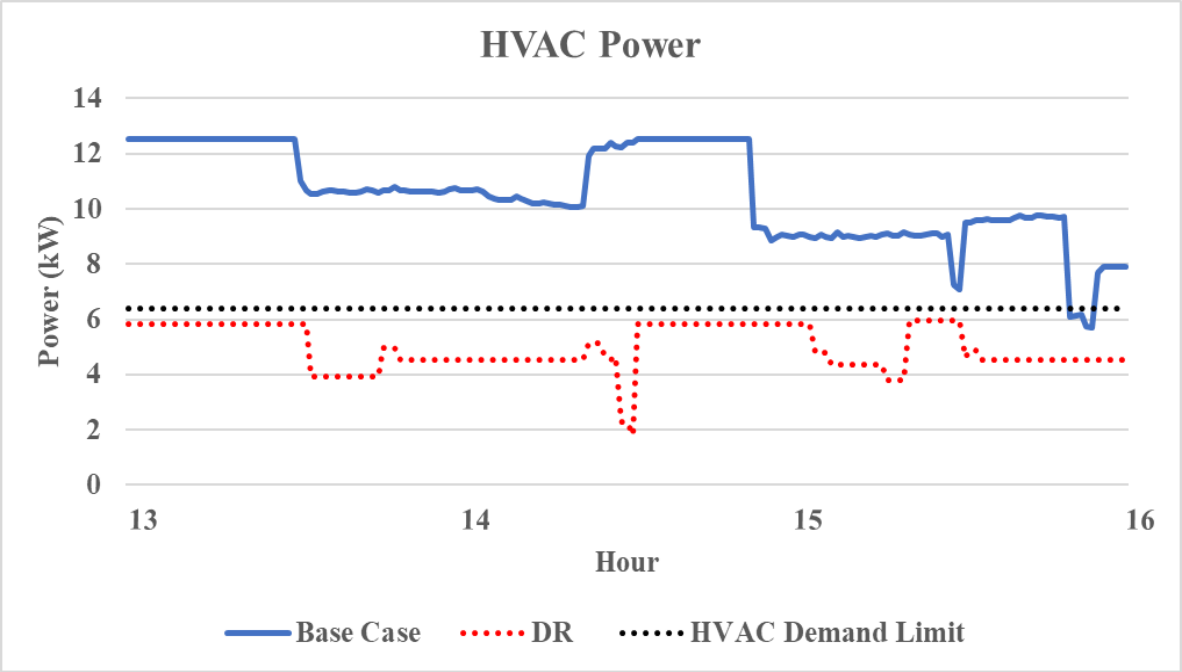

Figure 28. Comparison of HVAC power consumption for case 3.

From Fig. 28 we observe the red DR line stays below the DR limit of 6.37kW for HVAC loads, however the base case line reaches a maximum load of 12.54kW. During the DR event, the HVAC energy consumption using DR is 15.05kWh compared to 31.81kWh for the base case. The use of the DR algorithm yields a HVAC energy saving of 16.76kWh (52.70%).

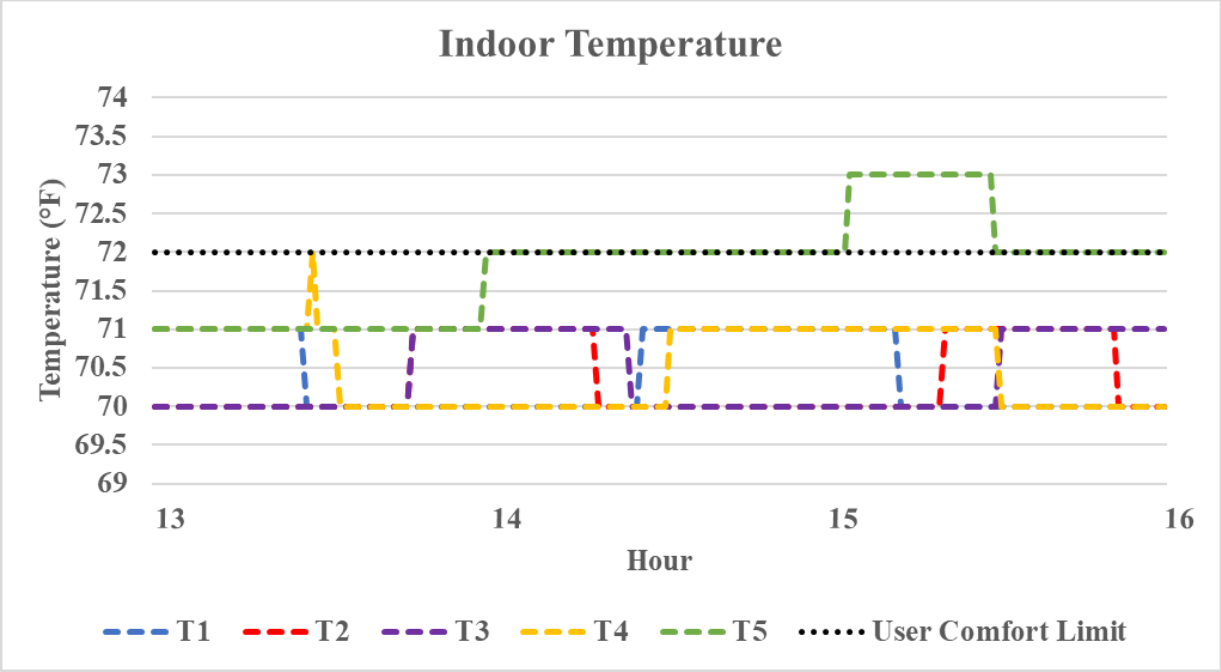

Figure 29. Variation of indoor temperatures during case 3.

Fig. 29 shows us that all the thermostats stay within the user comfort limit with the only exception being T5. Though this is the thermostat with least priority, it only violates the user comfort limit for 14% of the total DR time before coming back within the user comfort limit.

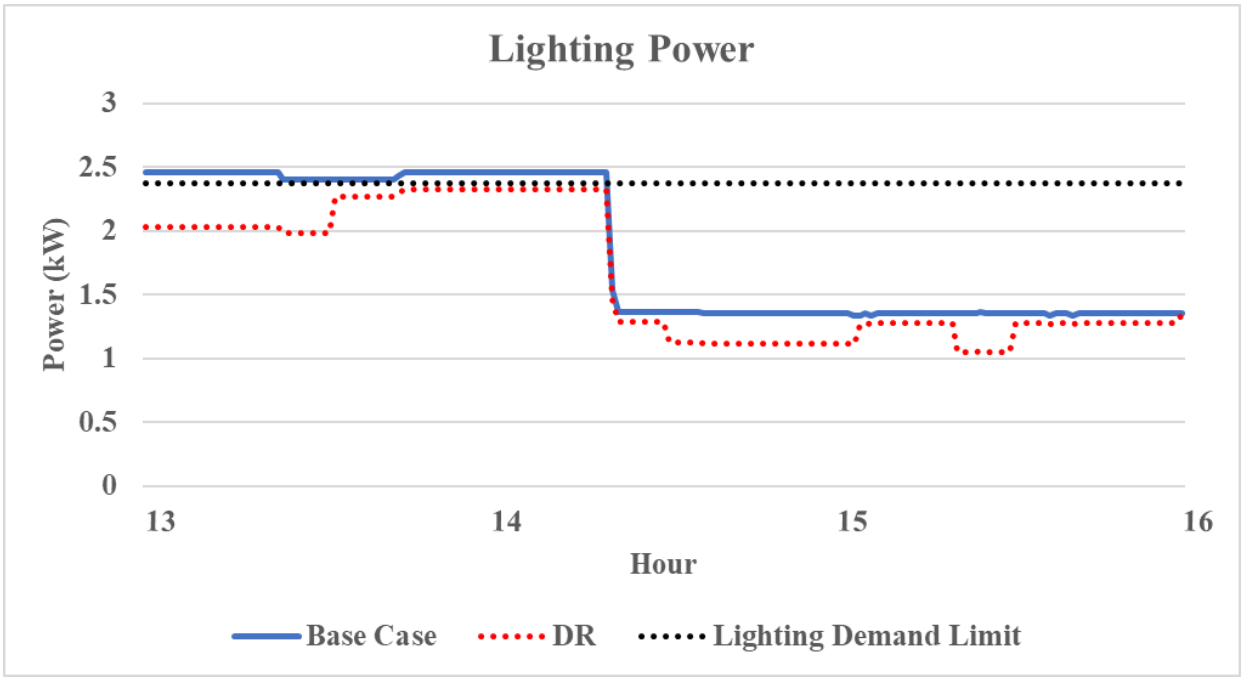

Figure 30. Comparison of lighting power consumption for case 3.

In Fig. 30 We see that the lighting power consumption using the DR algorithm always remains below the maximum demand limit, even though this limit is breached in the base case with a maximum power consumption of 2.49kW. During the DR event, the lighting energy consumption using DR is 4.94kWh compared to 5.53kWh for the base case. The DR algorithm yields lighting energy savings of 0.59kWh (10.60%).

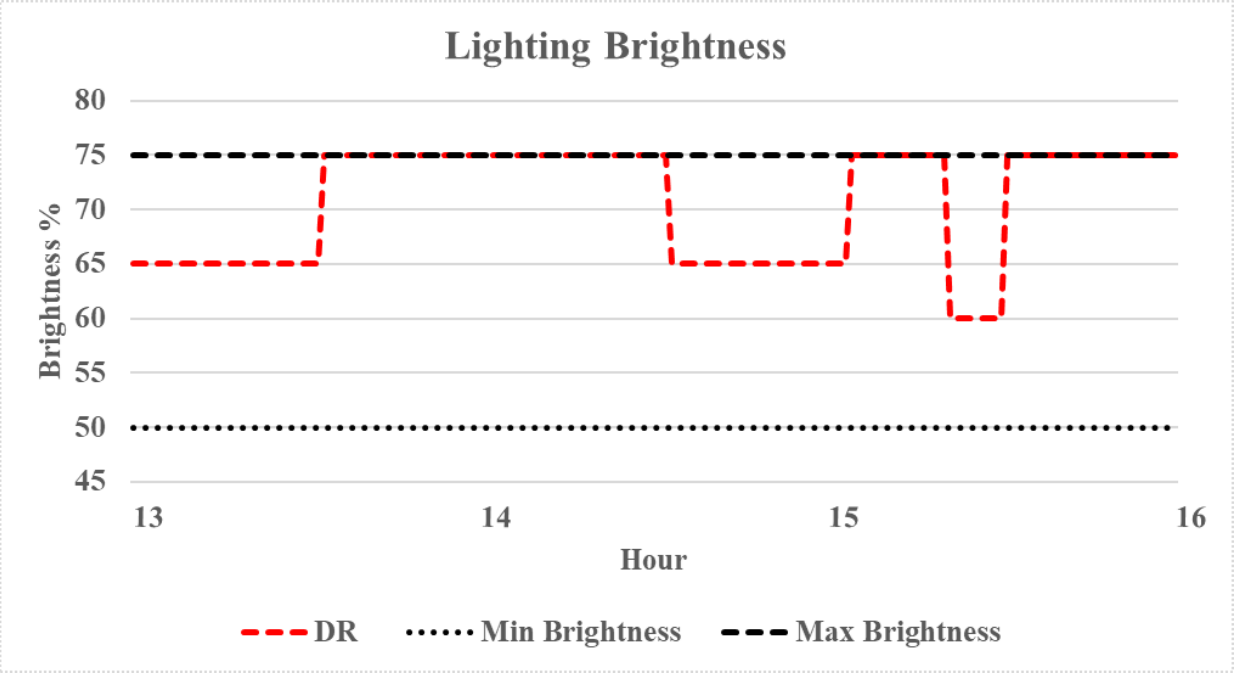

Figure 31. Variation of lighting brightness during case 3.

Fig. 31 Illustrates the fact that throughout the DR event, the lighting brightness is kept above the minimum brightness, and is kept at the maximum possible 75% brightness for most of the DR event. Initially when the HVACs controlled by thermostats T1 and T4 are active, the maximum possible brightness is 65%. Later the brightness rises to 75% when the HVAC controlled by T4 becomes inactive. The brightness drops to 65% for some time again when the HVAC controlled by T4 is active again, but returns to 75% when the HVAC controlled by T5 is activated in place of the HVAC controlled by T4, as its indoor temperature reaches 73°F. For a short period of time later on, the brightness drops to 60% when HVACs controlled by T2 and T5 are active, but returns to 75% when the HVAC controlled by T5 is turned off, and there is enough power left within the demand limit to maintain this level of brightness.

Case 4

In this test case, prior to the DR event when the user bid price is generated, only two of the five HVACs (T4 and T5) are active, as their thermostats have not reached the desired 70°F setpoint.

Table 13. Indoor temperatures, electricity prices and demand limit for case 4.

T1 (°F)	T2 (°F)	T3 (°F)	T4 (°F)	T5 (°F)	Bid Price ($/kWh)	Cleared Price ($/kWh)	Demand Limit (kW)
70	70	70	71	72	0.046	0.040	10

Table 13 shows that upon clearing of the bid price, a demand limit of 10kW is received from the DR server, leaving 6.37kW for HVACs to be active after curtailing the minimum power consumption for lighting and plug loads.

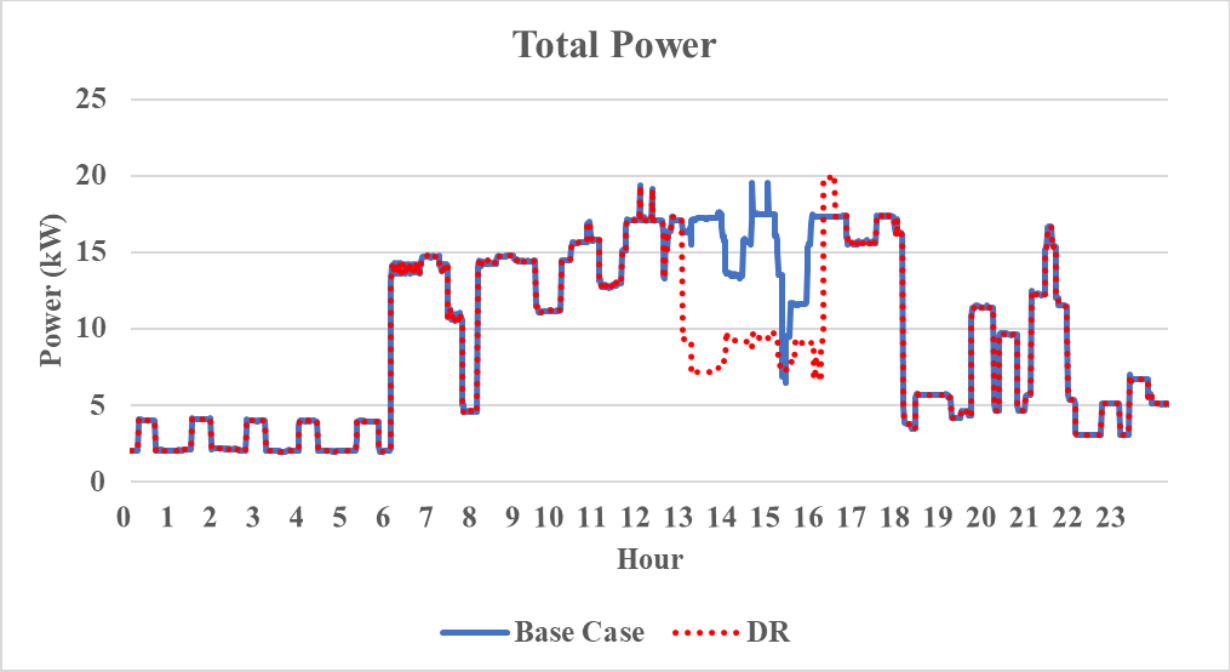

Figure 32. Comparison of 24-hour total power consumption for case 4.

From Fig. 32 we observe that throughout the DR event, the red DR line remains below the total load demand limit of 10kW, in contrast to the base case that reaches a maximum load of 19.58kW during this time. During the DR event, the total energy consumption using DR is 25.15kWh compared to 45.68kWh for the base case. The total energy savings as a result of using the DR algorithm in this case is 20.53kWh (44.94%).

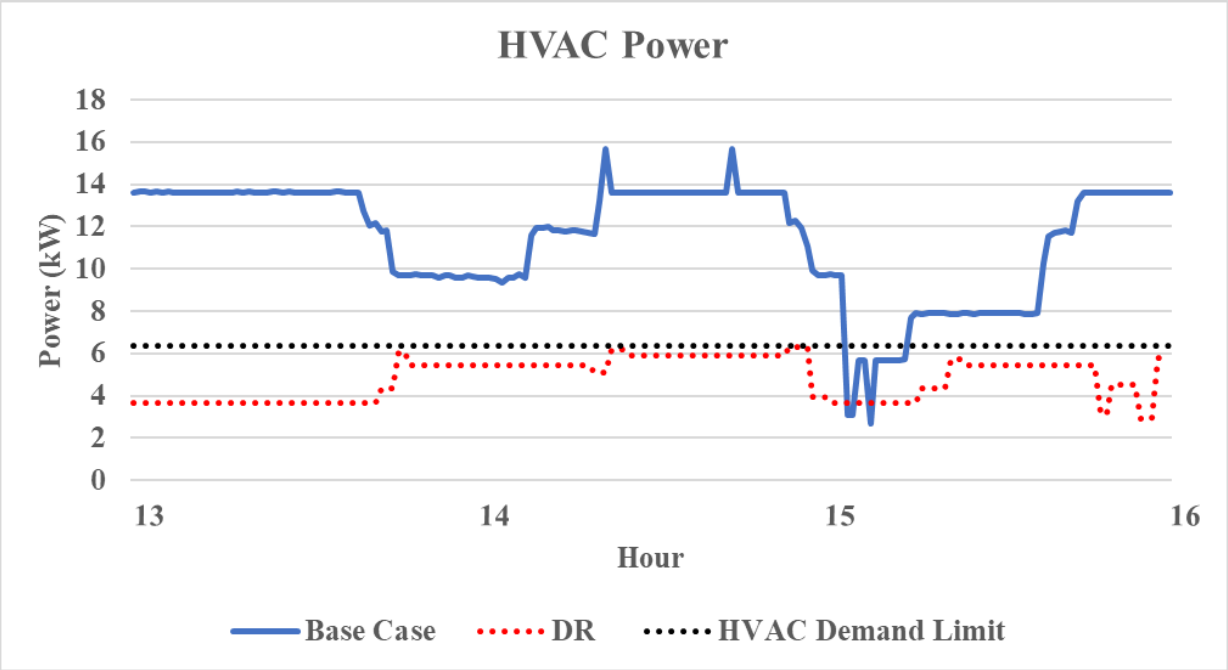

Figure 33. Comparison of HVAC power consumption for case 4.

Fig. 33 illustrates the trend in HVAC power consumption, which with the use of the DR algorithm is kept below the HVAC demand limit of 6.37kW, in comparison to the base case which reaches a maximum of 15.7kW. During the DR event, the HVAC energy consumption using DR is 14.51kWh compared to 34.55kWh for the base case. The HVAC energy savings achieved here is 20.04kWh (57.99%) throughout the duration of the DR event.

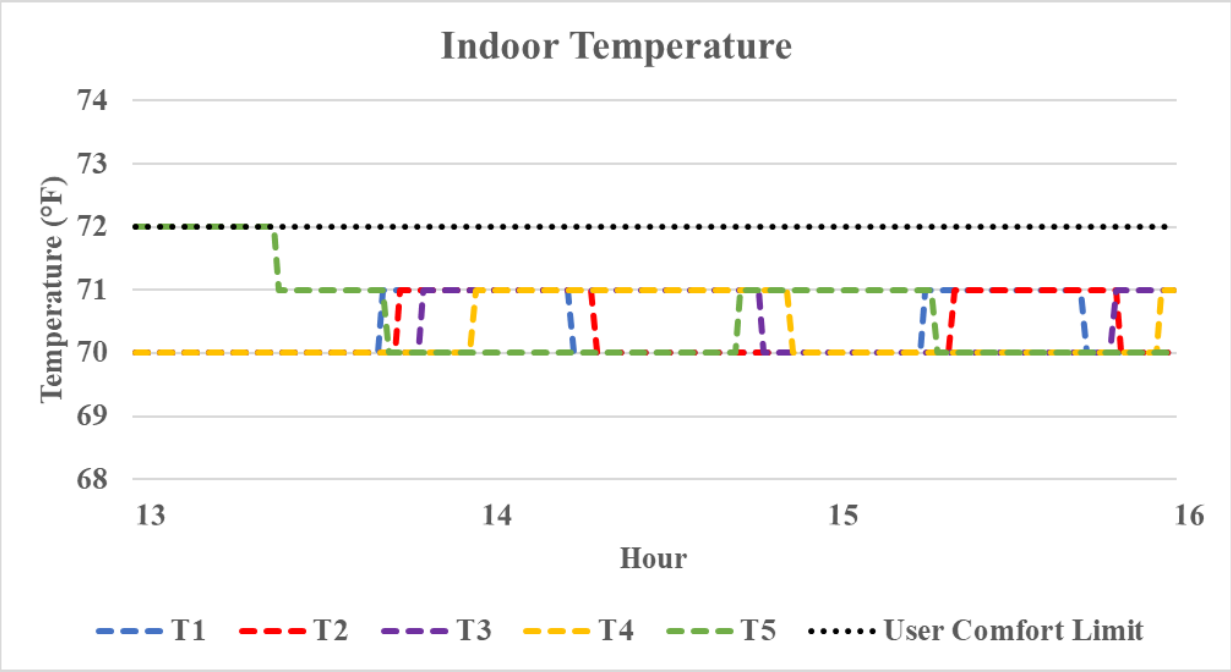

Figure 34. Variation of indoor temperatures during simulated case 4.

From Fig. 34 we observe that the DR algorithm is able to maintain the user comfort limits for all five thermostats, while also being able to bring them down to their desired setpoint at different points throughout the DR event.

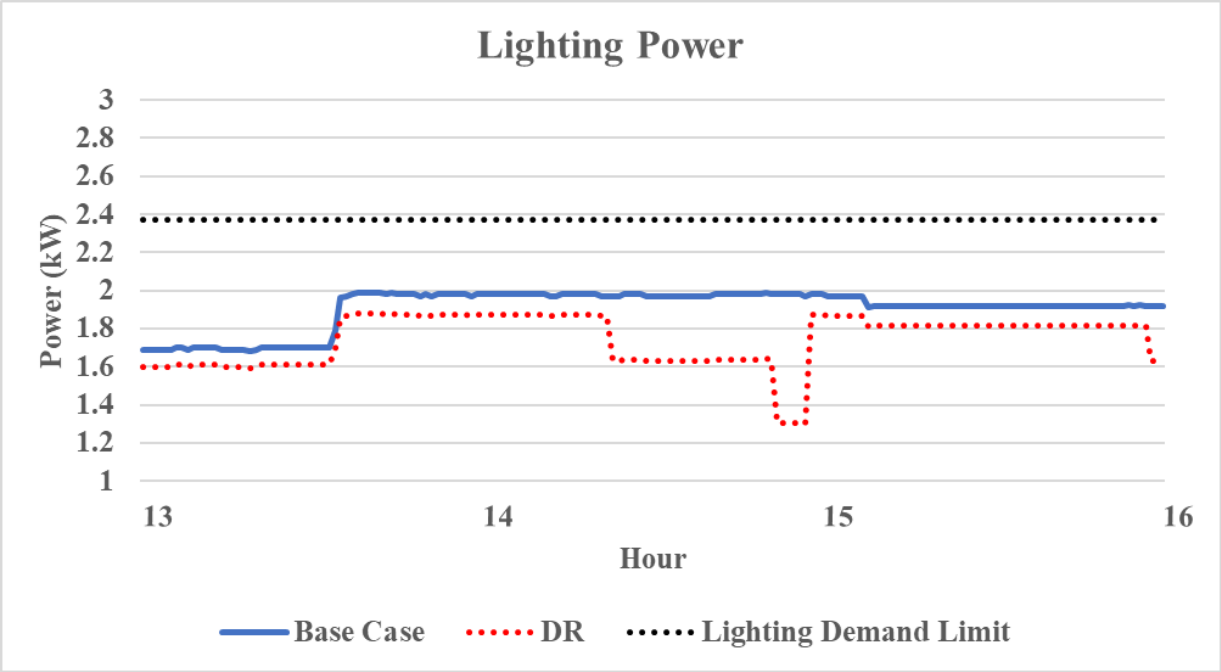

Figure 35. Comparison of lighting power consumption for case 4.

Fig. 35 shows us that the entire lighting load is not active during the DR event, and therefore the power consumption of both the DR and base cases are below the maximum lighting demand limit. During the DR event, the lighting energy consumption using DR is 5.23kWh compared to 5.72kWh for the base case. The total lighting energy savings amount to 0.49kWh (8.56%).

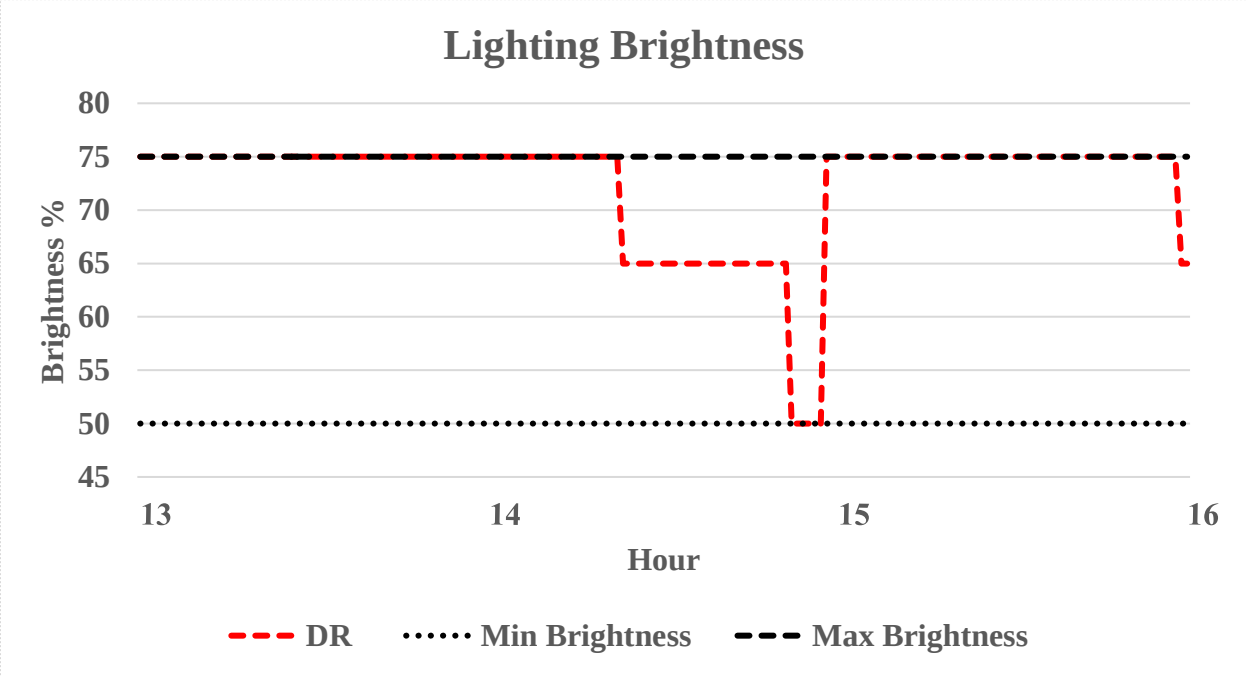

Figure 36. Variation of lighting brightness during case 4.

As can be seen in Fig. 36 for the majority of the DR event the lighting is at its maximum permitted brightness of 75% during the DR event. For less than 4% of the duration of the DR event, the brightness is at the minimum level of 50%. Initially only the HVAC controlled by thermostat T5 is active, and there is enough power within the demand limit to keep lighting brightness at 75%. This drops to 65% later on when HVACs controlled by T3 and T4 are active and then drops to the minimum 50% when the HVAC controlled by T5 is turned on, once T3 reaches its target setpoint. Once the HVAC controlled by T4 reaches its setpoint and becomes inactive, the brightness returns to 75%. Towards the end of the DR event, the brightness drops to 65% when HVACs controlled by T3 and T4 are again active.

4.4.2 Cases Using Simulated Data

Four additional test cases were simulated – two to investigate the performance of the DR algorithm when one or zero of the five HVACs (cases which could not be found in the recorded data) were active at the time of bid price generation, and another two cases to show how the DR algorithm would perform when total load is scaled up to 2 and 4 times the total load of the cases

in section 4.4.1. In all of these cases, the rate at which cooling or heating of the areas controlled by thermostats occurs, has been simulated based on historical data.

Simulated Case 1

In this test case, only one of the five HVACs is active prior to the DR event when the user bid price is generated. Thermostat T5 recorded an indoor temperature greater than the set point that was set to 70°F. Load priorities for HVACs controlled by their thermostats (T1-T5) are given in the following order- T1>T2>T3>T4>T5. It is assumed that the plug load is constant at 2kW whereas all the lighting load is turned on, leading to a power consumption of 2.5kW before the DR event.

Table 14. Indoor temperatures, electricity prices and demand limit for simulated case 1.

T1 (°F)	T2 (°F)	T3 (°F)	T4 (°F)	T5 (°F)	Bid Price ($/kWh)	Cleared Price ($/kWh)	Demand Limit (kW)
70	70	70	70	72	0.044	0.040	10

Based on the cleared user bid price in Table 14 the DR server allocates a demand limit of 10kW, making 6.37kW available to operate HVACs, whereas 2kW is allocated to the plug load and a minimum of 1.63kW is needed to maintain the minimum brightness of lighting loads.

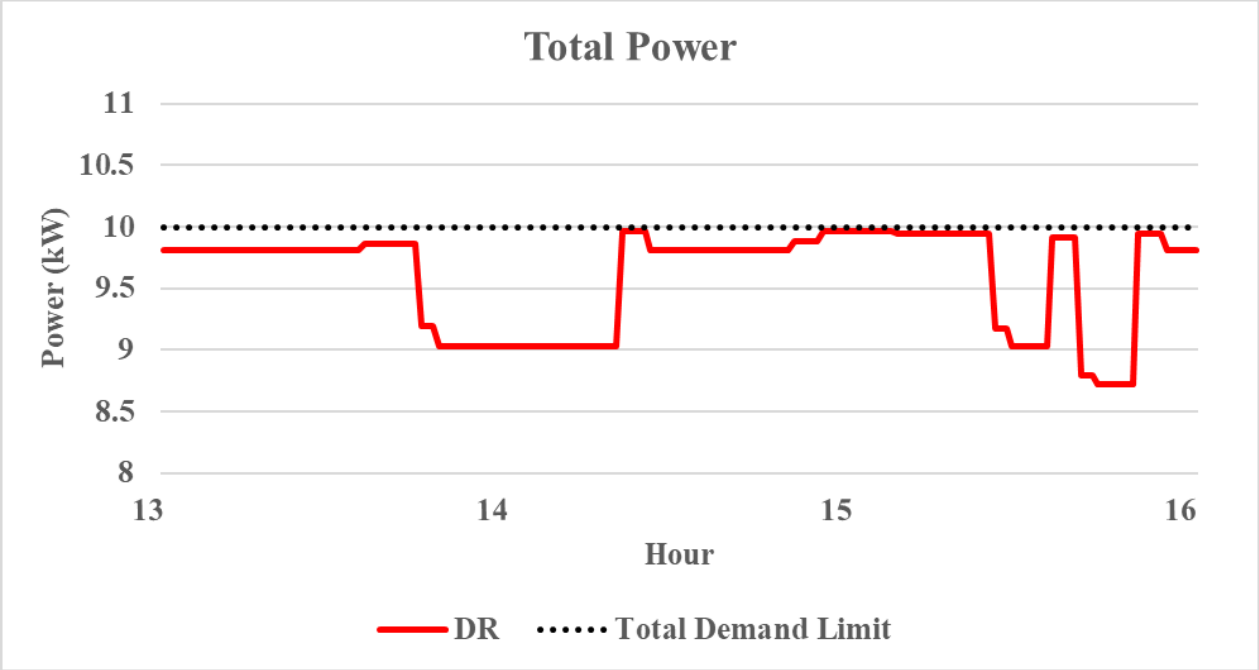

Figure 37. Total power consumption for simulated case 1.

From Fig. 37 we observe that throughout the DR event, the DR algorithm is capable of maintaining the total power consumption below the demand limit of 10kW, reaching a maximum value of 9.97kW. The total energy consumption throughout the DR event is 28.88kWh.

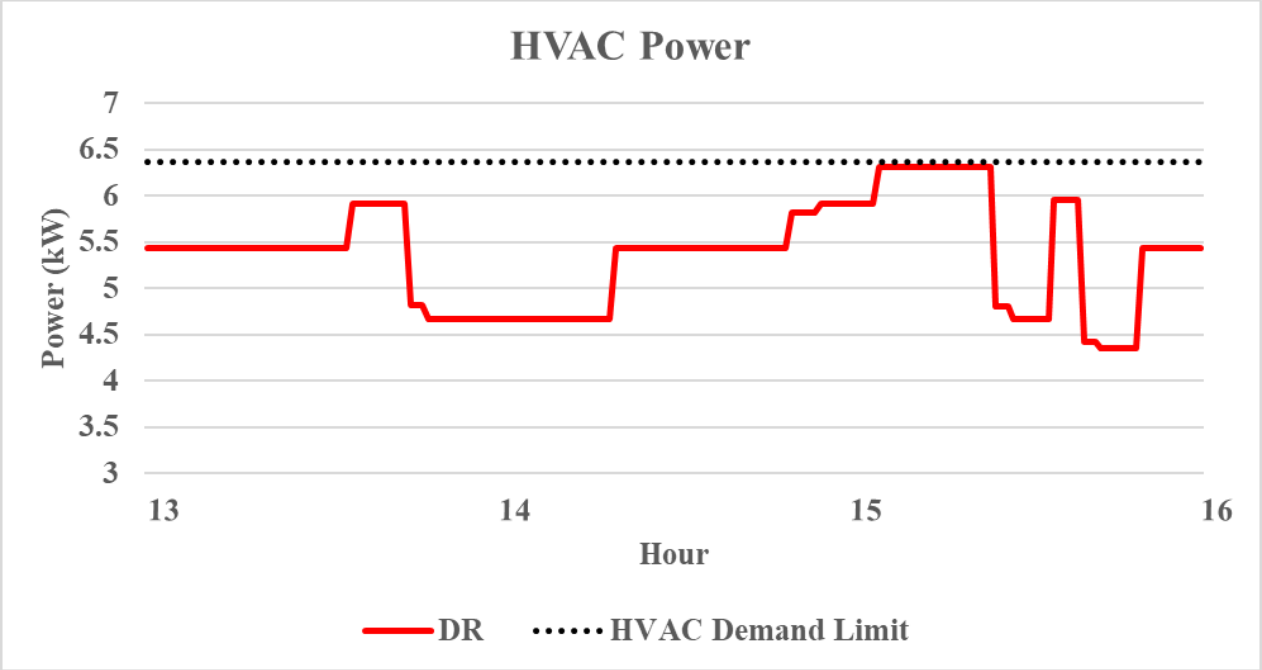

Figure 38. HVAC power consumption for simulated case 1.

Fig. 38 illustrates how the HVAC load varies during the DR event, as it is kept below the demand limit of 6.37kW. The maximum HVAC power consumption is 6.31kW while the total energy consumption during the DR event is 16.18kWh.

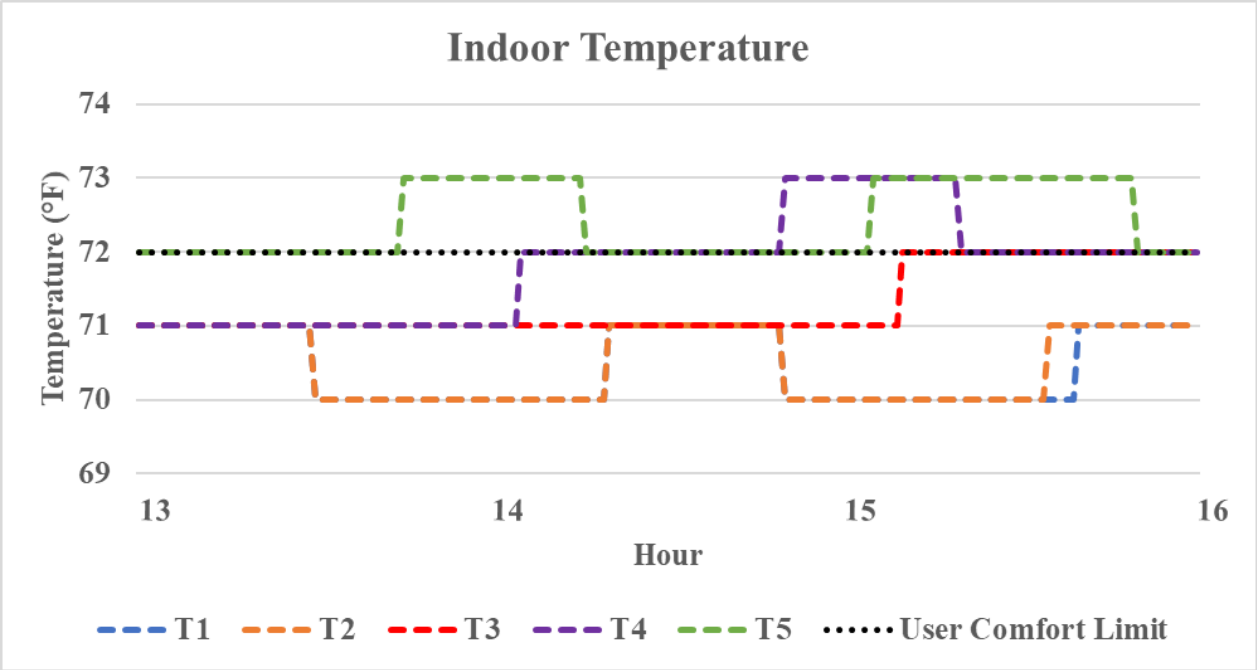

Figure 39. Variation of indoor temperatures during simulated case 1.

From Fig. 39 we see that by the start of the DR event, the indoor temperature of T1-T4 increases to 71°F whereas the indoor temperature of T5 is still at 72°F**.** The only two thermostats that violate the user comfort limit are T4 and T5, the two thermostats with the least priority. Even then T4 and T5 are above the user comfort limit for a maximum time of 16.67% and 25% of the DR event, spending most of the DR event duration within the comfort limit.

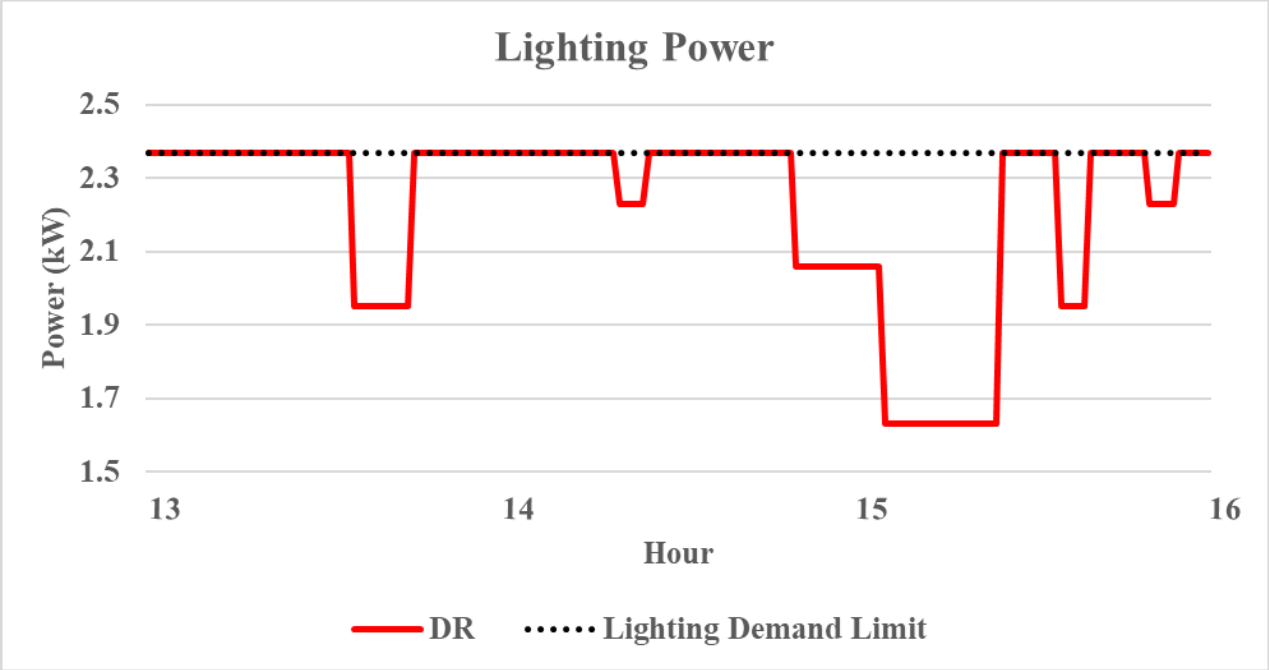

Figure 40. Lighting power consumption for simulated case 1.

Fig. 40 illustrates the lighting power that is kept at or below the lighting demand limit of 2.37kW by the DR algorithm. The total lighting energy consumption is 6.70kWh.

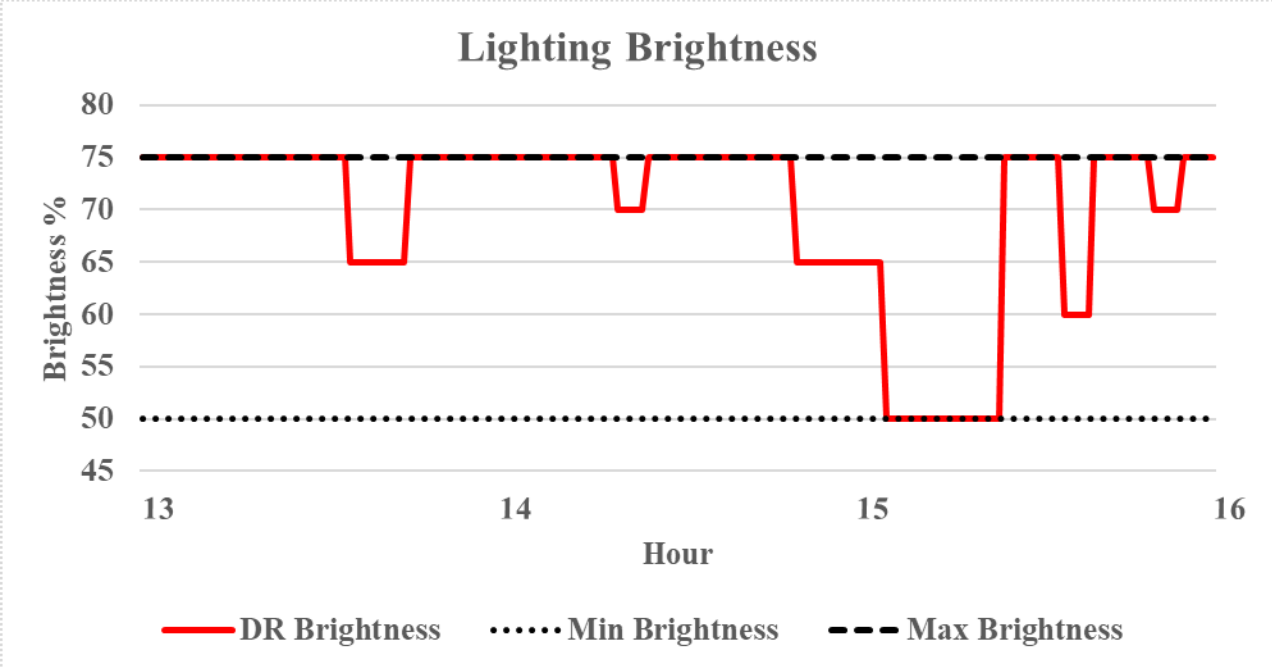

Figure 41. Variation of lighting brightness during simulated case 1.

From Fig. 41 we observe that throughout the DR event, the lighting brightness is kept within the specified limits, with brightness being at a minimum level of 50% for only 11.11% of the total DR event duration. Initially the brightness is set to 75% when HVACs controlled by T1 and T2 are active and there is enough power left over within the demand limit to maintain this level of brightness. This briefly falls to 65% when HVACs controlled by T3 and T4 are active but again rises to 75% when the HVAC controlled by T5 turns on in place of the HVAC of T4. Later on, the brightness falls to 70% for a short period of time, when HVACs controlled by T1 and T2 turn on due to higher priority in place of T3 and T5, but air handlers for the latter pair are active for a few minutes after the HVACs are turned off. Further into the DR event, the brightness reduces to 65% when the HVACs of T3 and T4 are again active, and then the brightness reaches the minimum 50% when HVACs of T4 and T5 are active, and there is not enough power left over within the demand limit to maintain a higher level of brightness. The brightness returns to 75% when the HVAC of T4 turns off as its indoor temperature is brought back within the comfort limit and the HVAC of T3 is activated in its place. The brightness drops to 60% for a short time when the HVAC of T2 takes the place of the HVAC of T3 due to higher priority, but comes back to 75% when the HVAC of T1 takes the place of the HVAC of T2. After this, for a short period of time, the brightness drops to 70% when the HVAC of T2 is activated in place of T5, while the air handler of T5 is still active, but soon the brightness climbs back up to 75%.

Simulated Case 2

In this simulated case, the areas controlled by all five thermostats are at the desired setpoint of 70°F, therefore none of the five HVACs are active when the bid price is generated for the DR event. Once again, load priorities for HVACs controlled by their thermostats (T1-T5) are given in the following order- T1>T2>T3>T4>T5, which all have a target setpoint of 70°F. It is assumed that the plug load is constant at 2kW whereas all the lighting load is turned on, leading to a power consumption of 2.5kW before the DR event.

Table 15. Indoor temperatures, electricity prices and demand limit for simulated case 2.

T1 (°F)	T2 (°F)	T3 (°F)	T4 (°F)	T5 (°F)	Bid Price ($/kWh)	Cleared Price ($/kWh)	Demand Limit (kW)
70	70	70	70	70	0.039	0.040	10

Table 15 shows that even when none of the HVACs are active, the total demand limit is 10kW, of which 2kW is for plug loads, a minimum of 1.63kW is for lighting therefore leaving 6.37kW for HVAC loads.

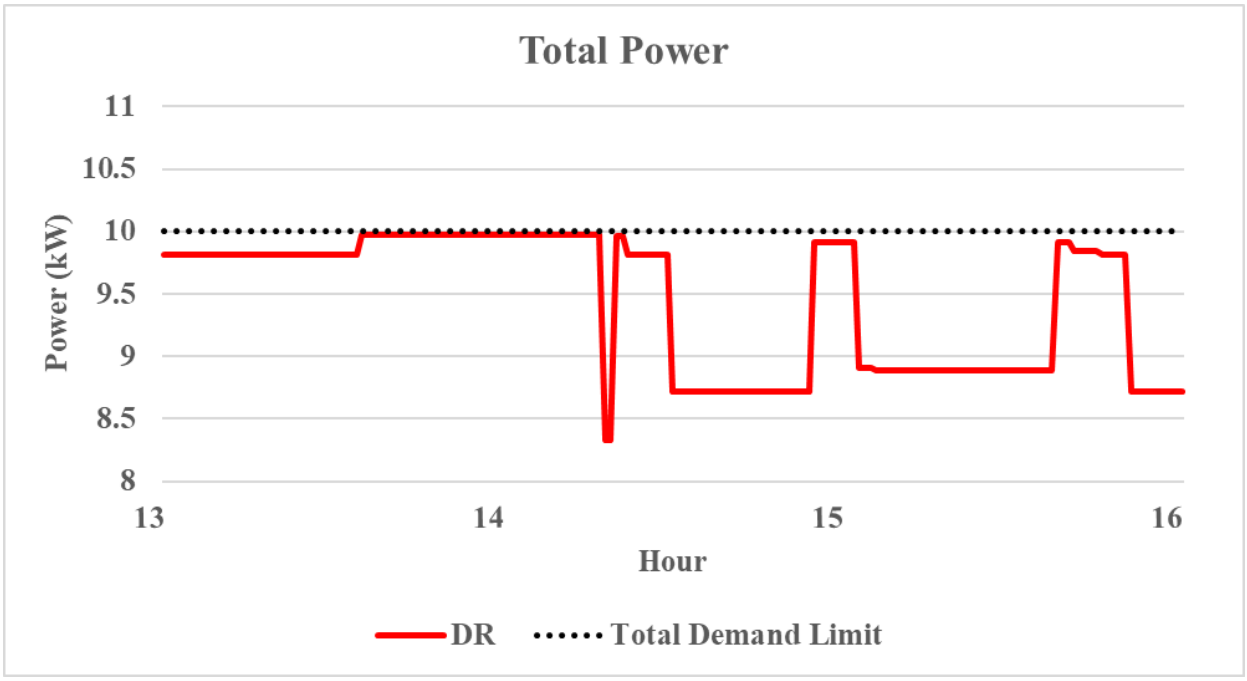

Figure 42. Total power consumption for simulated case 2.

The DR algorithm manages to keep the total power consumption below the 10kW demand limit as shown in Fig. 42 The total energy consumption during the DR event is 28.45kWh.

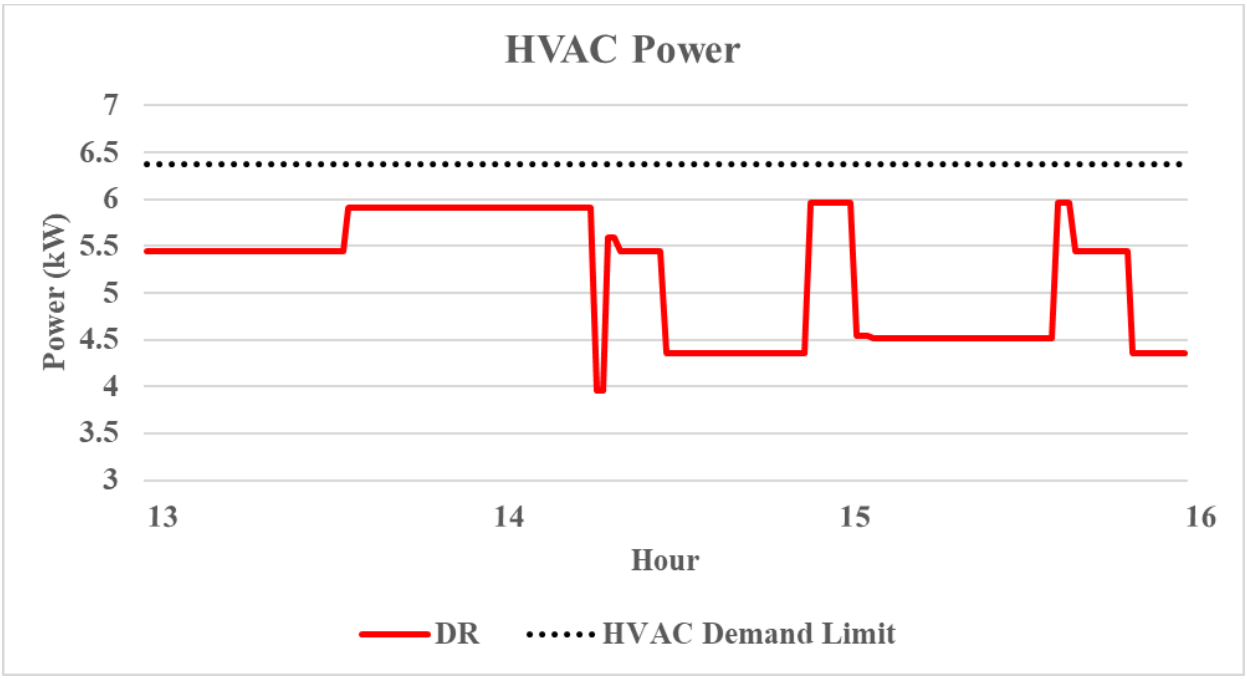

Figure 43. HVAC power consumption for simulated case 2.

As shown in Fig. 43 The total HVAC power is kept below the demand limit of 6.37kW, reaching a maximum value of 5.96kW. The total HVAC energy consumption is 15.63kWh.

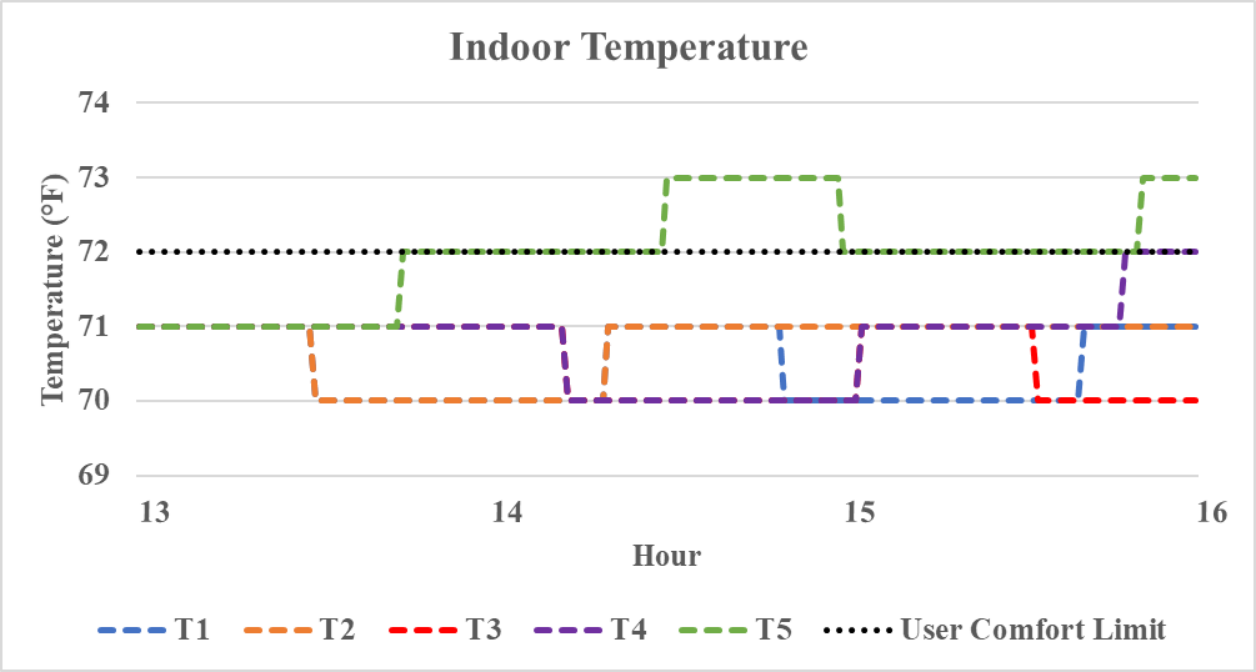

Figure 44. Variation of indoor temperatures during simulated case 2.

From Fig. 44 we observe that by the start of the DR event, the indoor temperature for all five thermostats has increased by one degree to 71°F. Even then the DR algorithm is able to cool T1-T4 to the setpoint of 70°F and keep them within the user comfort limit, whereas T5 exceeds the limit for a maximum of 22.22% of the DR event duration.

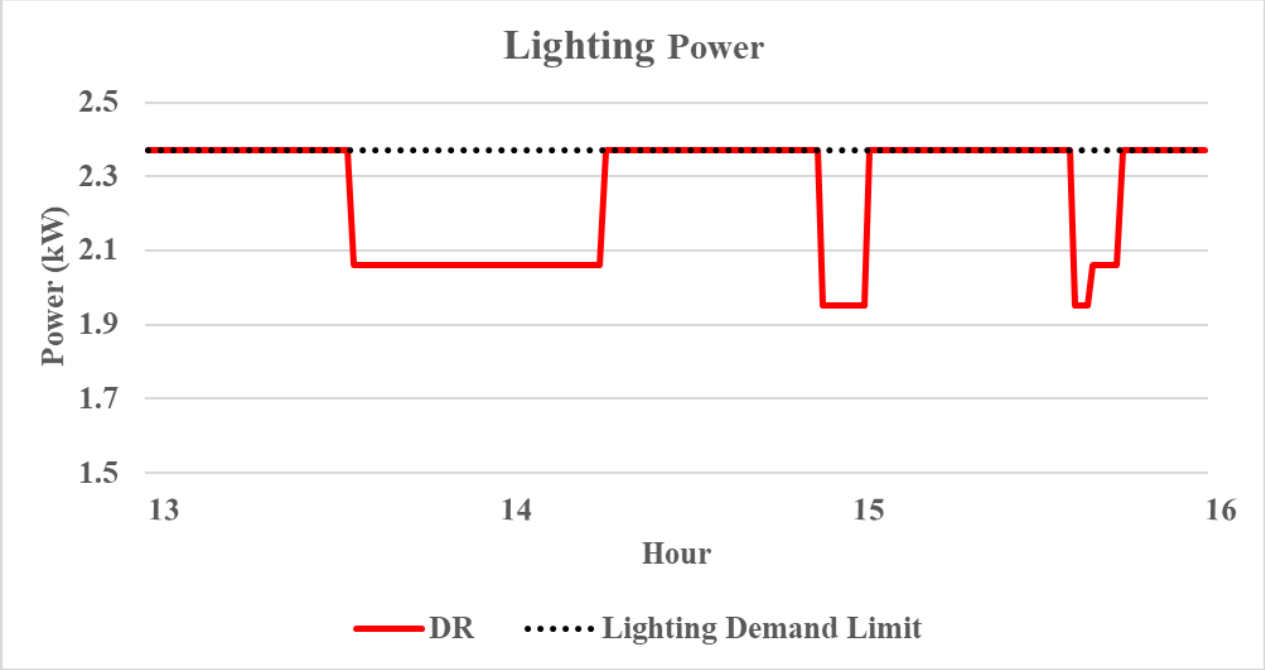

Figure 45. Lighting power consumption for simulated case 2.

Fig. 45 Illustrates the variation in lighting power throughout the DR event, which is kept at or below the maximum DR consumption level of 2.37kW. The total lighting load energy consumption is 6.82kWh.

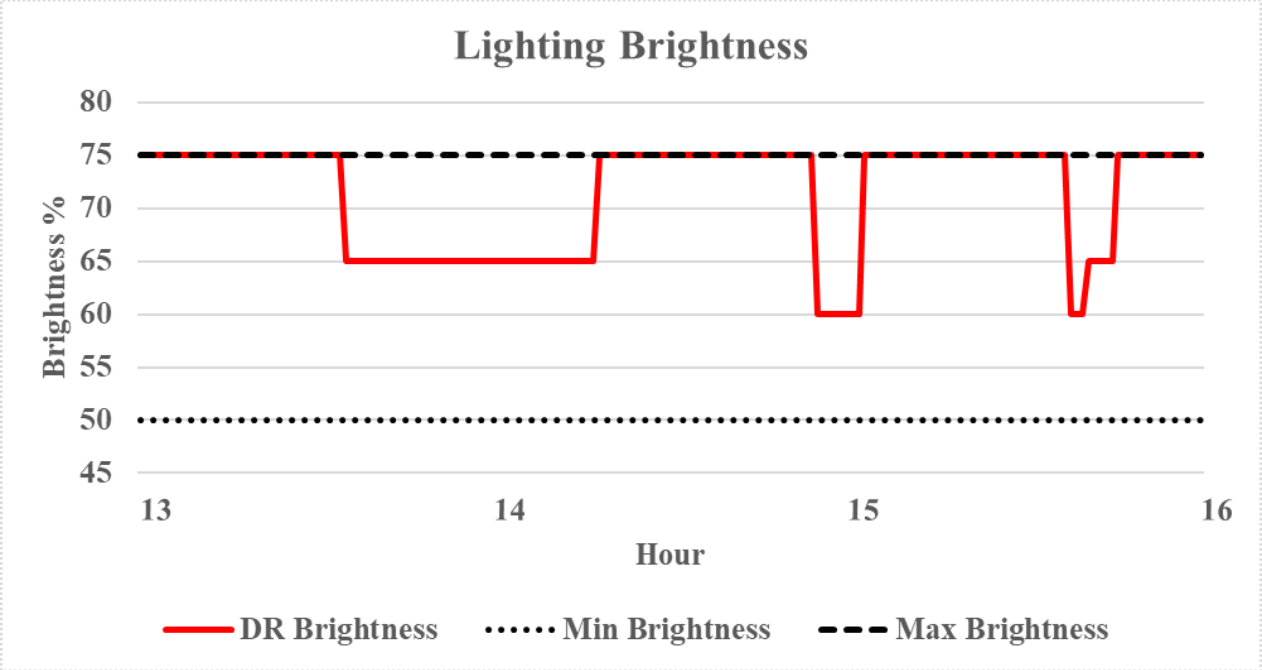

Figure 46. Variation of lighting brightness during simulated case 2.

The DR algorithm manages to keep the lighting brightness at 75% for the majority of the DR event without ever reaching the minimum brightness level of 50%. Initially the brightness is set to 75% when HVACs controlled by thermostats T1 and T2 are active. After some time into the DR event there is a drop in brightness to 65%, when the HVACs of T3 and T4 are active. The brightness returns to 75% when HVACs of T1 and T2 are active and those of T3 and T4 are turned off. Further into the DR event there is a drop in brightness to 60% when HVACs of T3 and T4 are on but the air handler for the HVAC of T1 is still active, given the HVAC was turned off only a few minutes before this. The brightness returns to 75% when the HVAC of T5 turns on in place of the HVAC of T3 as the comfort limit of T5 is reached, and beacuase there is enough power left over within the demand limit to maintain this level of brightness. Towards the end of the DR event, brightness varies between 60% and 65% as the configuration of HVACs of T1, T2, T3 and T5 change, due to load priorities, with the brightness eventually coming back to 75% when only the HVACs of T1 and T2 remain active.

Simulated Case 3

This test case is designed to demonstrate the ability of the DR algorithm to perform on a larger scale, where the load profile has been doubled from the previous cases. Here there are 10 HVACs, 5kW of active lighting load before the DR event and 4kW of constant plug load. Load priorities for HVACs controlled by their thermostats (T1-T10) are given in the following order- T1>T2>T3>T4>T5> T6>T7>T8>T9>T10, which again all have a target setpoint of 70°F.

In this case study, prior to the DR event when the user bid price is generated, five of the ten odd number HVACs are in operation, with areas being controlled by these HVACs having an indoor temperature above the user comfort limit at 73°F, while the other ten HVACs are inactive as their thermostats have reached the desired setpoint.

Table 16. Indoor temperatures, electricity prices and demand limit for simulated case 3.

T1 (°F)	T2 (°F)	T3 (°F)	T4 (°F)	T5 (°F)	T6 (°F)	T7 (°F)	T8 (°F)	T9 (°F)	T10 (°F)	Bid Price ($/kWh)	Cleared Price ($/kWh)	Demand Limit (kW)
73	70	73	70	73	70	73	70	73	70	0.081	0.080	20

After the bid price in Table 16 is cleared the DR server allocates a demand limit of 20kW, leaving 12.74kW for HVAC operation, as 4kW is reserved for plug load and another 3.26kW is needed to maintain the minimum brightness level of lighting load.

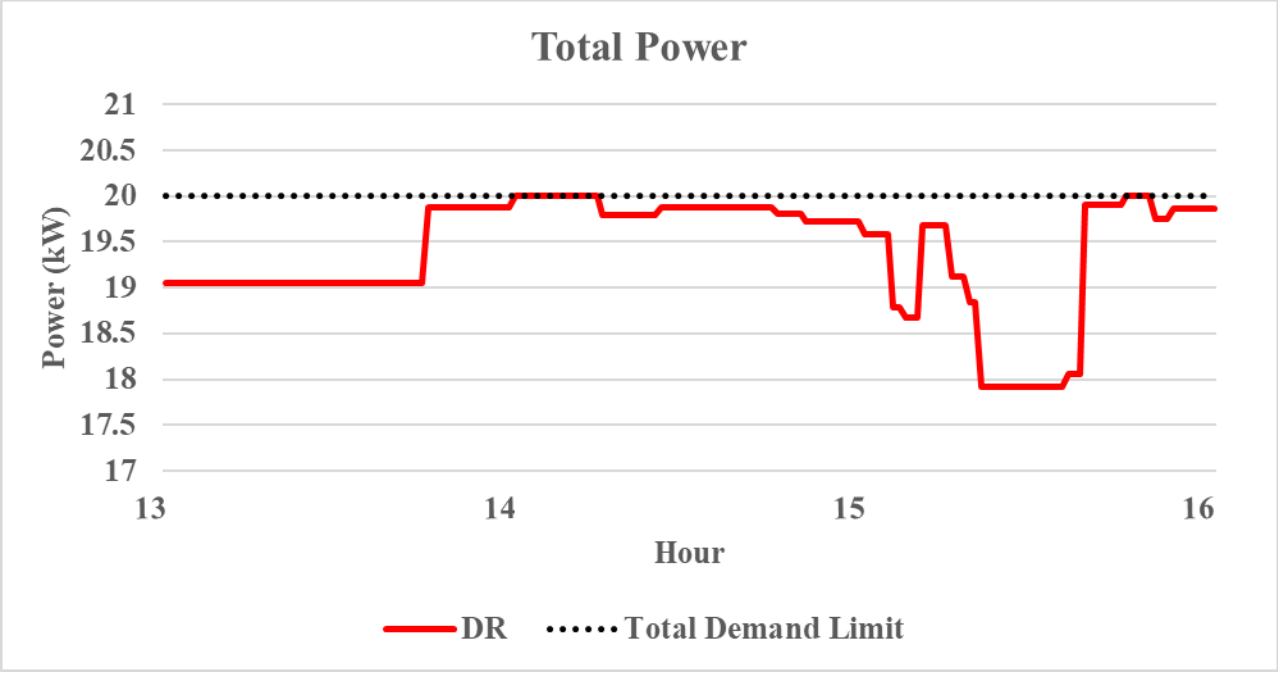

Figure 47. Total power consumption for simulated case 3.

As seen in Fig. 47 Using the DR algorithm, the total power consumption during the DR event is kept at or below the total demand limit of 20kW. The total energy consumption during this period is 58.49kWh.

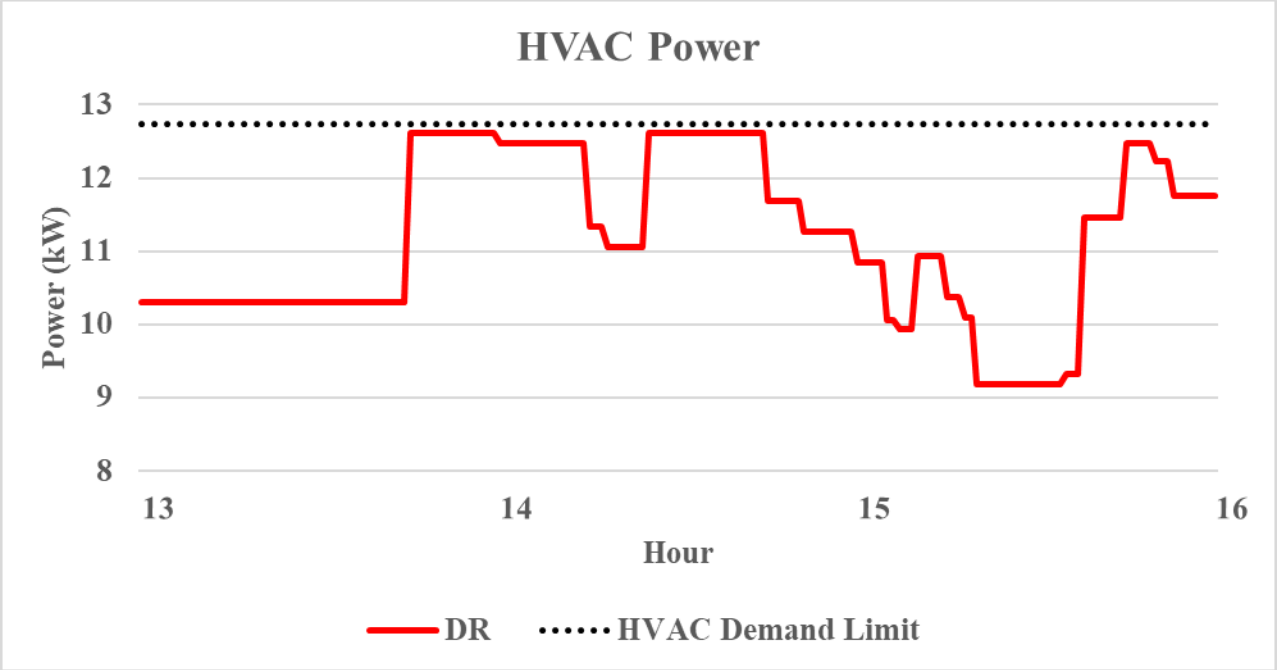

Figure 48. HVAC power consumption for simulated case 3.

Fig. 48 illustrates that the total HVAC power is kept below the demand limit of 12.74kW throughout the duration of the DR event, reaching a maximum of 12.48kW. The total HVAC energy consumption during the DR event is 33.75kWh.

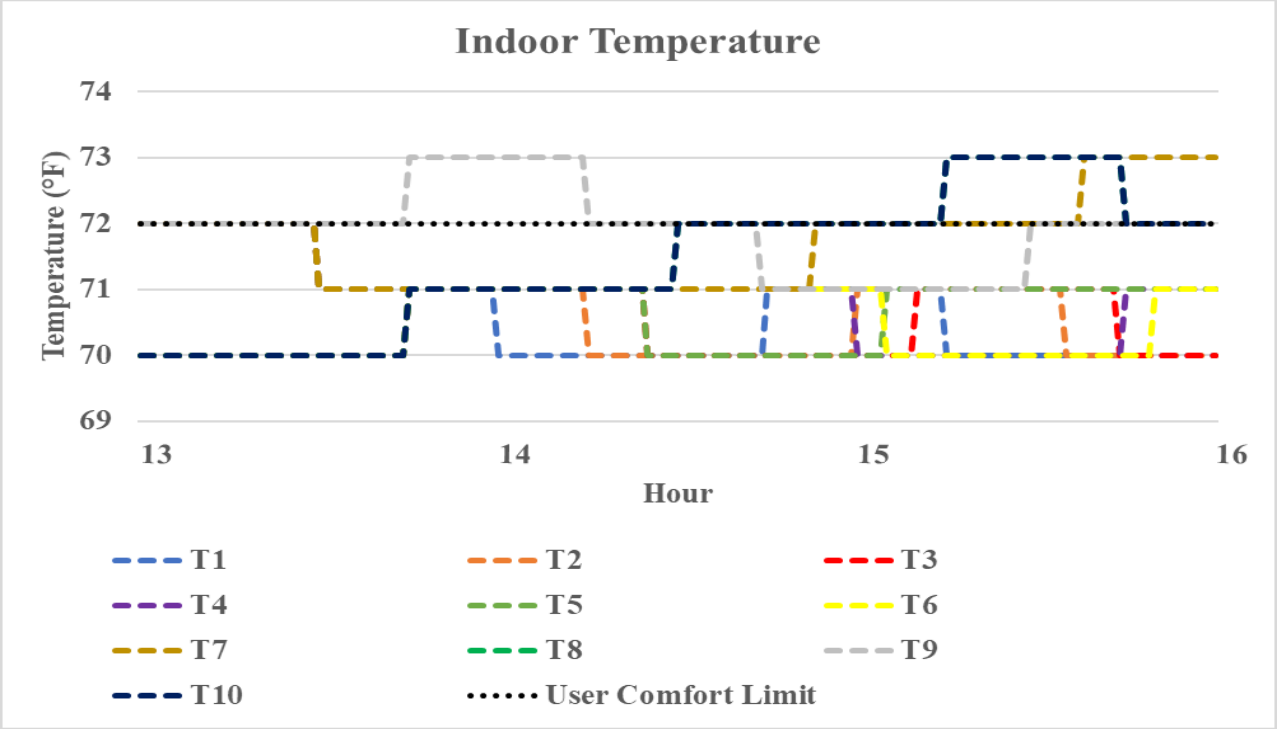

Figure 49. Variation of indoor temperatures during simulated case 3.

We observe from Fig. 49 that of the 10 thermostats, four of them- T7, T8, T9 and T10 cross the user comfort limit. However, this is only for a short period of time, before being brought back to within the comfort limits with T7 being above the comfort limit for a maximum of 12.78%, while T8-T10 are over for a maximum of 16.67% of the total DR event duration.

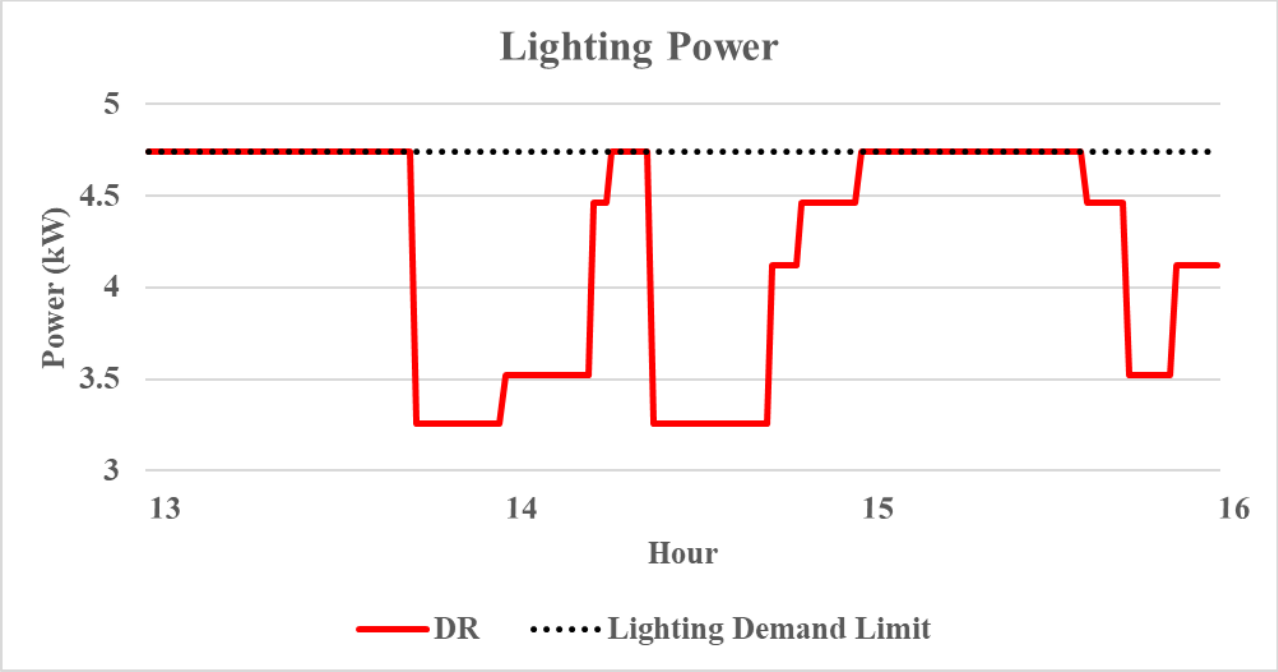

Figure 50. Lighting power consumption for simulated case 3.

From Fig.50 it can be seen that the total lighting load is kept at or below the demand limit of 4.74kW. The total energy consumption of lighting load during this time is 12.74kWh.

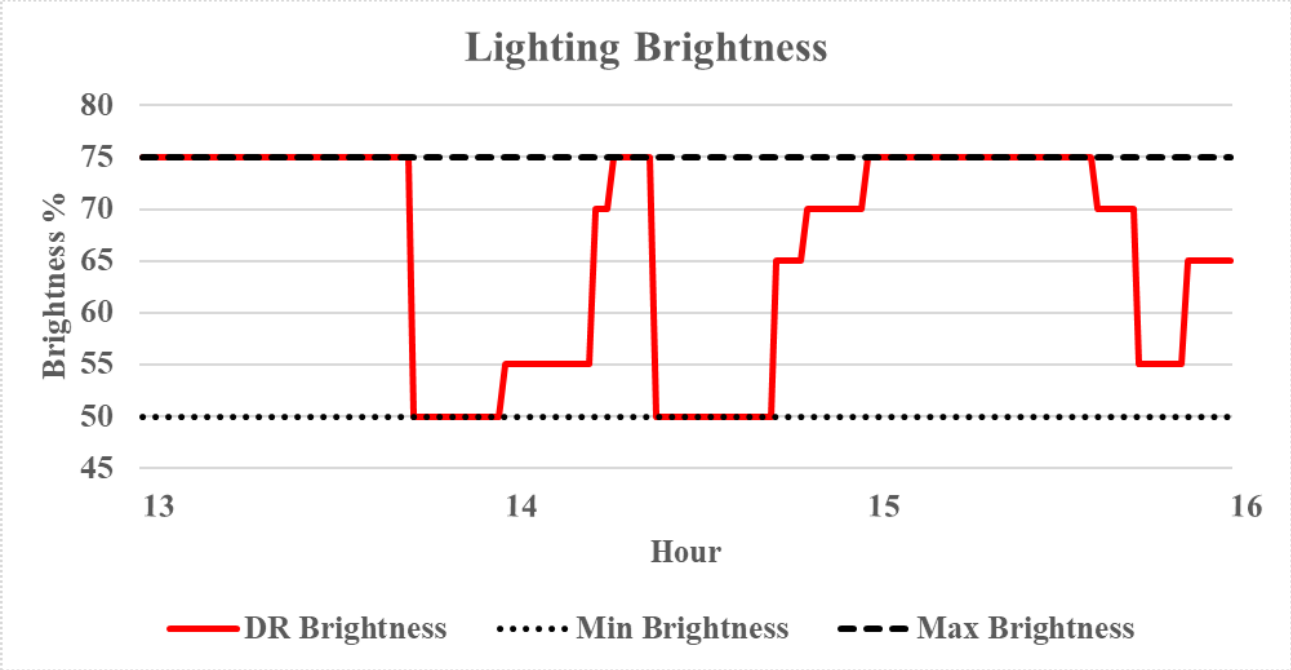

Figure 51. Variation of lighting brightness during simulated case 3.

As show in Fig. 51 the lighting brightness is maintained within the specified levels, with brightness reaching a minimum level for only 19.44% of the entire duration of the DR event. Initially the brightness is set to 75% when HVACs of T1, T3, T5 and T7 are active. The brightness varies as the configuration of active HVACs changes throughout the DR event, with a minimum of 50% reached on two occasions. First when HVACs of T1, T2, T4 and T9 are active, and then again later when HVACs of T1, T4, T6 and T7 are active. Towards the end of the DR event the brightness falls for a short period of time to 55% when HVACs of T4, T7, T8 and T10 are active, but the brightness changes back to 65% when HVACs of T5 and T6 take the place of the HVACs of T8 and T10, due to higher load priority.

Simulated Case 4

This test case is an extension of the previous case, where the load profile has again been doubled from the previous cases. Now there are 20 HVACs, 10kW of active lighting load before the DR event and 8kW of constant plug load. Load priorities for HVACs controlled by their thermostats (T1-T20) are given in the following order-T1>T2>T3>T4>T5>T6>T7>T8>T9>T10> T11>T12>T13>T14>T15> T16>T17>T18>T19>T20 which all have a common setpoint of 70°F.

In this case study, prior to the DR event when the user bid price is generated, ten of the twenty odd number HVACs are in operation, with an indoor temperature of the areas being controlled by these HVACs above the user comfort limit at 73°F, while the other ten HVACs are inactive as their thermostats have reached the desired setpoint.

Table 17. Indoor temperatures, electricity prices and demand limit for simulated case 4.

T1 (°F)	**T2 (°F)**	**T3 (°F)**	**T4 (°F)**	**T5 (°F)**	**T6 (°F)**	**T7 (°F)**	**T8 (°F)**	**T9 (°F)**	**T10 (°F)**	**Bid Price ($/kWh)**	**Cleared Price ($/kWh)**	**Demand Limit (kW)**
73	70	73	70	73	70	73	70	73	70	0.127	0.120	30
T11 (°F)	**T12 (°F)**	**T13 (°F)**	**T14 (°F)**	**T15 (°F)**	**T16 (°F)**	**T17 (°F)**	**T18 (°F)**	**T19 (°F)**	**T20 (°F)**			
73	70	73	70	73	70	73	70	73	70			

Once the bid price is cleared, the demand limit that is obtained is 30kW. Of this 8kW is reserved for constant plug load, 6.52kW is needed to maintain the minimum lighting brightness during the DR event and the remaining 15.48kW is available to operate HVACs.

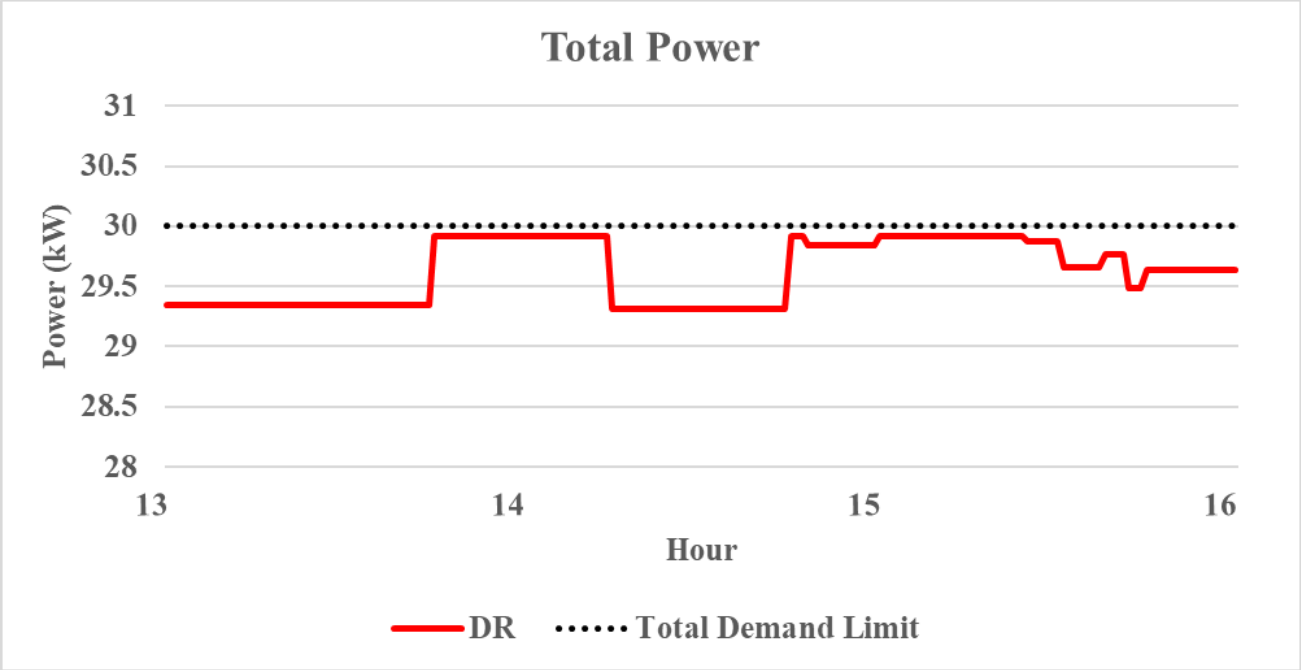

Figure 52. Total power consumption for simulated case 4.

Fig. 52 shows how the total power consumption at any given time is kept below the demand limit of 30kW, peaking at a value of 29.64kW. The total energy consumption during the DR event is 89.22kWh.

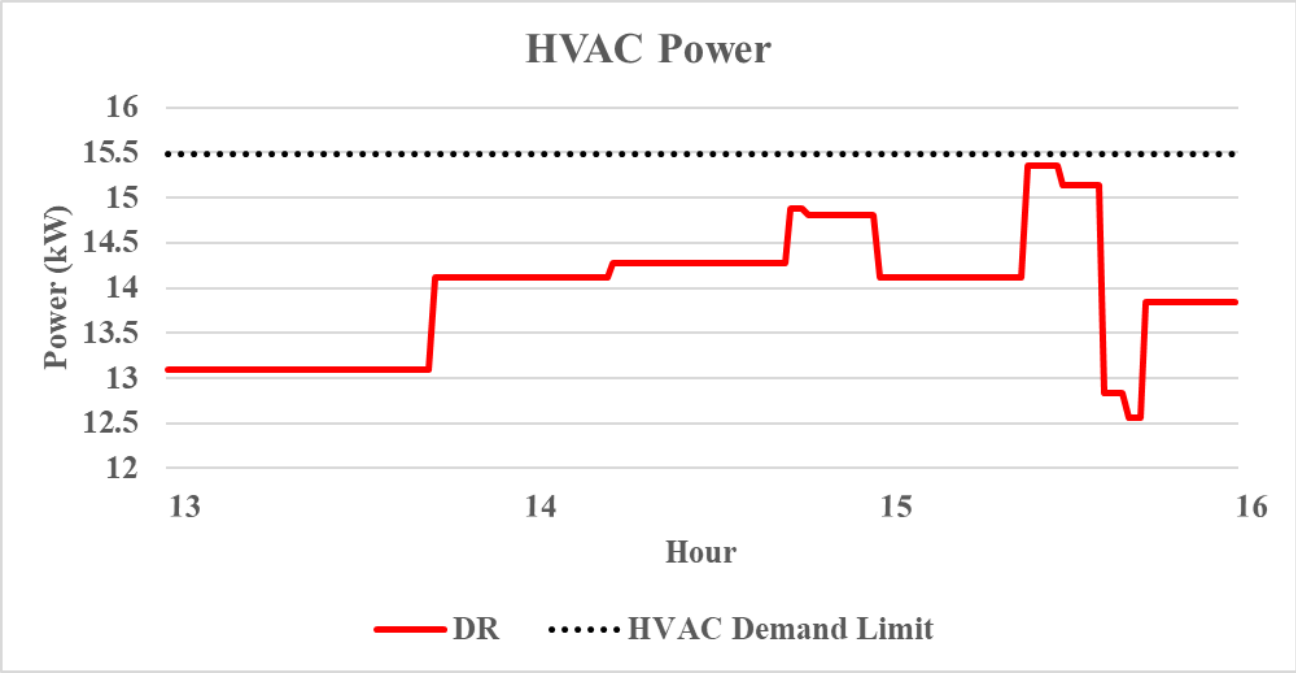

Figure 53. HVAC power consumption for simulated case 4.

The DR algorithm manages to keep the HVAC power within the specified demand limit as shown in Fig. 53 The highest HVAC power consumption is 15.35kW, whereas the total HVAC energy consumption is 42.08kWh.

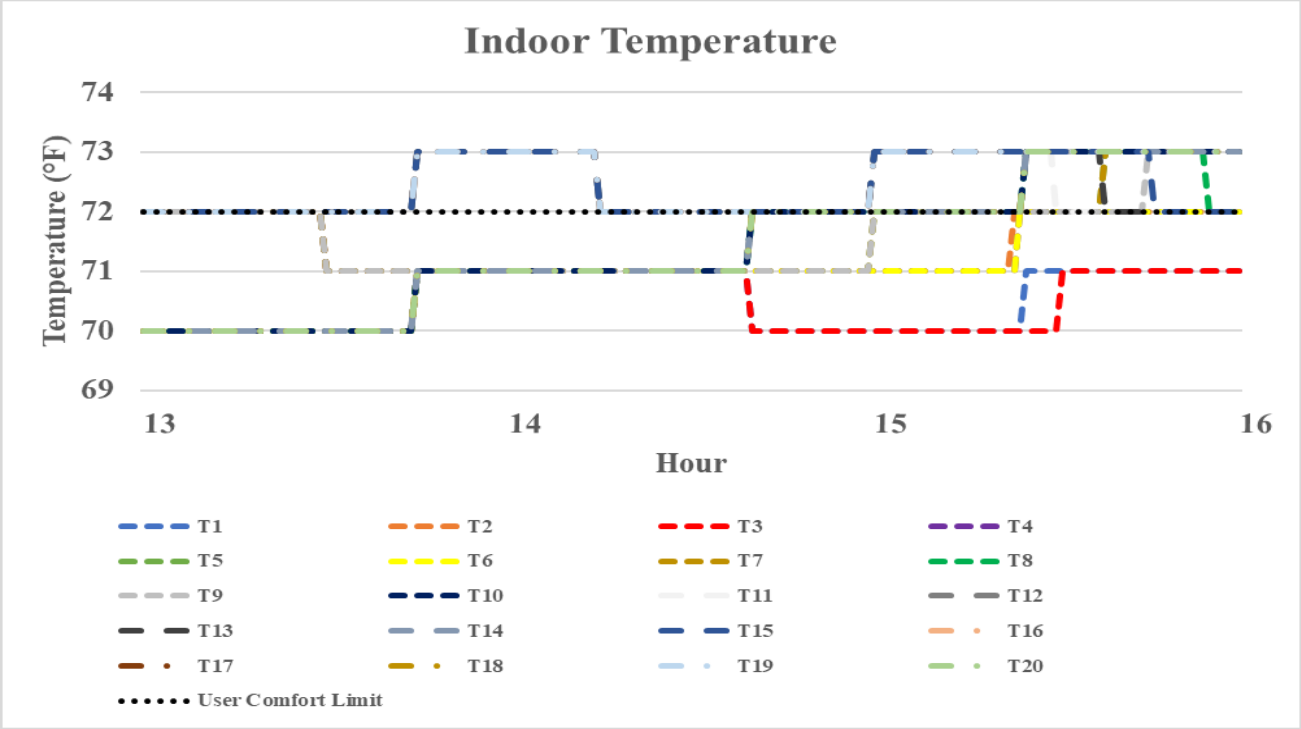

Figure 54. Variation of indoor temperatures during simulated case 4.

In this case, a larger number of thermostats record indoor temperatures going above the user comfort limit- T1-T4 and T6 are always within the comfort limit, T5 and T7 are over for a maximum of 12.78%, whereas T11, T13, T15, T17 and T19 are over the comfort limit for a maximum 33% of the DR event duration.

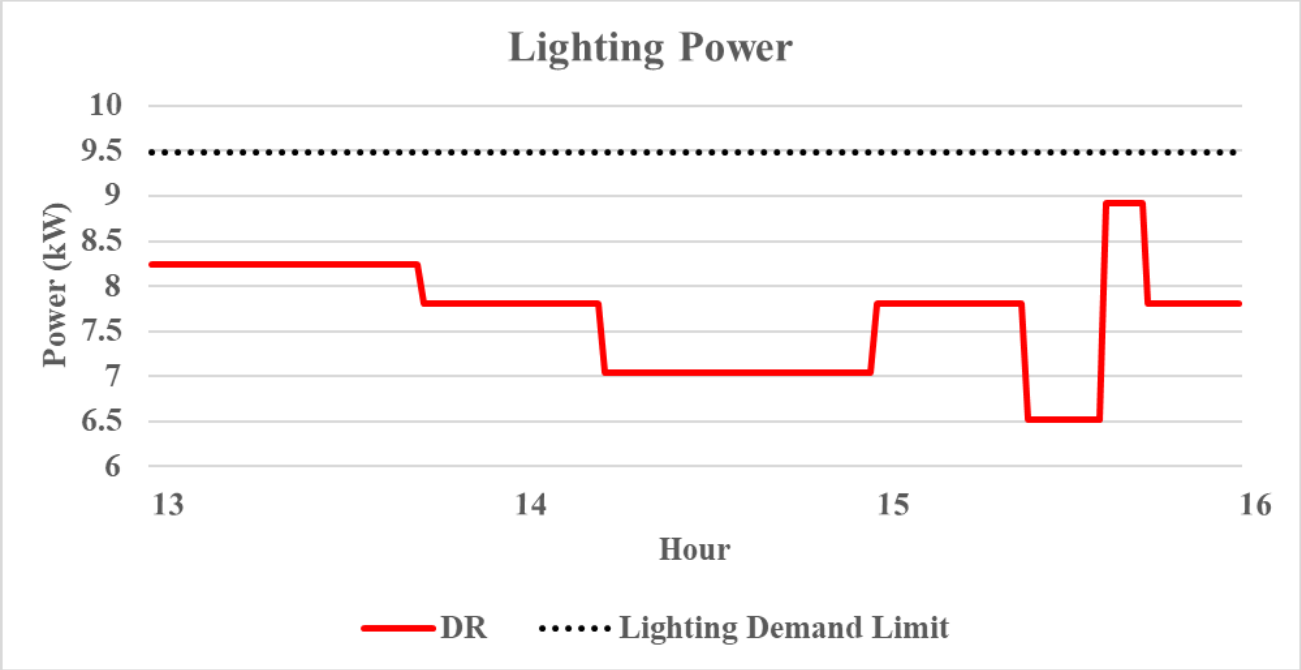

Figure 55. Lighting power consumption for simulated case 4.

From Fig. 55 We see that the DR algorithm is able to maintain the lighting power throughout the DR event below the demand limit of 9.48kW, reaching a maximum of 8.92kW. The total lighting energy consumption is 23.14kWh.

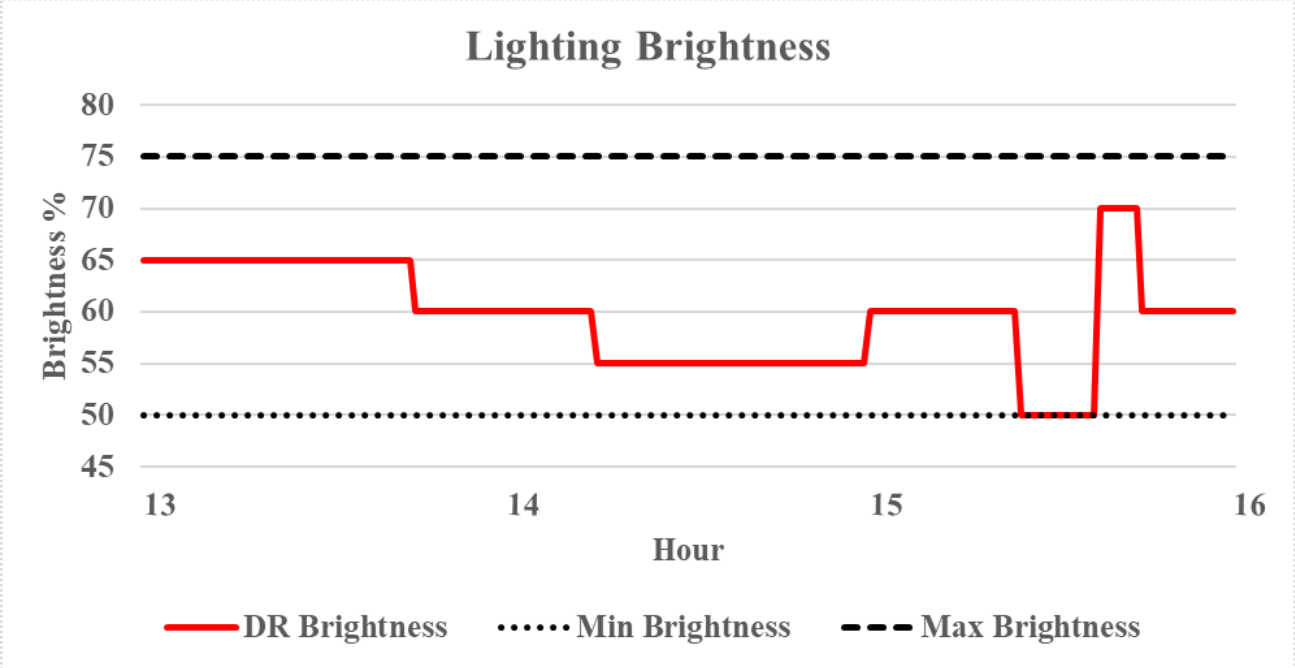

Figure 56. Variation of lighting brightness during simulated case 4.

The DR algorithm is able to maintain the lighting brightness within the desired brightness limits, while only operating at the minimum brightness level 7.22% of the total DR event duration. Initially the brightness is set to 65% when HVACs of thermostats T1, T3, T5, T7 and T9 are active, and this is the maximum brightness that can be achieved with the power left over within the demand limit. The brightness then varies at different times during the DR event based on the configuration of active HVACs. The brightness is set to a minimum level of 50% when the HVACs of T8, T10, T11, T12 and T14 are active, and there is not enough power to maintain a higher level of brightness. However, this is for a short period of time before the brightness rises back up to 70%, when the configuration of active HVACs changes again.

4.5 Results and Discussion

The demand response algorithm consisting of the user bid price calculation as well as a load scheduling technique for HVAC and lighting loads was tested in a number of real and simulated case studies.

A total of eight different case studies were carried out, based on different bid prices and demand limits summarized in Table 18.

Table 18. Summary of case study prices and demand limits.

Real			
Case	**Bid Price ($)**	**Cleared Price ($)**	**Demand Limit (kW)**
1	0.066	0.06	15
2	0.059	0.06	15
3	0.047	0.04	10
4	0.046	0.04	10
Simulated			
Case	**Bid Price ($)**	**Cleared Price ($)**	**Demand Limit (kW)**
1	0.044	0.04	10
2	0.039	0.04	10
3	0.081	0.08	20
4	0.127	0.12	30

From the Table 18, we observe that the bid price is matched to its nearest possible clearing price, after which the demand limit associated with that cleared price is allocated to the customer. In general, as the bid price increases, the allocated demand limit also increases, proving that the bid price equation developed in equation (12) can accurately model the increase in demand.

For the cases using real data, a summary of the energy savings and effect on user comfort limits and preferences are summarized in Table 19.

Table 19. Summary of case study results.

Case	Demand Limit (kW)	Total DR Energy Savings (kWh)	Total DR Energy Savings (%)	Max Time> Comfort Limit (%)	Lighting>Minimum DR Brightness (%)
1	15	15.22	27.45	10	100
2	15	16.83	29.70	0	100
3	10	17.35	40.38	14	100
4	10	20.54	44.94	0	96

As we go from Case 1 to Case 4 in Table 19 the demand limit decreases, leading to an increase in total energy savings. This is an expected result as in general a reduced demand limit, will lower the active time of each HVAC at any given time, increasing energy savings. Also, between cases having the same demand limit, if the bid price for one case is lower than the other, the energy savings are expected to be higher, as the lower initial bid price reflects a lower demand. In two out of the four cases, there is a short percentage of time during the DR event when the user comfort limit for indoor temperature is crossed. In each case, while the comfort limit is crossed, the corresponding HVAC gain highest priority and quickly bring the indoor temperature back within the user comfort limit. In case 1 this only happens because at the start of the DR event, the indoor temperature of the area controlled by T1 and T5 are above the user comfort level to begin with. In case 3 this happens only for the area controlled by T5, which has the lowest priority of all the thermostats.

The results also show that the DR algorithm is able to consistently maintain a level of lighting during the DR event higher than the specified minimum brightness level, with 4% being the most time spent with minimum lighting brightness, only in case 4.

The effect of the allocated demand limit on the 4 simulated cases are summarized in Table 20.

Table 20. Summary of simulated case study results.

Case	Demand Limit (kW)	Max Time> Comfort Limit (%)	Lighting>Minimum Brightness (%)
1	10	25	88.89
2	10	16.67	100
3	20	16.67	80.56
4	30	33	92.78

In both cases 1 and 2 only the area controlled by the thermostat T5 set to least priority, crosses for a short period of time the comfort limit of indoor temperature. The maximum time above this

level for case 1 is slightly higher, as in this case the indoor temperature of the area controlled by T5 is at 72°F from the beginning of the DR event. Given it has the least priority, it spends a longer period of time above the user defined comfort limit. In case 2, once again T5 has the lowest priority and therefore its corresponding indoor temperature eventually crosses the comfort limit having started with an indoor temperature of 71°F at the beginning of the DR event. In case 3, the demand limit increases as the total load has been doubled from before. The two thermostats given least priority T9 and T10 spend a relatively short maximum period of time above the indoor temperature comfort limit. In regards to case 4, the total load is now four times that of the cases using real data, meaning there are 20 HVACs that are to be controlled. The maximum time spent above the comfort limit is for the T11, T13, T15, T17, T19, which are among the thermostats with the bottom half of priority. The areas controlled by these thermostats started the DR event with an indoor temperature of 72°F, therefore it is expected that areas controlled by these thermostats will cross the comfort limit for some time.

From Table 20 we can also see that the level of lighting brightness maintained by the algorithm throughout the DR event is mostly above the minimum brightness level, with the least amount of time being spent above the minimum level recorded at 80.56% for case 3.

5. Conclusion

In this dissertation, two broad solutions for commercial building demand response have been presented. The first was a load disaggregation algorithm, used to disaggregate the power of several individual HVACs whose combined power data was collected using a single power meter. The second work focused on a demand response algorithm involving the determination of an optimal bid price for double-auctioning between the user and the electric utility, and then a load scheduling technique that controls single floor HVAC and lighting loads in a commercial building, considering user preferences and load priorities.

In the case of load disaggregation, a number of different machine learning classification algorithms were tested including: Decision Trees (DT), Discriminant Analysis (DA), Support Vector Machine (SVM) and k-Nearest Neighbors (k-NN). Using input features such as one-minute interval real and reactive power of the compressors and air handlers, in addition to phase currents of both, the k-NN model was found to be the most efficient model in solving the problem of aggregated power disaggregation. The error in each of the test cases was less than 10%, where the power consumption, in addition to the status of activity of each HVAC was predicted. This level of error is comparable and, in some cases lower than the error found in existing load disaggregation techniques for different load types. Therefore, the model developed here can be accurately used for the purpose of power disaggregation of identical loads.

Considering the demand response algorithm, a bid price equation has been developed which takes into consideration the current and desired state of HVAC and lighting loads as well as

considering the variations in electricity prices for 24-hours prior to the DR event. This equation is then able to generate a bid price for electricity that corresponds to a demand limit based on which an optimal load configuration is found. The load scheduling part of the algorithm involves using a k-NN classification algorithm to match the demand limit for controllable loads, to an optimal load configuration that effectively utilizes the demand limit.

The developed DR algorithm was tested in a number of real and also simulated case studies. During a DR event, HVAC and lighting loads were controlled by reasonably staying within user comfort limits of indoor temperature and lighting brightness. The minimum amount of energy saved from a three-hour DR event was found to be 27.5%, which is comparable and, in some cases, greater than savings found from using existing DR algorithms for a DR event of the same duration of time. When accumulated over a period of time, this will result in a significant reduction in electric bills for the user, and help to reduce stress conditions on the electric grid during peak load hours.

The main contributions of this dissertation can be summarized as follows:

1. A novel approach is presented to disaggregate the power data from an aggregated power usage signal, of multiple identical HVACs. This was done in order to identify which HVAC units are in operation at any given moment in time, and also to predict the power consumption, allowing the fine-grained monitoring of the individual devices whose data has been aggregated together, using only a single power meter therefore reducing costs and enhancing security.

2. A double-auction DR algorithm was developed that controls HVAC and lighting loads in commercial buildings, that takes into consideration the user's preferences and load priorities which results in the maximum possible peak reduction and energy savings for the customer.

3. A novel customer bid price equation was developed that considers the impact of HVAC and lighting loads.

4. A load scheduling technique was created based on machine learning that considers user preferences and load priorities.

6. Future Work

The load disaggregation technique that has been presented in this work focuses only on disaggregating HVAC loads. In the future this work could be extended, to disaggregate other load types such as lighting and plug loads. This would alleviate the need for individual power meters for different load types, making the system even more economically feasible and secure.

The demand response algorithm that has been developed can be extended to control plug loads in addition to HVAC and lighting loads. Examples of such loads could be: water heaters, electric vehicle charging points etc. The demand response algorithm could also be extended in the future to include the integration of renewables such as solar PV and wind generation, as energy sources.

The demand response algorithm uses a statistical building model to simulate indoor thermal behavior, which is based on historical data for the test building. The existing model could be replaced with a physical building model, using standards defined in the ASHRAE (American Society of Heating, Refrigerating and Air-Conditioning Engineers) handbook. This would enable the implementation of the demand response algorithm in newly designed buildings, that do not have historical data.

7. References

[1] G.W. Hart, “Nonintrusive appliance load monitoring,” *Proc. IEEE*, vol. 80, no. 12, pp. 1870–1891, Dec. 1992.

[2] C. Mavrokefalidis, D. Ampeliotis, E. Vlachos, K. Berberidis and E. Varvarigos, "Supervised energy disaggregation using dictionary — based modelling of appliance states," *2016 IEEE PES Innovative Smart Grid Technologies Conference Europe (ISGT-Europe)*, Ljubljana, 2016, pp. 1-6.

[3] R. Sinha, S. Spoorthy, P. Khurana and M. G. Chandra, "Power system load data models and disaggregation based on sparse approximations," *2016 IEEE 14th International Conference on Industrial Informatics (INDIN)*, Poitiers, 2016, pp. 292-299.

[4] C. Mavrokefalidis, D. Ampeliotis, E. Vlachos, K. Berberidis and E. Varvarigos, "Supervised energy disaggregation using dictionary — based modelling of appliance states," *2016 IEEE PES Innovative Smart Grid Technologies Conference Europe (ISGT-Europe)*, Ljubljana, 2016, pp. 1-6.

[5] A. Rogriguez, S. T. Smith, A. Kiff and B. Potter, "Small power load disaggregation in office buildings based on electrical signature classification," *2016 IEEE International Energy Conference (ENERGYCON)*, Leuven, 2016, pp. 1-6.

[6] N. K. Thokala, M. G. Chandra and K. Nagasubramanian, "On load disaggregation using discrete events," *2016 IEEE Innovative Smart Grid Technologies - Asia (ISGT-Asia)*, Melbourne, VIC, 2016, pp. 324-329.

[7] C. Dinesh, B. W. Nettasinghe, R. I. Godaliyadda, M. P. B. Ekanayake, J. Ekanayake and J. V. Wijayakulasooriya, "Residential Appliance Identification Based on Spectral Information of Low Frequency Smart Meter Measurements," in *IEEE Transactions on Smart Grid*, vol. 7, no. 6, pp. 2781-2792, Nov. 2016.

[8] M. Mahmoudi, J. Dong, K. Tomsovic, and S. Djouadi, “Application of distributed control to mitigate disturbance propagations in large power networks,” in *Proc. North Amer. Power Symp.*, 2015, pp. 1–6.

[9] M. Mahmoudi and K. Tomsovic, “A distributed control design methodology for damping critical modes in power systems,” in *Proc. Power Energy Conf. Illinois*, 2016, pp. 1–6.

[10] A. Asadinejad, K. Tomsovic, and M. G. Varzaneh, “Examination of incentive based demand response in western connection reduced model,” in *Proc. North Amer. Power Symp.*, 2015, pp. 1–6.

[11] A. Asadinejad,M.G.Varzaneh,K. Tomsovic, C.-f. Chen, and R. Sawhney, “Residential customers elasticity estimation and clustering based on their contribution at incentive based demand response,” in *Proc. IEEE Power Energy Soc. General Meeting*, 2016, pp. 1–6.

[12] A. Asadinejad and K. Tomsovic, “Optimal use of incentive and price based demand response to reduce costs and price volatility,” *Electr. Power Syst. Res.*, vol. 144, pp. 215–223, 2017.

[13] J. D. Guedes,D.D. Ferreira, and B.H.Barbosa, “A non-intrusive approach to classify electrical appliances based on higher-order statistics and genetic algorithm: A smart grid perspective,” *Electr. Power Syst. Res.*, vol. 140, pp. 65–69, 2016.

[14] S. M. Tabatabaei, S. Dick, and W. Xu, “Towards non-intrusive load monitoring via multi-label classification,” *IEEE Trans. Smart Grid*, vol. 8, no. 1, pp. 26–40, Jan. 2016.

[15] N.Henao, K. Agbossou, S. Kelouwani, Y. Dubé and M. Fournier, "Approach in Nonintrusive Type I Load Monitoring Using Subtractive Clustering," in *IEEE Transactions on Smart Grid*, vol. 8, no. 2, pp. 812-821, March 2017.

[16] M.Azaza and F. Wallin, "Supervised household's loads pattern recognition," *2016 IEEE Electrical Power and Energy Conference (EPEC)*, Ottawa, ON, 2016, pp. 1-5.

[17] V.Mehra, R. Ram and C. Vergara, "A novel application of machine learning techniques for activity-based load disaggregation in rural off-grid, isolated solar systems," *2016 IEEE Global Humanitarian Technology Conference (GHTC)*, Seattle, WA, 2016, pp. 372-378.

[18] S. Biansoongnern and B. Plangklang, "Nonintrusive load monitoring (NILM) using an Artificial Neural Network in embedded system with low sampling rate," *2016 13th International Conference on Electrical Engineering/Electronics, Computer, Telecommunications and Information Technology (ECTI-CON)*, Chiang Mai, 2016, pp. 1-4.

[19] J. Tian, Y. Wu, S. Liu and P. Liu, "Residential load disaggregation based on resident behavior learning and neural networks," *2017 IEEE Conference on Energy Internet and Energy System Integration (EI2)*, Beijing, 2017, pp. 1-5.

[20] D. C. Mocanu, E. Mocanu, P. H. Nguyen, M. Gibescu and A. Liotta, "Big IoT data mining for real-time energy disaggregation in buildings," *2016 IEEE International Conference on Systems, Man, and Cybernetics (SMC)*, Budapest, 2016, pp. 003765-003769.

[21] O. Van Cutsem, G. Lilis and M. Kayal, "Automatic multi-state load profile identification with application to energy disaggregation," *2017 22nd IEEE International Conference on Emerging Technologies and Factory Automation (ETFA)*, Limassol, 2017, pp. 1-8.

[22] W. Kong, Z. Y. Dong, J. Ma, D. Hill, J. Zhao and F. Luo, "An Extensible Approach for Non-Intrusive Load Disaggregation with Smart Meter Data," in *IEEE Transactions on Smart Grid*, vol. PP, no. 99, pp. 1-1.

[23] Aid, M., & Lee, P. H.” Unsupervised approach for load disaggregation with devices interactions.” *Energy and Buildings*, 2016, 116, pp. 96-103.

[24] Aid, M., & Lee, P. H.” Non-intrusive load disaggregation with adaptive estimations of devices main power effects and two-way interactions.” *Energy and Buildings*, 2016, 130, pp. 131-139.

[25] K. Kumar and M. G. Chandra, "Event and feature based electrical load disaggregation using graph signal processing," *2017 IEEE 13th International Colloquium on Signal Processing & its Applications (CSPA)*, Batu Feringgi, 2017, pp. 168-172.

[26] T.Ozaki, N. Uchida and H. Mineno, "Development of electric power disaggregation system for chain stores," *2016 IEEE 5th Global Conference on Consumer Electronics*, Kyoto, 2016, pp. 1-2.

[27] A. Miyasawa, M. Matsumoto, Y. Fujimoto and Y. Hayashi, "Energy disaggregation based on semi-supervised matrix factorization using feedback information from consumers," *2017 IEEE PES Innovative Smart Grid Technologies Conference Europe (ISGT-Europe)*, Torino, 2017, pp. 1-6.

[28] G. C. Koutitas and L. Tassiulas, "Low Cost Disaggregation of Smart Meter Sensor Data," in *IEEE Sensors Journal*, vol. 16, no. 6, pp. 1665-1673, March15, 2016.

[29] Rahimpour, H. Qi, D. Fugate and T. Kuruganti, "Non-Intrusive Energy Disaggregation Using Non-Negative Matrix Factorization With Sum-to-k Constraint," in *IEEE Transactions on Power Systems*, vol. 32, no. 6, pp. 4430-4441, Nov. 2017.

[30] Brown, R., Ghavami, N., Siddiqui, H., Adjrad, M., Ghavami, M. and Dudley, S. (2017). Occupancy based household energy disaggregation using ultra-wideband radar and electrical signature profiles. *Energy and Buildings*, 141, pp.134-141.

[31] E. Sala, K. Kampouropoulos, M. D. Prieto and L. Romeral, "Disaggregation of HVAC load profiles for the monitoring of individual equipment," *2016 IEEE 21st International Conference on Emerging Technologies and Factory Automation (ETFA)*, Berlin, 2016, pp. 1-6.

[32] T.D. Huang, W. S. Wang and K. L. Lian, "A New Power Signature for Nonintrusive Appliance Load Monitoring," in *IEEE Transactions on Smart Grid*, vol. 6, no. 4, pp. 1994-1995, July 2015.

[33] A.Filippi, R. Rietman, Y. Wang and S. Bertagna de Marchi, "Voltage only multi-appliance power disaggregation," *2012 IEEE International Energy Conference and Exhibition (ENERGYCON)*, Florence, 2012, pp. 915-920.

[34] Perez, K. X., Cole, W. J., Baldea, M., & Edgar, T. F. (n.d.). “Nonintrusive Disaggregation of Residential Air- Conditioning Loads from Sub-hourly Smart Meter Data”. *Energy and Buildings*.

[35] D.Egarter and W. Elmenreich, "Autonomous load disaggregation approach based on active power measurements," *2015 IEEE International Conference on Pervasive Computing and Communication Workshops (PerCom Workshops)*, St. Louis, MO, 2015, pp. 293-298.

[36] N.Czarnek, K. Morton, L. Collins, R. Newell and K. Bradbury, "Performance comparison framework for energy disaggregation systems," *2015 IEEE International Conference on Smart Grid Communications (SmartGridComm)*, Miami, FL, 2015, pp. 446-452.

[37] T.Liu, X. Ding and N. Gu, "A Generic Energy Disaggregation Approach: What and When Electrical Appliances are Used," *2015 IEEE International Conference on Data Mining Workshop (ICDMW)*, Atlantic City, NJ, 2015, pp. 389-397.

[38] T.Bernard, D. Wohland, J. Klaaßen and G. vom Bögel, "Combining several distinct electrical features to enhance nonintrusive load monitoring," *2015 International Conference on Smart Grid and Clean Energy Technologies (ICSGCE)*, Offenburg, 2015, pp. 139-143.

[39] JianLiang, S. Ng, G. Kendall and J. Cheng, "Load signature study ¡V part I: Basic concept, structure and methodology," *IEEE PES General Meeting*, Minneapolis, MN, 2010, pp. 1-1.

[40] J.T. Chiang, T. Zhang, B. Chen and Y. C. Hu, "Load disaggregation using harmonic analysis and regularized optimization," *Proceedings of The 2012 Asia Pacific Signal and Information Processing Association Annual Summit and Conference*, Hollywood, CA, 2012, pp. 1-4.

[41] Norford, L. K., & Leeb, S. B. "Non-intrusive electrical load monitoring in commercial buildings based on steady-state and transient load-detection algorithms." *Energy and Buildings*, 1996, 24, pp. 51-64.

[42] Ji, Y., Xu, P., & Ye, Y. "HVAC terminal hourly end-use disaggregation in commercial buildings with Fourier series model." *Energy and Buildings*, 2015, 97, pp. 33-46.

[43] C.Elbe and E. Schmautzer, "Appliance-specific energy consumption feedback for domestic consumers using load disaggregation methods," *22nd International Conference and Exhibition on Electricity Distribution(CIRED 2013)*, Stockholm, 2013, pp. 1-4.

[44] GuanchenZhang, G. Wang, H. Farhangi and A. Palizban, "Residential electric load disaggregation for low-frequency utility applications," *2015 IEEE Power & Energy Society General Meeting*, Denver, CO, 2015, pp. 1-5.

[45] G.Elafoudi, L. Stankovic and V. Stankovic, "Power disaggregation of domestic smart meter readings using dynamic time warping," *2014 6th International Symposium on Communications, Control and Signal Processing (ISCCSP)*, Athens, 2014, pp. 36-39.

[46] R.Dong, L. Ratliff, H. Ohlsson and S. S. Sastry, "A dynamical systems approach to energy disaggregation," *52nd IEEE Conference on Decision and Control*, Firenze, 2013, pp. 6335-6340.

[47] M. Mirhosseini, M. Marzband and M. Oloomi, "Short term load forecasting by using neural network structure," *2009 6th International Conference on Electrical Engineering/Electronics, Computer, Telecommunications and Information Technology*, Pattaya, Chonburi, 2009, pp. 240-243.

[48] Guillermo Escrivá-Escrivá, Carlos Álvarez-Bel, Carlos Roldán-Blay, Manuel Alcázar-Ortega, "New artificial neural network prediction method for electrical consumption forecasting based on building end-uses," *Energy and Buildings*, Volume 43, Issue 11, 2011, Pages 3112-3119.

[49] Marino, Daniel & Amarasinghe, Kasun & Manic, Milos. (2016). Building Energy Load Forecasting using Deep Neural Networks. 10.1109/*IECON*.2016.7793413.

[50] W. Mai, C. Y. Chung, T. Wu and H. Huang, "Electric load forecasting for large office building based on radial basis function neural network," *2014 IEEE PES General Meeting | Conference & Exposition*, National Harbor, MD, 2014, pp. 1-5.

[51] L. Li, K. Ota and M. Dong, "When Weather Matters: IoT-Based Electrical Load Forecasting for Smart Grid," in *IEEE Communications Magazine*, vol. 55, no. 10, pp. 46-51, Oct. 2017.

[52] S. S. Reddy and J. A. Momoh, "Short term electrical load forecasting using back propagation neural networks," *2014 North American Power Symposium (NAPS)*, Pullman, WA, 2014, pp. 1-6.

[53] G. M. Khan, A. R. Khattak, F. Zafari and S. A. Mahmud, "Electrical load forecasting using fast learning recurrent neural networks," *The 2013 International Joint Conference on Neural Networks (IJCNN)*, Dallas, TX, 2013, pp. 1-6.

[54] Enric Sala-Cardoso, Miguel Delgado-Prieto, Konstantinos Kampouropoulos, Luis Romeral, "Activity-aware HVAC power demand forecasting," *Energy and Buildings*, Volume 170, 2018, Pages 15-24.

[55] H. Park, B. Lee, J. Son and H. Ahn, "A comparison of neural network-based methods for load forecasting with selected input candidates," *2017 IEEE International Conference on Industrial Technology (ICIT)*, Toronto, ON, 2017, pp. 1100-1105.

[56] M.C. Leung, Norman C.F. Tse, L.L. Lai, T.T. Chow, "The use of occupancy space electrical power demand in building cooling load prediction," *Energy and Buildings*, Volume 55, 2012, Pages 151-163.

[57] J. Berardino and C. Nwankpa, "Inclusion of temporal effects in forecasting building electrical loads for demand resource planning," *2013 IEEE Grenoble Conference*, Grenoble, 2013, pp. 1-6.

[58] Zeyu Wang, Yueren Wang, Ruochen Zeng, Ravi S. Srinivasan, Sherry Ahrentzen, "Random Forest based hourly building energy prediction," *Energy and Buildings*, Volume 171, 2018, Pages 11-25.

[59] C. Sandels, J. Widén, L. Nordström, E. Andersson, "Day-ahead predictions of electricity consumption in a Swedish office building from weather, occupancy, and temporal data," *Energy and Buildings*, Volume 108, 2015, Pages 279-290.

[60] Yibo Chen, Hongwei Tan, Umberto Berardi, "Day-ahead prediction of hourly electric demand in non-stationary operated commercial buildings: A clustering-based hybrid approach," *Energy and Buildings*, Volume 148, 2017, Pages 228-237.

[61] L. W. Chong, D. Rengasamy, Y. W. Wong and R. K. Rajkumar, "Load prediction using support vector regression," *TENCON 2017 - 2017 IEEE Region 10 Conference*, Penang, 2017, pp. 1069-1074.

[62] Yan Ding, Qiang Zhang, Tianhao Yuan, Kun Yang, "Model input selection for building heating load prediction: A case study for an office building in Tianjin," *Energy and Buildings*, Volume 159, 2018, Pages 254-270.

[63] K. Palapanyakul and P. Siripongwutikorn, "Prediction model of short-term electrical load in an air conditioning environment," *2017 International Electrical Engineering Congress (iEECON)*, Pattaya, 2017, pp. 1-4.

[64] N. K. Thokala, A. Bapna and M. G. Chandra, "A deployable electrical load forecasting solution for commercial buildings," *2018 IEEE International Conference on Industrial Technology (ICIT)*, Lyon, 2018, pp. 1101-1106.

[65] S. Ajmera, A. K. Singh and V. Chauhan, "An approach towards medium term forecasting based on support vector regression," *2016 IEEE 7th Power India International Conference (PIICON)*, Bikaner, 2016, pp. 1-6.

[66] L. Cheng, Y. Zhang, L. Suo, S. Shen, F. Fang and L. Jin, "Short-term cooling, heating and electrical load forecasting in business parks based on improved entropy method," *2017 36th Chinese Control Conference (CCC)*, Dalian, 2017, pp. 10611-10616.

[67] K. P. Warrior, M. Shrenik and N. Soni, "Short-term electrical load forecasting using predictive machine learning models," *2016 IEEE Annual India Conference (INDICON)*, Bangalore, 2016, pp. 1-6.

[68] Tanveer Ahmad, Huanxin Chen, "Short and medium-term forecasting of cooling and heating load demand in building environment with data-mining based approaches," *Energy and Buildings*, Volume 166, 2018, Pages 460-476.

[69] P. Saatwong and S. Suwankawin, "Short-term electricity load forecasting for Building Energy Management System," *2016 13th International Conference on Electrical Engineering/Electronics, Computer, Telecommunications and Information Technology (ECTI-CON)*, Chiang Mai, 2016, pp. 1-6.

[70] X. Yang *et al*., "A forecasting method of air conditioning energy consumption based on extreme learning machine algorithm," *2017 6th Data Driven Control and Learning Systems (DDCLS)*, Chongqing, 2017, pp. 89-93.

[71] Zhongjiao Ma, Jialin Song, Jili Zhang, "Energy consumption prediction of air-conditioning systems in buildings by selecting similar days based on combined weights," *Energy and Buildings*, Volume 151, 2017, Pages 157-166.

[72] Danielle Monfet, Maria Corsi, Daniel Choinière, Elena Arkhipova, "Development of an energy prediction tool for commercial buildings using case-based reasoning," *Energy and Buildings*, Volume 81, 2014, Pages 152-160.

[73] Xiwang Li, Jin Wen, “Building energy consumption on-line forecasting using physics based system identification,” *Energy and Buildings*, Volume 82, 2014, Pages 1-12.

[74] Y. Kim, "Optimal Price Based Demand Response of HVAC Systems in Multizone Office Buildings Considering Thermal Preferences of Individual Occupants Buildings," in *IEEE Transactions on Industrial Informatics*, vol. 14, no. 11, pp. 5060-5073, Nov. 2018.

[75] Y. M. Lee, R. Horesh and L. Liberti, "Simulation and optimization of energy efficient operation of HVAC system as demand response with distributed energy resources," *2015 Winter Simulation Conference (WSC)*, Huntington Beach, CA, 2015, pp. 991-999.

[76] X. Pan and B. Lee, "An Approach of Reinforcement Learning Based Lighting Control for Demand Response," *PCIM Europe 2016; International Exhibition and Conference for Power Electronics, Intelligent Motion, Renewable Energy and Energy Management*, Nuremberg, Germany, 2016, pp. 1-8.

[77] Zhijin Cheng, Qianchuan Zhao, Fulin Wang, Yi Jiang, Li Xia, Jinlei Ding, “Satisfaction based Q-learning for integrated lighting and blind control,” *Energy and Buildings*, Volume 127, 2016, Pages 43-55.

[78] J. Vasudevan and K. S. Swarup, "Price based Demand Response strategy considering load priorities," *2016 IEEE 6th International Conference on Power Systems (ICPS)*, New Delhi, 2016, pp. 1-6.

[79] S. A. Husen, A. Pandharipande, L. Tolhuizen, Ying Wang and Meng Zhao, "Lighting systems control for demand response," *2012 IEEE PES Innovative Smart Grid Technologies (ISGT)*, Washington, DC, 2012, pp. 1-6.

[80] R. Çakmak and İ. H. Altaş, "Optimal scheduling of time shiftable loads in a task scheduling based demand response program by symbiotic organisms search algorithm," *2017 Saudi Arabia Smart Grid (SASG)*, Jeddah, 2017, pp. 1-7.

[81] B. Sivaneasan, K. Thachinamoorthi and K. P. Goh, "Interruptible load scheme: Demand response management for buildings," *2016 IEEE Region 10 Conference (TENCON)*, Singapore, 2016, pp. 1716-1719.

[82] M. B. Kjærgaard *et al*., "Demand response in commercial buildings with an Assessable impact on occupant comfort," *2016 IEEE International Conference on Smart Grid Communications (SmartGridComm)*, Sydney, NSW, 2016, pp. 447-452.

[83] Krystian X. Perez, Michael Baldea, Thomas F. Edgar, “Integrated HVAC management and optimal scheduling of smart appliances for community peak load reduction,” *Energy and Buildings*, Volume 123, 2016, Pages 34-40.

[84] Diana Manjarres, Ana Mera, Eugenio Perea, Adelaida Lejarazu, Sergio Gil-Lopez, “An energy-efficient predictive control for HVAC systems applied to tertiary buildings based on regression techniques,” *Energy and Buildings*, Volume 152, 2017, Pages 409-417.

[85] Luís L. Fernandes, Eleanor S. Lee, Dennis L. DiBartolomeo, Andrew McNeil, “Monitored lighting energy savings from dimmable lighting controls in The New York Times Headquarters Building,” *Energy and Buildings*, Volume 68, Part A, 2014, Pages 498-514.

[86] Erhan E. Dikel, Guy R. Newsham, Henry Xue, Julio J. Valdés, “Potential energy savings from high-resolution sensor controls for LED lighting,” *Energy and Buildings*, Volume 158, 2018, Pages 43-53.

[87] Andrea Peruffo, Ashish Pandharipande, David Caicedo, Luca Schenato, “Lighting control with distributed wireless sensing and actuation for daylight and occupancy adaptation,” *Energy and Buildings*, Volume 97, 2015, Pages 13-20.

[88] R. Adhikari, M. Pipattanasomporn, M. Kuzlu and S. Rahman, "Simulation study of transactive control strategies for residential HVAC systems," *2016 IEEE PES Innovative Smart Grid Technologies Conference Europe (ISGT-Europe)*, Ljubljana, 2016, pp. 1-5.

[89] H. Hao, C. D. Corbin, K. Kalsi and R. G. Pratt, "Transactive Control of Commercial Buildings for Demand Response," in *IEEE Transactions on Power Systems*, vol. 32, no. 1, pp. 774-783, Jan. 2017.

[90] R. R. Nejad and S. M. M. Tafreshi, "A new method for demand response by real-time pricing signals for lighting loads," *2012 Power Engineering and Automation Conference*, Wuhan, 2012, pp. 1-5.

[91] A. Albert and R. Rajagopal, "Strategic scheduling of residential energy consumers," *2015 54th IEEE Conference on Decision and Control (CDC)*, Osaka, 2015, pp. 3260-3265.

[92] H. Huang, Y. Cai, H. Xu and H. Yu, "A Multiagent Minority-Game-Based Demand-Response Management of Smart Buildings Toward Peak Load Reduction," in *IEEE Transactions on Computer-Aided Design of Integrated Circuits and Systems*, vol. 36, no. 4, pp. 573-585, April 2017.

[93] J. Cao, B. Yang, K. Ma, C. Chen and X. Guan, "Residential HVAC load control strategy based on game theory," *2017 Chinese Automation Congress (CAC)*, Jinan, 2017, pp. 5933-5938.

[94] P. Faria, Â. Pinto, Z. Vale, M. Khorram, F. B. de Lima Neto and T. Pinto, "Lighting consumption optimization using fish school search algorithm," *2017 IEEE Symposium Series on Computational Intelligence (SSCI)*, Honolulu, HI, 2017, pp. 1-5.

[95] Azim Keshtkar, Siamak Arzanpour, Fazel Keshtkar, “Adaptive residential demand-side management using rule-based techniques in smart grid environments,” *Energy and Buildings*, Volume 133, 2016, Pages 281-294.

[96] S. Zou, Z. Ma, Y. Shao, L. Ran and X. Liu, "Efficient and dynamic double auctions for resource allocation," 2016 IEEE 55th Conference on Decision and Control (CDC), Las Vegas, NV, 2016, pp. 6062-6067.

[97] M. Khorasany, Y. Mishra and G. Ledwich, "Auction based energy trading in transactive energy market with active participation of prosumers and consumers," 2017 Australasian Universities Power Engineering Conference (AUPEC), Melbourne, VIC, 2017, pp. 1-6.

[98] M. N. Faqiry and S. Das, "Double-Sided Energy Auction in Microgrid: Equilibrium Under Price Anticipation," in IEEE Access, vol. 4, pp. 3794-3805, 2016.

[99] B. P. Majumder, M. N. Faqiry, S. Das and A. Pahwa, "An efficient iterative double auction for energy trading in microgrids," 2014 IEEE Symposium on Computational Intelligence Applications in Smart Grid (CIASG), Orlando, FL, 2014, pp. 1-7.

[100] S. Thakur, B. P. Hayes and J. G. Breslin, "Distributed Double Auction for Peer to Peer Energy Trade using Blockchains," 2018 5th International Symposium on Environment-Friendly Energies and Applications (EFEA), Rome, 2018, pp. 1-8.

[101] P. G. Flikkema, "A multi-round double auction mechanism for local energy grids with distributed and centralized resources," 2016 IEEE 25th International Symposium on Industrial Electronics (ISIE), Santa Clara, CA, 2016, pp. 672-677.

[102] Huiye Ma and Ho-fung Leung, "An adaptive attitude bidding strategy for agents in continuous double auctions," 2005 IEEE International Conference on e-Technology, e-Commerce and e-Service, Hong Kong, 2005, pp. 38-43.

[103] B. Ramachandran, S. K. Srivastava, D. A. Cartes and C. S. Edrington, "Distributed energy resource management in a smart grid by risk based auction strategy for profit maximization," IEEE PES General Meeting, Providence, RI, 2010, pp. 1-7.

[104] B. Ramachandran, S. K. Srivastava, C. S. Edrington and D. A. Cartes, "An Intelligent Auction Scheme for Smart Grid Market Using a Hybrid Immune Algorithm," in IEEE Transactions on Industrial Electronics, vol. 58, no. 10, pp. 4603-4612, Oct. 2011.

[105] M. N. Faqiry and S. Das, "Double Auction With Hidden User Information: Application to Energy Transaction in Microgrid," in IEEE Transactions on Systems, Man, and Cybernetics: Systems.

[106] N. K. Sharma, A. Banshwar, J. Kaur Saini, Y. R. Sood and R. Shrivastava, "Economic Profit Maximization by Optimal Allocation and Sizing of WPG in Double Auction Competitive Electricity Market," 2018 International Conference on Power Energy, Environment and Intelligent Control (PEEIC), Greater Noida, India, 2018, pp. 254-257.

[107] W. El-Baz and P. Tzscheutschler, "Autonomous coordination of smart buildings in microgrids based on a double-sided auction," 2017 IEEE Power & Energy Society General Meeting, Chicago, IL, 2017, pp. 1-5.

[108] D. An, Q. Yang, W. Yu, X. Yang, X. Fu and W. Zhao, "SODA: Strategy-Proof Online Double Auction Scheme for Multimicrogrids Bidding," in IEEE Transactions on Systems, Man, and Cybernetics: Systems, vol. 48, no. 7, pp. 1177-1190, July 2018.

[109] P. G. Flikkema, "A multi-round double auction mechanism for local energy grids with distributed and centralized resources," 2016 IEEE 25th International Symposium on Industrial Electronics (ISIE), Santa Clara, CA, 2016, pp. 672-677.

[110] J. C. Fuller, K. P. Schneider and D. Chassin, "Analysis of Residential Demand Response and double-auction markets," 2011 IEEE Power and Energy Society General Meeting, Detroit, MI, USA, 2011, pp. 1-7.

[111] Y. Sun, A. Somani and T. E. Carroll, "Learning based bidding strategy for HVAC systems in double auction retail energy markets," 2015 American Control Conference (ACC), Chicago, IL, 2015, pp. 2912-2917.

[112] D. Li, Q. Yang, W. Yu, D. An, X. Yang and W. Zhao, "A strategy-proof privacy-preserving double auction mechanism for electrical vehicles demand response in microgrids," 2017 IEEE 36th International Performance Computing and Communications Conference (IPCCC), San Diego, CA, 2017, pp. 1-8.

[113] D. Li, Q. Yang, W. Yu, D. An and X. Yang, "Towards double auction for assisting electric vehicles demand response in smart grid," 2017 13th IEEE Conference on Automation Science and Engineering (CASE), Xi'an, 2017, pp. 1604-1609.

[114] D. Li, Q. Yang, D. An, W. Yu, X. Yang and X. Fu, "On Location Privacy-Preserving Online Double Auction for Electric Vehicles in Microgrids," in IEEE Internet of Things Journal, vol. 6, no. 4, pp. 5902-5915, Aug. 2019

[115] Y. Li, C. Liao, Y. Wang and C. Wang, "Energy-Efficient Optimal Relay Selection in Cooperative Cellular Networks Based on Double Auction," in IEEE Transactions on Wireless Communications, vol. 14, no. 8, pp. 4093-4104, Aug. 2015.

[116] N. Reyhanian, B. Maham, V. Shah-Mansouri and C. Yuen, "Double-auction-based energy trading for small cell networks with energy harvesting," 2016 IEEE International Conference on Communications (ICC), Kuala Lumpur, 2016, pp. 1-6.

[117] L. Tang and H. Chen, "Double auction mechanism for request outsourcing in cloud federation," 2015 IEEE International Conference on Communication Workshop (ICCW), London, 2015, pp. 1889-1894.

[118] L. Deng, F. Xu, Y. Ren, S. Bao, H. He and C. Li, "Resource allocation method based on combinatorial double auction mechanism in cloud computing," 2018 13th IEEE Conference on Industrial Electronics and Applications (ICIEA), Wuhan, 2018, pp. 801-806.

[119] Yang Bai, Haiwang Zhong and Qing Xia, "Real-time demand response potential evaluation: A smart meter driven method," *2016 IEEE Power and Energy Society General Meeting (PESGM)*, Boston, MA, 2016, pp. 1-5.

[120] T. Lu, C. Gao, L. Sun, F. Liu, Y. Han and J. Zhang, "A calculation of power users' demand response potential under the angle of big data," *2015 5th International Conference on Electric Utility Deregulation and Restructuring and Power Technologies (DRPT)*, Changsha, 2015, pp. 127-134.

[121] B. J. Johnson, M. R. Starke, O. A. Abdelaziz, R. K. Jackson and L. M. Tolbert, "A dynamic simulation tool for estimating demand response potential from residential loads," *2015 IEEE Power & Energy Society Innovative Smart Grid Technologies Conference (ISGT)*, Washington, DC, 2015, pp. 1-5.

[122] M. Ali, A. Safdarian and M. Lehtonen, "Demand response potential of residential HVAC loads considering users preferences," *IEEE PES Innovative Smart Grid Technologies, Europe*, Istanbul, 2014, pp. 1-6.

[123] Sergi Rotger-Griful, Rune Hylsberg Jacobsen, Dat Nguyen, Gorm Sørensen, "Demand response potential of ventilation systems in residential buildings," *Energy and Buildings*, Volume 121, 2016, Pages 1-10.

[124] Limei Shen, Zhengwei Li, Yongjun Sun, "Performance evaluation of conventional demand response at building-group-level under different electricity pricings," *Energy and Buildings*, Volume 128, 2016, Pages 143-154.

[125] Markus Puchegger, "Electric load behaviour and DSM potential of office buildings," *Energy and Buildings*, Volume 100, 2015, Pages 43-49.

[126] V. A. H. Vajjala and W. Jewell, "Demand response potential in aggregated residential houses using GridLAB-D," *2015 IEEE Conference on Technologies for Sustainability (SusTech)*, Ogden, UT, 2015, pp. 27-34.

[127] S. Ghaemi and S. Schneider, "Potential analysis of residential Demand Response using GridLAB-D," *IECON 2013 - 39th Annual Conference of the IEEE Industrial Electronics Society*, Vienna, 2013, pp. 8039-8045.

[128] K. O. Aduda, W. Vink, G. Boxem, Yang Zhao and W. Zeiler, "Evaluating cooling zonal set point temperature operation strategies for peak load reduction potential: Case based analysis of an office building," *2015 IEEE Eindhoven PowerTech*, Eindhoven, 2015, pp. 1-5.

[129] Michael Dahl Knudsen, Steffen Petersen, "Demand response potential of model predictive control of space heating based on price and carbon dioxide intensity signals," *Energy and Buildings*, Volume 125, 2016, Pages 196-204.